UNIVERSITY OF CALIFORNIA
RIVERSIDE

Characterization of the Non-Receptor GEF, RIC8 with Genetic, Chemical, and Biochemical Analyses.

A Dissertation submitted in partial satisfaction
of the requirements for the degree of

Doctor of Philosophy

in

Genetics, Genomics and Bioinformatics

by

Patrick Carl Schacht

December 2013

Dissertation Committee:

Dr. Katherine A. Borkovich, Chairperson
Dr. Thomas Girke
Dr. Howard S. Judelson

The Dissertation of Patrick Carl Schacht is approved:

_____

_____

_____

Committee Chairperson

University of California, Riverside

Acknowledgements:

There are many individuals to whom I am deeply indebted for my success in this endeavor. I must begin by thanking Dr. Katherine A. Borkovich for training me to be a productive researcher, meticulous scientific writer, and effective communicator of scientific ideas. I am also indebted to Dr. Sara Wright for her initiation of the RIC8 project and training me on its methods, and Dr. Asharie Campbell for the fruitful collaboration in GEF analysis of RIC8 mutant proteins. I am also grateful the entire Borkovich lab for the healthy environment of research collaboration and communication we have enjoyed.

My academic success is in no small part due to a sustained string of excellent educators, far too many to name exhaustively. I cannot forget Mrs. Emma Slabbert who in 3rd grade offered opportunities to pursue mathematical problems beyond what the curriculum required with real world application. I am most specifically grateful for Dr. Luman Wing and his guest lecture in my 8th grade advanced computing class where I first learned of Bioinformatics and set as my goal to pursue a Ph.D. in the field. Enthusiastic teachers like Mr. David Fitzgerald and Dr. Heckman poured fuel on my passion for Biology and Chemistry respectively. In college, my mentor Dr. Joe Henderson and program director Dr. John Mark Reynolds challenged and honed my critical thinking and writing abilities. Within the sciences, Dr. Jim Rynd challenged me to rigorously engage in scientific learning, and Dr. Matt Cruzen was a constant source of encouragement throughout my education. Dr. Lee always knew how to push me within

an inch of my breaking point, and keep me pursuing my studies to the absolute limits of my ability. Finally, Dr. Gerard Manning gave me an introduction to research that beyond teaching me practical skills, exposed me to an environment of collaboration and perpetual learning I was eager to enter.

In the end, it is not possible to engage in a project of this scale without incredibly support from family. From the start, my parents have encouraged me to pursue my scientific interests and have empowered me to succeed by ensuring I was given ample educational opportunities. My brother Mitch has been a great encouragement as well as we have studied together and spurred one another onto success without animosity. My wife Karen has been a great support throughout this process, as she endured my working weekends and late nights necessary to complete this task, and my daughter Rebecca has been an incredible motivation through these last nine months. Finally, I must thank my Lord and Savior, Jesus Christ for the countless blessings and providential encounters I have had throughout this entire process.

Dedication:

I dedicate this dissertation to my wife, Karen, for her forbearance with me as I pursued this graduate degree. Through the long hours, delays, and frustrations she has been supportive and my primary motivation throughout the course of my graduate career.

ABSTRACT OF THE DISSERTATION

Characterization of the Non-Receptor GEF, RIC8
with Genetic, Chemical, and
Biochemical Analyses.

by

Patrick Carl Schacht

Doctor of Philosophy, Graduate Program in Genetics, Genomics and Bioinformatics
University of California, Riverside, December 2013
Dr. Katherine A. Borkovich, Chairperson

RIC8 plays a critical role in the regulation of G protein signaling. In this study, a specific chemical inhibitor of the RIC8-GNA-1 interaction is identified. In addition to disrupting the interaction *in vitro*, compound F2342-0045 elicits many of the defects associated with loss of *ric8* or *gna-1*. A suppressor screen identified a novel suppressor of Δ*ric8*, predicted to be a *ham-5* mutant by mapping and sequencing. Suppressors of Δ*ric8*, Δ*pde-1* and Δ*rgs-1*, were also identified by crosses with G protein related mutants further implicating RIC8 in Gα and cAMP regulation. Systematic mutagenesis of the RIC8 protein revealed multiple structure-function relationships. The N-terminus of the protein is essential for binding to GNA-1, while the C-terminus is dispensable for this action. Mutations of conserved residues along the front face of the C-terminus generally inhibit the GEF activity of the RIC8 protein towards GNA-1 and GNA-3 alike, while mutations in the central third of the protein have less effect on GEF activity. Residues that cluster together on the top face of the C-terminus show varied but potent effects, either inhibiting or enhancing GEF activity by 50% or more. These data combine to suggest that the N-terminus of RIC8 is involved in binding of Gα proteins, while the C-terminus is involved in GEF activity.

Table of Contents

List of Tables

List of Figures

Chapter 2

Chapter 3

Chapter 1

Introduction

Neurospora crassa as a model organism

The filamentous fungus *Neurospora crassa* (*N. crassa*) is a highly tractable organism for the study of heterotrimeric G protein signaling because of the conservation with mammalian systems, short life cycle, and breadth of genetic tools (Rowland H. Davis, 2000; L. Li, Wright, Krystofova, Park, & Borkovich, 2007). *N. crassa* is a haploid multi-cellular organism which can progress through the asexual and sexual sporulation pathways in a few days or two weeks, respectively (Rowland H. Davis, 2000). As a haploid organism, genetic modification is simplified, having only a single allele for each gene. Transformation is made more efficient using the Δ*mus-51* and Δ*mus-52* mutants, which lack genes essential for non-homologous end joining, and exhibit nearly 100% homologous recombination (Ninomiya, Suzuki, Ishii, & Inoue, 2004). Using these strains and high throughput methodology, the *N. crassa* community has undertaken a project to "knockout" each gene by replacement with the hygromycin resistance gene, *hph*, and has already created knockout strains for the majority of the genome (Colot et al., 2006).

The life cycle of *N. crassa*

N. crassa has a complex life cycle with a variety of tissue types. The organism is capable of undergoing both sexual and asexual sporulation in response to nutrient and environmental cues (Springer & Yanofsky, 1989). Under laboratory growth conditions, such as Vogel's minimal medium (VM), *N. crassa* will establish a mycelium and elaborate hyphae radially from the point of inoculation (R.H. Davis & de Serres, 1970). These hyphae are separated into cell

compartments by crosswalls termed septa, but a septal pore exists in each wall allowing for the flow of cytoplasmic material, and even nuclei (Plamann, 2009). The colony expands via tip extension, forming basal hyphae along the surface of the medium. In the mature colony, aerial hyphae are also formed, extending vertically from the medium surface. The ends of these hyphae constrict, forming multinucleate, fully separated cells in a "beads on a string" configuration. These so-called macroconidia separate completely upon maturation, and are easily distributed by wind or mechanical agitation (Springer, 1993). Macroconidia, hereafter referred to simply as conidia, are robust spores which can survive freezing, but are susceptible to heat. When these spores encounter adequate nutrients (sugar, salts, and a few trace elements will suffice) they establish a new colony completing the primary asexual life cycle (Metzenberg, 1995). A less common sporulation pathway also exists where in response to specific stresses, including the presence of iodoacetic acid, mono-nucleate spores called microconidia are generated directly from mature hyphae (Maheshwari, 1999; Rossier, Ton-That, & Turian, 1977; Springer, 1993; Springer & Yanofsky, 1989).

N. crassa exists in both *mat a* and *mat A* mating types, each of which can function as a male or female in the sexual cycle (Raju & Leslie, 1992). When it is grown under nitrogen deprivation conditions, such as are induced on synthetic crossing medium (SCM), the formation of female sexual structures (protoperithecia) is induced (Westergaard & Mitchell, 1947). Within one week, hyphae coil together to form protoperithecia, which appear as light-brown bodies. Protoperithecia elaborate hyphae known as trychogynes which grow towards an opposite mating type male cell (macroconidium, microconidium or hyphal fragment) using a pheromone response pathway (Bobrowicz, Pawlak, Correa, Bell-Pedersen, & Ebbole, 2002; Kim & Borkovich, 2004, 2006). Upon fusion, the nuclei from the male cell are transported into the

protoperitheicium where fertilization takes place (Bistis, 1981; Kim & Borkovich, 2004). The protoperithecia subsequently enlarge, melanize and orient the tip of the developing perithecium in the direction of the light source. As these macroscopic changes take place, in each ascus a pair of meiotic divisions followed by a single mitotic division occur, forming thousands of asci, each containing eight sexual spores, termed ascospores (Raju, 1980; Springer, 1993). Once the perithecium has matured, it will violently eject the haploid ascospores in the direction of the light. These spores are resistant to and even activated by heat, after which they germinate readily to establish a new colony (Metzenberg, 1995).

Heterotrimeric G protein signaling in *N. crassa*

Heterotrimeric G proteins play a critical role in transmitting extracellular stimuli into intracellular signals. Signal transduction begins when a ligand stimulates a G protein coupled receptor (GPCR) (L. Li et al., 2007). These proteins, defined by their seven transmembrane helical domains, represent the largest point of diversity within G protein signaling, with mammals possessing almost 800 GPCRs (Fredriksson, Lagerstrom, Lundin, & Schioth, 2003). Heterotrimeric G proteins, comprised of subunits termed α, β and γ, are the next step in the signaling pathway. The Gα subunit can be bound to either guanosine di-phosphate (GDP) or guanosine tri-phosphate (GTP). When the Gα is in its GDP-bound state, it is inactive and sequestered at the membrane with the tightly bound Gβγ heterodimer (L. Li et al., 2007). Upon stimulation, the GPCR acts as a Guanine Nucleotide Exchange Factor (GEF), facilitating the exchange of GDP for GTP on the Gα subunit. This activates the Gα, causing it and the Gβγ dimer to dissociate from the GPCR, where they each activate downstream effectors (L. Li et al., 2007). The Gα protein has a native GTPase activity and eventually hydrolyzes a phosphate, converting

its GTP to GDP, and then returns to the membrane where it re-associates with the Gβγ dimer. A total of 20 different Gα proteins have been identified in mammals, which can be divided into four distinct classes: $G\alpha_s$, $G\alpha_i/G\alpha_o$, $G\alpha_q/G\alpha_{11}$ and $G\alpha_{12}/G\alpha_{13}$, each of which has a diverse range of functions (Neves, Ram, & Iyengar, 2002).

The G protein signaling pathway in *N. crassa* is well characterized and shares similarities with higher eukaryotes, making discoveries in *N. crassa* relevant to studies in mammalian systems. At present, 25 GPCR genes have been predicted in *N. crassa*, but analysis of knockout mutants have revealed only subtle phenotypes for most, presumably due to gene redundancy (Kays & Borkovich, 2004; L. Li et al., 2007). *N. crassa* possesses three Gα subunits termed GNA-1, GNA-2 and GNA-3, one Gβ subunit (GNB-1), and one Gγ subunit (GNG-1). GNA-1 has the highest similarity to $G\alpha_i$ from mammals (Turner & Borkovich, 1993). Regulators of G Protein Signaling (RGS) proteins exist in both *N. crassa* and mammals (Borkovich et al., 2004; Hollinger & Hepler, 2002). These RGS proteins stimulate the native GTPase activity of the Gα subunit, accelerating its return to the inactive GDP bound form (Wilkie & Kinch, 2005). One RGS gene, *rgs-1*, was identified in the initial genome annotation, but four additional RGS genes have been since identified (Li, Wright and Borkovich, unpublished). These additional genes have been named *rgs-2*, *rgs-3*, *rgs-4* and *rgs-5* based on their homology to characterized genes in *Aspergillus nidulans* (L. Li et al., 2007; Yu, 2006).

The many roles of RIC8

RIC8 provides a unique exception to canonical G protein signaling, as it acts as a GEF for Gα proteins, but is not a GPCR. RIC8 was initially discovered in *C. elegans* where it was implicated as a possible upstream regulator of $G\alpha_q$ in neurons (Miller, Emerson, McManus, &

Rand, 2000). It was found to be localized to the cytoplasm, presenting a significant difference from GPCR GEF proteins that are located in the plasma membrane. (Miller et al., 2000) At the same time, RIC8 was also linked to roles in centrosome movement (Miller & Rand, 2000). A few years later, the homologue in mammals, Ric-8A, was confirmed to have GEF activity towards Gα proteins (Tall, Krumins, & Gilman, 2003). Continued work in *C. elegans* revealed that RIC8 also played a critical role in asymmetrical cell division during embryogenesis (Afshar et al., 2004). Work in *Drosophila* confirmed that RIC8 was involved in maintaining polarity during asymmetrical cell division, and identified that it was essential for sensing of extracellular ligands (Hampoelz, Hoeller, Bowman, Dunican, & Knoblich, 2005). A few suppressors of the *ric-8* mutation were identified in *C. elegans*, including hyperactive alleles of the Gα subunits, as well as activated alleles of adenylyl cyclase and protein kinase A (PKA) (Schade, Reynolds, Dollins, & Miller, 2005). Genomic studies also revealed that *ric8* was present in most eukaryotes, but not in yeasts or plants (Wilkie & Kinch, 2005).

N. crassa possesses a RIC8 homolog, the loss of which induces severe pleiotropic effects (Wright, Inchausti, Eaton, Krystofova, & Borkovich, 2011). The Δ*ric8* mutant grows much more slowly than wild type, does not produce aerial hyphae, conidiates inappropriately in submerged culture and is female-sterile (Wright et al., 2011). *N. crassa* hyphae grow via polar apical extension, serving as a useful model for asymmetric cell division in higher eukaryotes (Schmid & Harold, 1988). Thus, one of the main functions of *ric8* in other eukaryotes – asymmetric cell division – may partially explain the growth rate defects of the N. crassa mutant (Wright et al., 2011). Using the yeast two hybrid system, RIC8 was shown to interact with GNA-1 and GNA-3, but not GNA-2 (Wright et al., 2011). Previous work on the Gα mutants in *N.* crassa showed that the loss of *gna*-1 and *gna*-3 or the loss of all three Gα genes led to many of the same phenotypic

defects as observed in Δ*ric8* strains (Kays & Borkovich, 2004). Based on this and previous *C. elegans* data, hyperactive mutations for the three Gα genes were introduced into the Δ*ric8* background, with *gna-1* and *gna-3* partially suppressing the Δ*ric8* mutant phenotypes (Wright et al., 2011).

cAMP signaling is activated by Gα proteins and has been implicated as a downstream effector of *ric8* in animals (Neves et al., 2002; Schade et al., 2005). To test for a similar function in *N. crassa*, a mutation in *mcb*, encoding the regulatory subunit of cAMP-dependent protein kinase (Bruno, Aramayo, Minke, Metzenberg, & Plamann, 1996) was introduced into the Δ*ric8* background. This mutation, predicted to lead to elevated cAMP levels, had previously been shown to suppress defects of Δ*gna-1* mutants to be epistatic to the Δ*gna-3* mutation (Kays, Rowley, Baasiri, & Borkovich, 2000). Similarly, *mcb* was able to suppress the Δ*ric8* phenotype (Wright et al., 2011). These results support the hypothesis that RIC8 regulates G protein signaling similarly in *N. crassa* and higher eukaryotes, and that discoveries in *N. crassa* will be useful and relevant for progressing work on RIC8 in animal systems.

Hypothesis and Objectives

The severe phenotypes arising from the loss of *ric8* demonstrate its vital importance to the cell. Current knowledge of its signaling roles is only partial and a structural understanding of its function has remained elusive. The hypothesis of this thesis is that the pleiotropic effects due to loss of *ric8* suggest critical roles in regulation of Gα proteins. Additionally, it is predicted that genes regulated by RIC8 through Gα pathways will represent a specific subset of all Gα-related genes. Consequently, hyperactive mutations in genes up-regulated by RIC8 and loss of function mutations in genes repressed by RIC8 should at least partially suppress phenotypes seen in the Δ*ric8* mutant.

Aim 1: Identify chemical inhibitors of the RIC8-Gα interaction

Chemical inhibitors can phenocopy genetic mutations and afford additional options for future analysis (Bedalov, Gatbonton, Irvine, Gottschling, & Simon, 2001; Fitzsimmons et al., 2011). These chemicals ideally target a specific binding pocket and block only a single interaction. Chemicals can be added to and subsequently removed from any strain for time-based analysis of morphology and protein localization. Based on the broad and powerful applications of a chemical inhibitor, a screen was pursued for inhibitors of the RIC8-GNA-1 protein interaction. For this screen, a yeast two hybrid system was utilized, where the production of a nutrient by the yeast cell is contingent on the interaction between RIC8 and its Gα. Using robotic automation to dispense media and diverse compounds into microplates, a rapid testing platform was developed to identify chemical inhibitors of this interaction that could be used for future analysis of RIC8.

Aim 2: Identify ric8-related genes using suppressor screens

As the pathways regulated by *ric8* are only partially understood, a two-fold approach to identifying genes having a genetic interaction with *ric8* was proposed. To best leverage current knowledge, the Δ*ric8* mutation was crossed into backgrounds harboring mutations implicated as suppressors of Δ*ric8* based on literature studies. Utilizing the library of knockout mutants, a genetic cross followed by genotyping of progeny was used to generate and identify double mutants. Phenotypic assays identified double mutants which grew better than the Δ*ric8* mutant alone, revealing genes that suppress the *ric8* mutation.

In conjunction with the targeted approach, a random mutagenesis project was also pursued. Mutagenesis with ultraviolet (UV) light allows for an unbiased suppressor screen. Utilization of single nucleotide polymorphisms to efficiently map mutations and next generation sequencing to rapidly sequence genomes, offers an efficient mechanism for discovering the genetic basis of suppressor mutations.

Aim 3: Determine functionally critical regions of RIC8

Current knowledge of the structure-function relationships of RIC8 residues is minimal. By removing large regions of RIC8 and testing for an interaction with GNA-1 in the yeast two hybrid system, broad regions of RIC8 essential for interaction were identified. GEF assays performed on the same truncations showed that every truncation fully eliminated GEF activity. Mutation of individual conserved amino acids in the open reading frame (ORF) was more revealing, with the GEF assay identifying specific amino acids and regions within RIC8 that were essential for activity.

CHAPTER 2

Chemical inhibition of the interaction between RIC8 and GNA-1

Abstract:

The regulation of Gα proteins, specifically GNA-1, is one of the primary functions of RIC8. In most systems this function cannot be studied using traditional knockout mutants, as the loss of *ric8* is lethal in all studied higher eukaryotes. However, such studies can be accomplished in filamentous fungi such as *N. crassa*, where although leading to slow growth, loss of *ric8* is not lethal. The identification of a chemical inhibitor would be useful not only for temporally assaying the effects of disrupting RIC8 function in *N. crassa*, but also in systems where analysis of traditional knockout mutants is not possible. In this chapter, a reverse genetic yeast two-hybrid screen was performed, testing 25,000 compounds for their ability to disrupt the interaction between RIC8 and GNA-1. One inhibitor of the interaction was identified. Analysis of available analogs revealed that even modest changes to the compound eliminated its potency. Application of this compound to *N. crassa* resulted in reversible, partial phenocopying of the defects of the Δ*ric8* mutant in a dose-dependent manner.

Introduction

Heterotrimeric G protein signaling revolves around the guanine nucleotide-bound state Gα proteins (Neves et al., 2002). Historically, these proteins are known to be regulated by a large family of GPCR proteins (Oldham & Hamm, 2008). In recent years, RIC8 has been shown to act as a cytosolic GEF, in the absence of a GPCR (Romo et al., 2007; Tall & Gilman, 2004). To accomplish this activity, RIC8 directly interacts with Gα proteins, specifically GNA-1 and GNA-3 in *N. crassa* (Wright et al., 2011). Additionally, the loss of *gna-1* and *gna-3* combined phenocopies the Δ*ric8* mutant, with *gna-1* contributing most significantly to this effect (Wright et al., 2011).

The role of *ric8* remains an important area of study, but the essential nature of the gene makes working with knockout mutants difficult in animal systems. In *Caenorhabditis elegans*, where RIC8 was first characterized, only partial loss of function mutants were viable, and no viable null mutants were ever obtained (Miller et al., 2000). Similarly, research in *Drosophila melanogaster* (*Drosophila*) revealed that reduction-of-function mutants were able to undergo asymmetric cell division, but no null mutants were viable (Wang et al., 2005). Further, research in *Mus musculus* revealed that while heterozygous knockout mice were sick but viable, the homozygous loss of *ric8* resulted in embryonic lethality (Tonissoo et al., 2006). Finally, research in *Xenpus laevis* revealed that the *ric8* null mutant was likewise inviable (Romo et al., 2007). With each of these organisms the loss of *ric8* has been found to produce lethality at such an early stage that a homozygous knockout could not be studied. In contrast, in *N. crassa*, although loss of *ric8* produces severe defects in development and growth, mutants are still viable and can be studied for phenotypes (Wright et al., 2011).

The inability to work with a mammalian organism lacking RIC8 has resulted in gaps in our knowledge regarding the role of RIC8, particularly in higher eukaryotes. To fill this gap, one could engineer a temperature-sensitive mutant or control the expression of *ric8* with an inducible promoter in each of these organisms and selectively express it until the organism matures. This semi-classical approach, however, is not as efficient as would be finding a chemical that specifically disrupts the function of RIC8 *in vivo* (Spring, 2005). The benefits to a chemical inhibitor are not merely the complement of the difficulties associated with using an inducible promoter, but include a number of unique positives. For one, the use of a chemical is completely reversible, and is limited only by the rate of diffusion into the cell. An inducible promoter must be activated, or repressed, and then a cascade of events must occur before the protein reemerges or disappears respectively. Translation of the existing mRNA still proceeds and turnover of existing protein product must occur before the effect is observed. With a chemical inhibitor, the reaction is immediately reversible, as one can add the compound and observe its effect as fast as it can diffuse through the membrane, and then wash with fresh media to remove the compound and the effect as fast as diffusion allows (Stockwell, 2004; Wells & McClendon, 2007). Additionally, a compound can be applied to any existing mutant to mimic the effects of a double mutant without the lengthy workup and possible issues of lethality associated with generating a double mutant.

Given the difficulty, or even impossibility, of working with a *ric8* null mutant the identification of a compound which specifically disrupts the function of RIC8 should provide a significant benefit to the community attempting to dissect the roles of RIC8. In order to obtain such a compound, a number of techniques and considerations from the field of Chemical Genomics must be assessed (MacBeath, 2001). First, just as in classical genetics and genomics,

one must consider whether forward or reverse chemical genomics is best suited for the task. Forward chemical genomics produces a higher hit rate, and has been effective in finding chemicals involved in general growth and developmental pathways, such as in *Danio rerio* (Peterson, Link, Dowling, & Schreiber, 2000). This forward method is attractive, in large part due to its high hit rate, but it fails to provide one critical piece of information: the mechanism of action of any hit compound. Subsequent to any forward chemical screen, akin to a forward genetic screen, one must dissect exactly what proteins are targeted by the bioactive compound. As this project seeks to identify a specific disruptor of the function of RIC8, the additional work of characterizing hits, as well as the improbability that a compound identified for its effect on growth or development would be specifically targeting RIC8, makes forward chemical genomics a sub-optimal approach.

Instead, the technique of reverse chemical genomics is more amenable to the project of finding an inhibitor of RIC8. Using reverse chemical genomics, a specific protein pair is identified and used in an *in vitro* system where the unique disruption of their interaction can be assessed in the presence of various compounds (Spring, 2005). This technique yields a drastically lower hit rate given the specificity it requires, but provides the critical benefits of already knowing the target protein. Consequently, to effectively conduct a reverse genetic screen it is necessary to have a robust system with controls, a mechanism of automation to increase throughput, and an optimized and very large set of chemicals to analyze.

For the reverse chemical genetic screen of RIC8, the yeast two hybrid system provides a system that is highly reproducible and easy to scale. Yeast two hybrid analysis has been used to prove RIC8 interacts with Gα in multiple organisms including human (Klattenhoff et al., 2003). In *N. crassa*, RIC8 interacts with the Gα protein GNA-1. This interaction occurs specifically between

GNA-1 in the GAD vector and RIC8 in the GBK vector within the yeast two hybrid system (Wright et al., 2011).

Given the sheer numbers of chemicals and protein-protein interactions, many preliminary studies were necessary to make the screening for a chemical inhibitor feasible. To begin, chemical screening was restricted to drugs which adhered to the Lipinski's 'rule of five' (Lipinski, Lombardo, Dominy, & Feeney, 2001). This set of factors that are multiples of five: less than five hydrogen bond donors, no more than 10 hydrogen bond acceptors, molecular mass of less than 500 Daltons, less than five rotatable bonds, and a Log(P) of less than five, represent a general set of criteria for molecules most likely to permeate the plasma membrane and elicit an effect within a cell. With these considerations, three libraries of compounds were chosen that optimally represent these criteria.

Two main library types exist for obtaining diversity in high throughput screening: synthetic and natural products (Brenk et al., 2008). Each has their benefits and drawbacks. A natural products library often produces more bioactives (Spring, 2005). Most synthetic libraries are built in a combinatorial manner, where the same building blocks are re-arranged to efficiently produce a large set of compounds (Weber, 2000). Greater diversity can be achieved, but only with significantly higher cost, and in either case, the purification away from intermediates is more difficult, often resulting in mixtures rather than pure products (Burke & Schreiber, 2004). Ultimately there is a tradeoff to be made, where artificial diversity can be had cheaply in combinatorial synthetic libraries, but carefully curated natural product libraries can often represent more bioactives that tend to target already known pathways and proteins. To balance these tradeoffs, mixed and synthetic libraries were used in the screening to offer the most diversity and potential bioactives, without redundancy and excessive expense.

Finally, screening on the scale necessary to find a chemical inhibitor requires a great deal of automation. Various systems exist for this, ranging from multichannel pipettes and 96 well pin tools to robotic automation. The specifications of the robot used will be described in the Materials and Methods, but this screening can occur on the order of 25-96 well plates per day, or with controls, nearly 1000 compounds assessed in a single day. Only with this level of efficiency is it possible to traverse the vast chemical space in search of a unique compound that disrupts the interaction between RIC8 and GNA-1.

The ultimate goal of the chemical screening is to isolate a potent, specific inhibitor that offers a wide array of benefits. Given the vastness of chemical space it is expected that there should be a specific compound which drugs a single interface, allowing for careful targeting of the mechanism desired (Haggarty, Koeller, Wong, Grozinger, & Schreiber, 2003). Finally, there is also the possibility of a commercial application of any chemical inhibitor (Cases & Mestres, 2009; Dean, 2007). It could be viable in pharmaceutical applications, and given the absence of RIC8 in plants, but its importance in fungi and insects, a specific inhibitor of RIC8 could also serve as an effective fungicide or pesticide (Cases & Mestres, 2009; Dean, 2007).

Materials and Methods:

Fungal Strains:

Two *N. crassa* strains were used in this study. For a base comparison, wild type *mat A* (FGSC #4200) was used as wild type. The *ric8* deletion mutant, ∆*ric8 mat a* was used for comparison (Wright et al., 2011). Yeast diploids from previous studies were used. Positive and negative control strains were obtained from Clontech (Mountain View, CA). The assay strain containing RIC8-GAD and GNA-1-GBK vector was generated in a previous study (Wright et al., 2011).

Chemical Libraries:

The compounds were supplied to UCR in powdered form, and dissolved in equal volumes of DMSO to facilitate both optimal solubility and stable storage (Frearson & Collie, 2009). All chemical libraries were stored in 384 well plates. The plates were sealed to prevent water from entering the solution, and stored at -20^{o}C between uses. Because of transfer loss and compounds having variable molecular weights within a library, there was some variability, but the DMSO stock concentrations were on average 10mM.

Screening was begun in using the Microsource Spectrum Collection (Microscource Discovery Systems, CT, USA). This 2,000 compound library is a mixture of 600 natural products, 1,000 known drugs, and 400 other known bioactives (Kocisko et al., 2003). It is devised to be a control set with a very high hit rate and general bioactive rate, in order to calibrate the sensitivity of a screen. The second library screened was the 20,000 ChemBridge DiverSet (ChemBridge Corporation, CA, USA). This library is completely synthetic library built upon a set

of 430 scaffold molecules. The last library screened was the 12,000 compound LifeChem library (Life Chemicals, Ontario, Canada). This library is also a synthetic library, but is based on a larger set of roughly 2,300 scaffolds, offering greater diversity.

Calibration of screening:

All chemical libraries available contain samples dissolved in DMSO. To utilize this system the maximum volume of DMSO that would not significantly affect the growth rate of yeast strains was determined. DMSO concentrations of 0.0, 0.2, 0.5, 1.0, 1.5, and 2.0 μL/200 μL were each tested for inhibition of yeast growth after 20 hours of 30^{o}C 200 RPM shaking. The results showed that at a concentration of 0.5 μL/200 μL, the growth rate was still 94% that of 0.0 μL/200 μL. At 1.0 μL/200 μL, DMSO growth was reduced to 80% that of no DMSO. Therefore, 0.5 μL of DMSO in a 200 μL cell suspension was used for all screening experiments in order to deliver the maximum concentration of chemical, without significantly altering the growth of yeast.

Robotic Screening Protocols:

Robotic screening was conducted using a Biomek FX fluid handling robot with an attached Cytomat. Before screening, yeast two hybrid strains were grown in SD-Trp-Leu for a positive control, and SD-Trp-Leu-His for the assay (Appendix A). An 18x150 mm glass tube containing 5mL of liquid medium was inoculated with a single colony of yeast from a plate and grown at 30^{o}C with shaking at 200 RPM for 48 hours. This 5 mL culture was used to inoculate 50 mL of medium in a 125 mL baffle flask, which was then grown for 24 hours under the same conditions as the tube culture. Finally, the 50 mL culture was diluted into 450 mL of the same

medium, and dispensed using a Biomek FX fluid handling robot (Beckman Coulter, Brea CA), at 200 μL per well on a 96 well plate. Chemicals were then added in a volume of 0.5 μL to wells B1 through H11, leaving all wells in columns A and I free of chemicals for control purposes (Figure 2.1). Four 96 well plates for each of the assay and control cell suspensions were used in conjunction with a single 384 well plate of compounds. In this system, the A plate contained chemicals from wells C1, C3, C5 in column B, E1, E3, E5 in column C, and so forth using a grid pattern to equally dispense the 384 columns into 4-96 well plates (Figure 2.1). Plates B, C, and D followed the same pattern for chemical dispersal, beginning in wells D1, C2, and D2, respectively. Each plate containing cell suspension and chemical was sealed with breathable sealing tape, closed with a plastic lid, and incubated at 30^{o}C with shaking at 250 RPM for 20 hours. Finally, the Optical Density at 600 nm (OD_{600}) of each well was read in a microplate reader to determine the relative absorbance, which is directly proportional to the concentration of yeast cells in each well.

Data analysis of screening data

Data collected from the microplate reader were processed using Excel (Microsoft, Seattle, WA). Absorbance values for all eight plates corresponding to a 384 well plate of chemicals were copied into a single Excel sheet. An average growth for each plate was first established by calculating the average absorbance of all cells in columns A and I (the cells without compound). The absorbance of each cell where compound was added was then divided by the average control growth rate for the plate to determine a percent growth inhibition. This data was then aligned for both the assay and control media for each compound and assessed on two criteria. First, did the compound inhibit the growth of the assay strain greater than 25

percent? Second, did the compound inhibit growth of the control strain greater than 25 percent? From these two questions four conclusions could be drawn. If growth in the assay was inhibited, but not the control, then the compound was deemed a possible hit and flagged for rescreening. If growth of assay and control were both inhibited, the compound was deemed a potential general fungicide and not considered for further analysis within this study. If the growth of the assay and control were both unaffected, the compound was deemed not to have any fungicidal or specific activity and not considered further.

Rescreening protocols

Compounds deemed to be leads were re-screened to determine if the observed suppression was reproducible. Screening was performed in a manner identical to that of robotic screening with one exception. Chemical was added manually instead of robotically, and two wells of each medium type were allocated for each chemical to be re-screened.

***N. crassa* Growth Conditions**

For all growth assays, *N. crassa* strains were first grown on slants under the conditions described in Appendix B (Slant Growth). Conidia from these slant cultures were then inoculated onto a variety of different medium for different assays. For radial hyphal growth analysis, a sterile wood stick was used to inoculate a small (1 mm) spot of conidia on the center of a petri dish. The petri dish was prepared with VM medium (see recipe in Appendix A) supplemented with either 5 μL of pure DMSO per mL of medium or the same volume of DMSO containing 4, 8, 16, or 32 μg/μL of compound. These concentrations produced media with 20, 41, 82, and 165 μg/mL compound respectively, or 60, 120, 240, and 480 μM. Conidial germination assays were

performed as described in Appendix C, with chemical concentrations as described for the hyphal growth analysis.

Results:

Calibration screening confirmed ideal conditions and cutoffs

Screening for inhibitors of the RIC8-GNA-1 interaction in the yeast two hybrid system was initiated using the 2,000 compound Microsource library. This library is rich in bioactives, including fungicides, and served as a calibration control for larger-scale screening. The growth of the assay strain in the presence of a compound was compared with the growth of the positive control strain. A total of 100 of the 2,000 compounds were selected for retesting, based on inhibition of the assay strain by more than 25%, while allowing for less than a 20% reduction in growth of the control strain. These 100 compounds were retested under conditions identical to the initial assays, but duplicates of both the assay and control strain were used and all were found to be false positives. This initial control screen thus revealed a baseline for future screening: a 5% hit rate was to be expected in a bioactive rich library. Of these, the vast majority would be expected to be noise in the data resulting from not using replicates. This false positive rate was high, but it was partially expected as a symptom of the type of library represented by Microsource.

High throughput screening of 27,000 compounds revealed one inhibitor

Screening continued with the first 15,000 compounds of the ChemBridge DiverSet library. This library contained fewer bioactives, and only 200 potential hits were deemed worthy of follow-up. Re-testing of these 200 compounds revealed no compounds which specifically inhibited the interaction between RIC8 and GNA-1. While screening the ChemBridge DiverSet library, anecdotal evidence from concurrent screens in other labs suggested that the LifeChem

library had a high rate of bioactives. Therefore, screening of the ChemBridge DiverSet library was set aside to pursue a screen of the LifeChem library.

The LifeChem library was the third and final library screened, representing 12,000 compounds. Initial screening revealed 250 leads, a higher hit rate than the ChemBridge DiverSet library, validating the anecdotal evidence regarding bioactives. Re-screening of these leads revealed a single inhibitor of the RIC8 GNA-1 interaction, compound F2342-0045 (Figure 2.2). This compound inhibited growth of the RIC8, GNA-1 yeast two hybrid strain by 43%, while having no effect on the positive control.

Analog testing revealed no chemicals with activity

Upon identification of the hit compound, analogs were immediately tested from within the libraries available at UCR. *In silico* searching for similar compounds was conducted using ChemMineR (Backman, Cao, & Girke, 2011). This search revealed 44 available analogs with atom pair similarities of 0.300 or greater (Figure 2.3). Testing of these analogs was conducted in the same manner as re-testing: each compound was tested in duplicate in both the positive control and the assay medium. The strongest inhibitor-analogue, F2342-0083, displayed only a 13% inhibition of growth. This degree of inhibition is well within the noise of the assay. Consequently, none of these analogs were determined to produce any significant inhibition of the RIC8-GNA-1 interaction.

Compound F2342-0045 follows Lipinski's rule of five and was pure

Identification of the F2342-0045 hit compound was immediately followed by an analysis of its chemical properties. By Lipinski's rule, it was found to fulfill all criteria generally

established to describe a likely bioactive molecule. The compound had only one hydrogen bond donor, meeting the criterion of less than five hydrogen bond donors, and only five hydrogen bond acceptors, meeting the criterion of no more than 10 hydrogen bond acceptors. Its molecular mass of 331.4 Daltons was well below the 500 Dalton threshold that describes molecules most likely to pass through the membrane. It was highly conjugated, with double bonds making it more rigid, and possessed less than five rotable bonds. Finally, the Log(P) of 2.463 is well less than five, which is established in the Lipinski rule of five, indicating that the compound is only slightly more soluble in non-polar solvents than in water (Lipinski, 2000).

The library stock of the compound contained only a few microliters of 10 mM compound, necessitating purchasing more of the compound. The entire commercially available stock of the compound was initially ordered (700 mg) and subsequently another 1 g was custom synthesized for our use by Life Chemicals Inc. (Life Chemicals Inc., Ontario, Canada). With both the original compound and the new aliquots, it was necessary to determine if the compound was pure, and if it matched its described formula. To determine this, mass spectroscopy analysis was performed on each batch of the compound obtained (Figure 2.4). The findings of this analysis revealed that the dominant peak corresponded to a compound of the predicted structure of F2342-0045, and negligible contamination with byproducts and reactants was observed.

In vivo application of compound revealed partial phenocopying of Δ*ric8* defects

Upon obtaining usable quantities of compound F2342-0045, *in vivo* analysis of its effect was conducted. As described above, loss of *ric8* results in defects in growth rate, hyphal morphology, germination and sexual development. Working under the hypothesis that addition

of F2342-0045 would disrupt the interaction between RIC8 and GNA-1, thus mimicking the effects of losing *ric8* in *N. crassa*, phenotypes were assessed in the presence of the compound.

The most drastic effect of the Δ*ric8* mutation is the reduction of growth rate. The Δ*ric8* mutant grows at approximately 10% the rate of wild type *N. crassa*. Application of F2342-0045 resulted in a dose-dependent reduction in growth rate (Figure 2.5). Using equal volumes of DMSO bearing successively higher concentrations of compound, it was found that while 21 μg/mL (60 μM) inhibited growth approximately 10%, increasing the concentration to 165 μg/mL (480 μM) reduced growth by 35%.

In addition to growth rate, the hyphal morphology of a wild-type strain grown in the presence of F2342-0045 approximated some of the defects of the Δ*ric8* mutant. Approximate quantification of the branching rate revealed that while the loss of *ric8* results in over a five-fold increase in branch rate, the addition of 165 μg/mL (480 μM) compound induced a roughly 2 fold increase in branch rate in wild type (Figure 2.6). Furthermore, while the hyphal diameter of wild type grown in the presence of compound was greater than that of Δ*ric8*, the overall hyphal diameter appeared smaller than that of wild type grown in the presence of DMSO as a negative control.

Conidial germination analysis revealed a significant, but transient inhibition by compound. In *N. crassa*, 45% of wild-type spores germinate by two hours, 88% by four hours, and nearly 100% by six hours, while the Δ*ric8* mutant exhibits only 7% germination at four hours, and 12.6% by six hours (Figure 2.7). The addition of compound at 165μg/mL (480μM) to wild type results in only 17% of spores germinating at two hours. The defect begins to reverse itself by four hours, reaching two thirds the rate of wild type at that time point, with germination being indistinguishable from that of the wild type control by six hours suggesting

the compound inhibits the function of RIC8 in a reversible manner, inducing an initial delay in germination but not a total stop in the process. Furthermore, wild-type *N. crassa* conidia will normally form a single germ tube from each conidium, and none with two germ tubes were observed in the course of this study (Figure 2.8). Mutants with polarity defects will display multiple germ tubes, and in this study conidia grown in the presence of F2342-0045 periodically elaborated multiple germ tubes per conidia, consistent with the compound eliciting Δ*ric8* like polarity defects.

Discussion:

The objective of this aim, to isolate and characterize a chemical inhibitor of the interaction between RIC8 and GNA-1, was achieved. Compound F2342-0045 reproducibly inhibits the growth of the yeast two hybrid strain bearing RIC8 and GNA-1, and also partially phenocopies Δ*ric8* defects in wild-type *N. crassa*. Clearly, the vastness of chemical space was not underestimated by the expectations of needing to screen tens of thousands of compounds. Only after screening nearly 30,000 compounds was a single inhibitor obtained. The structure of this inhibitor was also highly specific, as 44 distinct analogs with only minor functional group changes had no effect on the yeast two hybrid strain. This result indicates an incredibly narrow target for a successful inhibitor. The specificity of the compound suggests that attempting to cover all of chemical space shallowly in order to find a weak hit and then hone in on a related potent inhibitor through subsequent analysis might be less than ideal. Indeed, in this instance such an approach would have had less than a 3% chance of success if only one compound with the common backbone were included in the screen. Consequently, it seems that the decision to screen the more bio-active rich LifeChem library was more efficient than screening a synthetically diverse library, at the least for the specific interaction between GNA-1 and RIC8. In total, the results of this experiment support the notion that diversity alone is insufficient to establish a hit, but large scale screening of presumably bioactive compounds enriches the target area and yields the greatest chance of success.

During assessment of the hit compound, it became apparent that aspirations of identifying an active pesticide or a potent drug were slightly overambitious. The compound must be applied at a very high dose, nearly mM concentrations, before eliciting a modest phenotype. Consequently, it is unlikely that F2342-0014 would be of commercial relevance, but

this minor shortfall should not overshadow its potential research applications. This compound reduced the the apical extension rate of hyphae and the conidial germination rate in *N. crassa*. With the addition of more compound, it is possible that a more severe phenotype might be induced. The results suggest that it would be reasonable to expect that studies of RIC8 in *M. musculus*, *D. melanogaster*, *C. elegans*, and even *H. sapiens* could benefit greatly by using this compound to induce Δ*ric8* phenotypes. Additionally, in all eukaryotes where RIC8 is present, this compound offers unique opportunities to observe the changes in localization of fluorescently tagged proteins, including RIC8 and GNA-1, as well as their downstream signals, in direct response to the disruption of the RIC8-GNA-1 interaction. This opportunity could be used to shed further light not just on the biochemical mode of action of RIC8, but also on the exact subcellular locations where these actions are occurring. In conclusion, this screen successfully identified a specific inhibitor of the RIC8-GNA-1 interaction that replicates known defects associated with the loss of *ric8* and presents a large array of new opportunities for its further study.

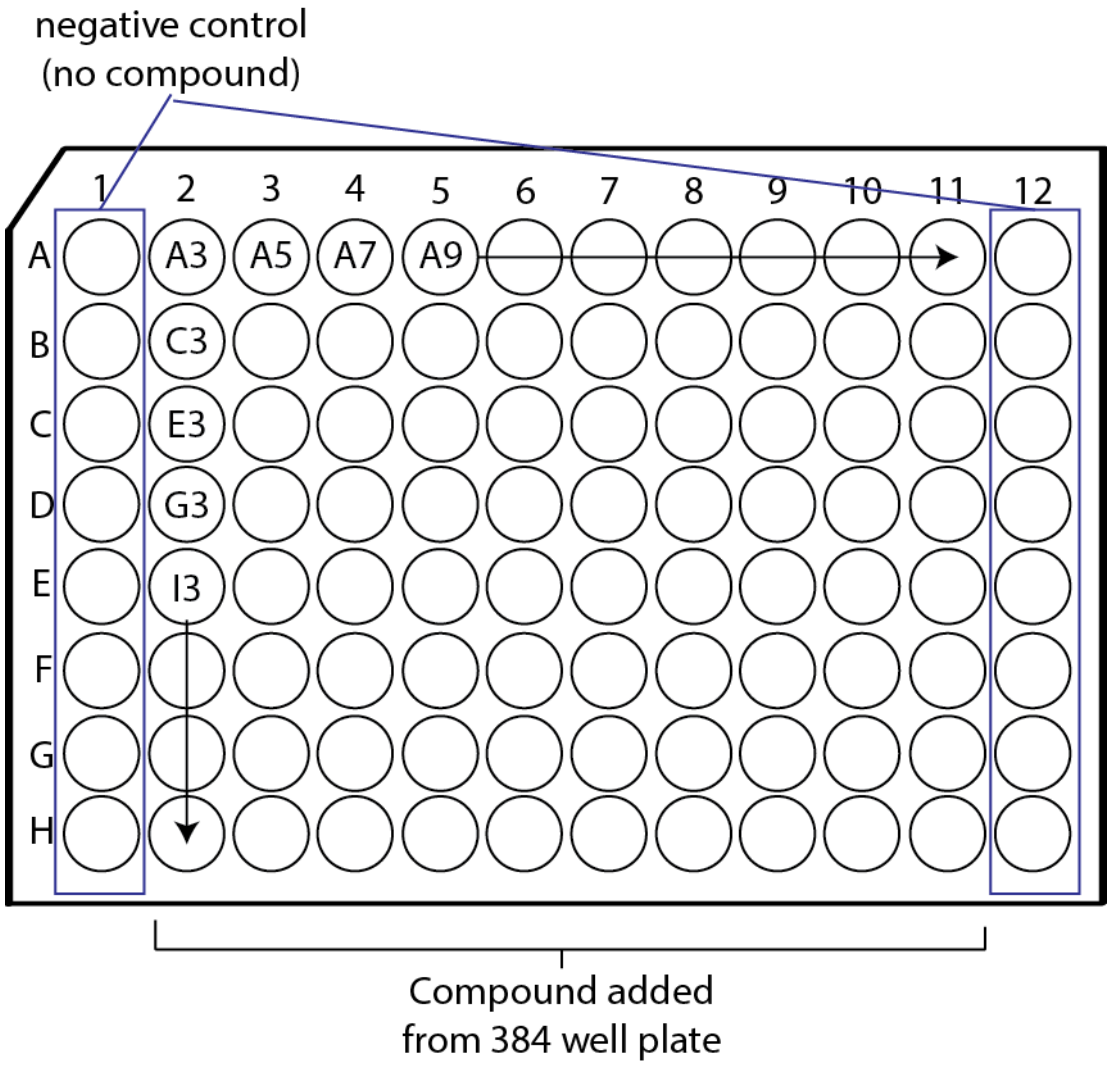

Figure 2.1: Plate mapping for dispensing of chemical library. Each 96 well plate contains empty wells in columns 1 and 12 for controls. The central 80 wells in columns 2-11 are inoculated with compound from the 384-well chemical plate. This plate shows the pattern for plate A, while plates B, C, & D would show the same pattern but begin with a compound from the 384-well plate wells A4, B3, and B4 respectively in well A2.

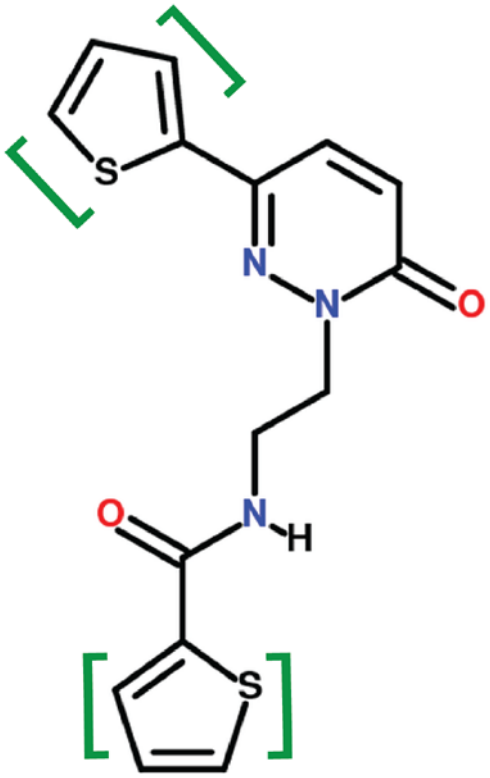

Figure 2.2: Structure of hit compound F2342-0045. The hit compound has a chemical formula of $C_{15}H_{13}N_3O_2S_2$, and a molecular mass of 331.413 Daltons. It meets all criteria of the Lipinski's rule of five. The two thiofuran groups (indicated by green brackets) distinguish this molecule from others in the library with a similar structure. The pair of amide groups, one of which is cyclic, was common to many other structures in the chemical library, indicating that while this substructure is likely necessary for activity, it is not sufficient to elicit the desired effect when the thiofuran groups are missing or modified.

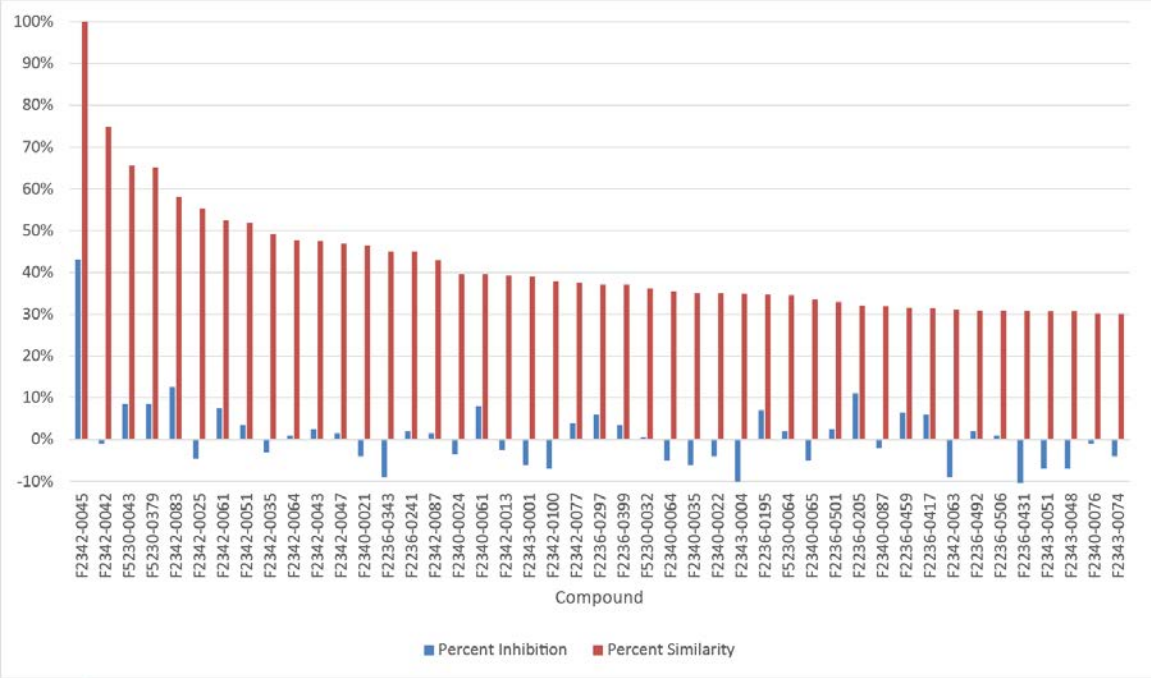

Figure 2.3: Activity of analogs of F2342-0045. The first entry on the x-axis is the hit compound F2343-0045, which inhibits growth of the yeast two hybrid strain by 43%. All other entries are successively less similar hits, based on atom pair similarity (red bars). All percent inhibitions were determined in duplicate, but none revealed a growth inhibition over the threshold value of 25% (blue bars). The greatest inhibition of any analog was observed for F2342-083 and F2236-0205, which inhibit growth by 13% and 11% respectively, well below the threshold of being considered robust inhibitors.

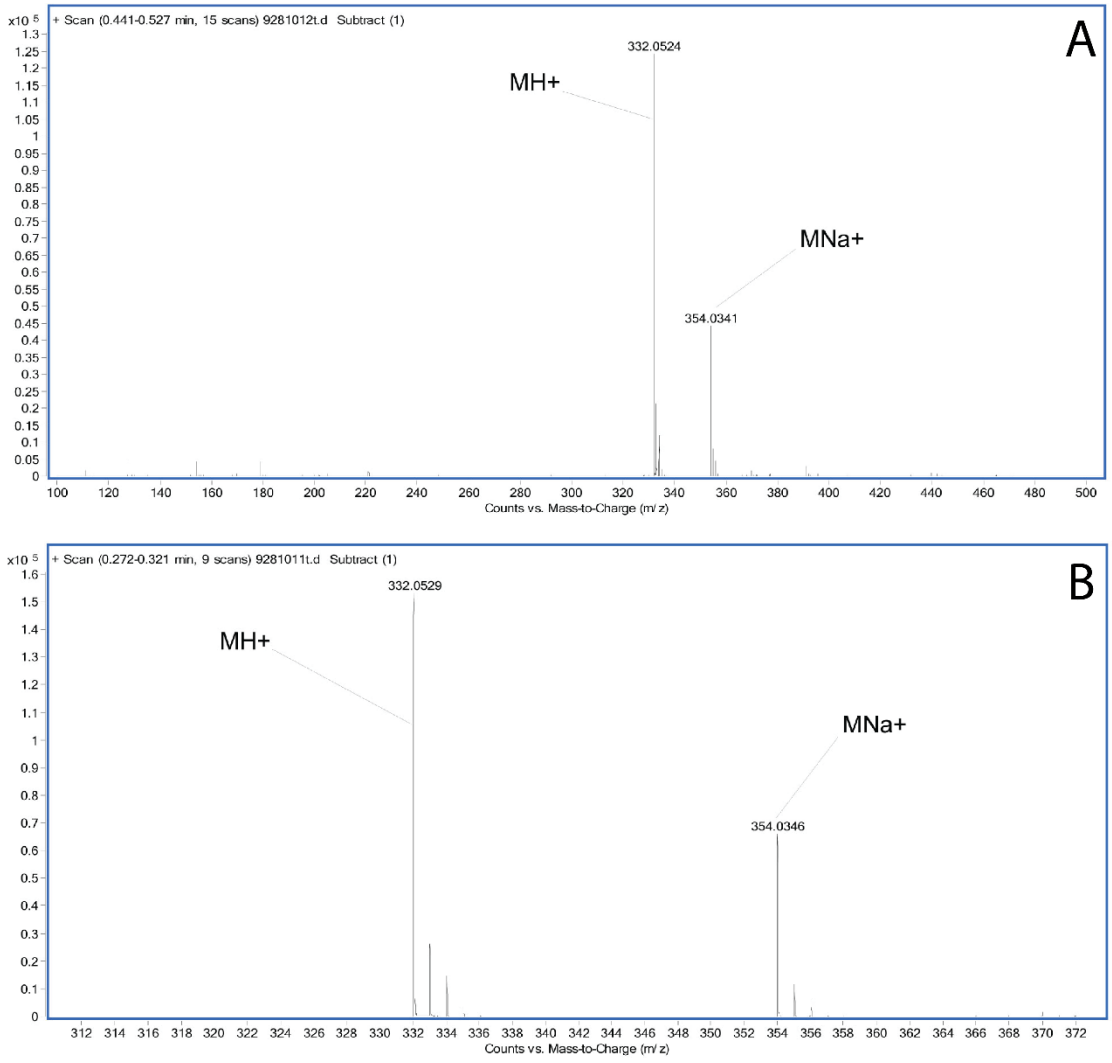

Figure 2.4: Mass spectroscopy of two lots of hit compound F2342-0045. Commercially obtained compound was subjected to analysis by proton mass spectroscopy at the Mass Spectroscopy Core Facility at UCR. Analysis of both the first (A) and second (B) lots revealed compounds with measured masses of 332.0524 and 332.0529 Daltons, respectively, and a compound with a predicted formula of $C_{15}H_{14}N_3O_2S$, identical to the expected formula of F2342-0045. Although purity was not quantified, no peaks except the expected proton and sodium peaks contributed significantly to the sample spectrum.

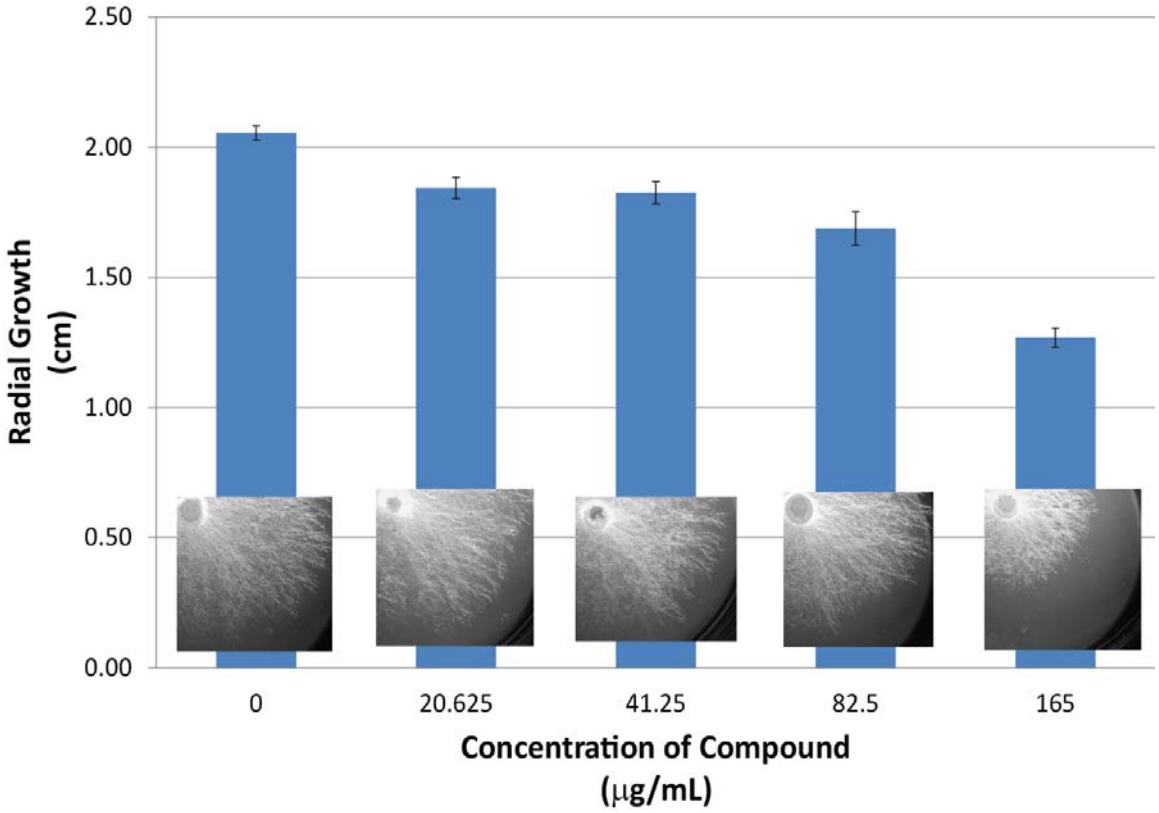

Figure 2.5: The effect of compound F2342-0045 on radial growth of *N. crassa*. VM plates containing 0, 20.625, 41.25, 82.5 and 165 μg/mL of F2342-0045 were inoculated with wild type conidia and grown in the dark for 18 hours at 30°C. The average diameter and standard deviation were calculated. *N. crassa* shows a dose dependent response to the compound.

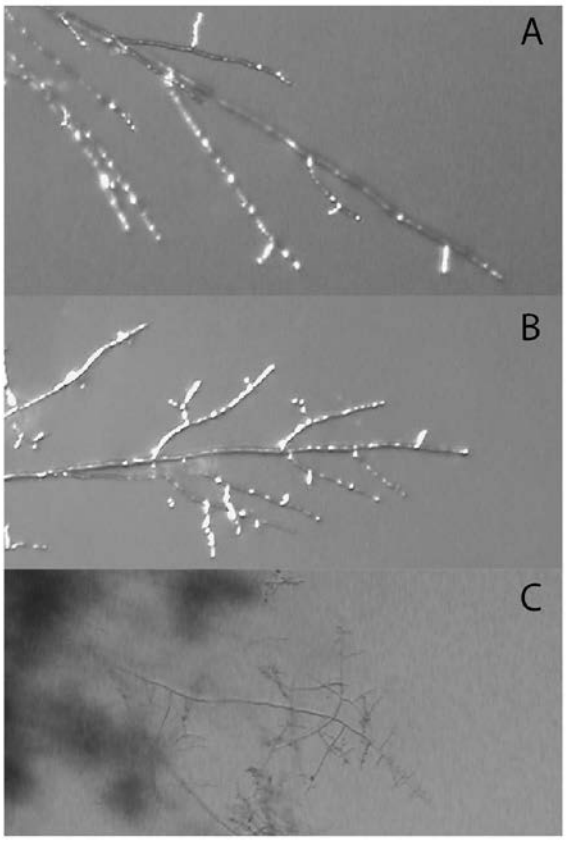

Figure 2.6: Colony edge photos of *N. crassa* grown in the presence of compound F2342-0045. 3.0 cm plates were inoculated with conidia in the center, and pictures were taken after 18 hours of growth at 30°C in the dark. Morphology of wild-type cultured on VM (A), and VM in the presence of 165 μg/mL (480 μM) compound F2342-0045 (B) as well as the Δ*ric8* mutant on VM alone (C) were imaged using an Olympus SZX9 (Olympus, Tokyo, Japan) microscope at 57x magnification with an attached Canon (Canon Inc., Tokyo, Japan) G11 camera. Addition of compound increases branching and decreases hyphal diameter, although not as severely as that induced by deletion of *ric8*.

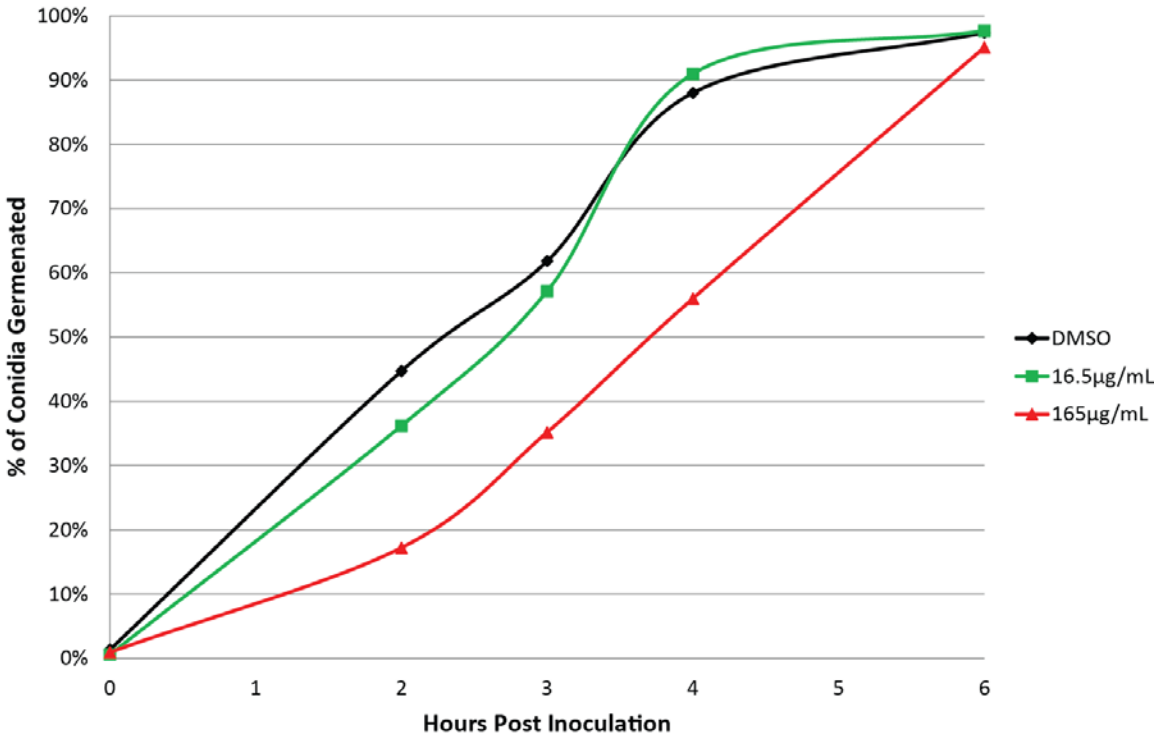

Figure 2.7: The effect of compound F2342-0045 on conidial germination. VM plates with DMSO only, or 16.5 mg/mL and 165 mg/mL F2342-0045 were spread with $1x10^6$ conidia. Samples were incubated in the dark at 30°C, and 100 or more conidia were scored for each time point, and the proportion germinated was reported.

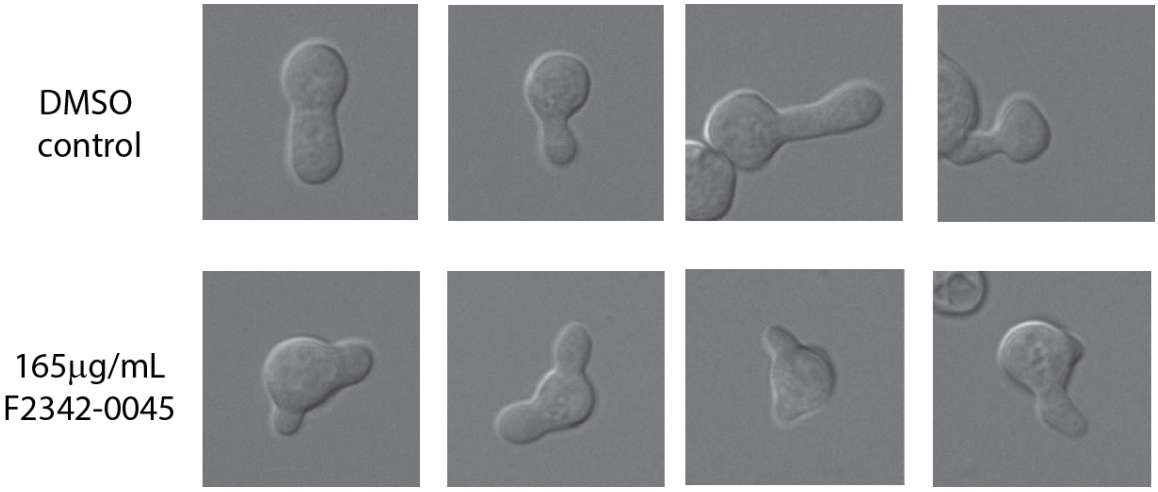

Figure 2.8: Germination assay of *N. crassa* conidia grown in the presence of compound F2342-0045. This experiment was conducted with identical conditions to Figure 2.7. The top panel shows that DMSO alone, and all observed conidia germinated under these conditions elaborated a single germ tube. In the bottom panel, wild-type conidia grown in the presence of F2342-0045 elaborate multiple germ tubes at a small but detectable rate.

Chapter 3

Screening and analysis of suppressors of the Δ*ric8* mutation

Abstract:

The loss of *ric8* induces severe pleotropic effects in *N. crassa*. Previous work with double mutants demonstrated that RIC8 is a positive regulator of Gα proteins and cAMP production in both *C. elegans* and *N. crassa*. To expand our understanding of the regulatory roles of RIC8, random mutagenesis was used in the Δ*ric8* genetic background to isolate suppressor mutations. A single suppressor was identified and SNP-based mapping and high throughput sequence analysis implicated an allele of the hyphal anastomosis gene for *ham-5* with a premature stop codon, as the suppressor. However, complementation with the gene in *trans* was unsuccessful, despite multiple attempts, leaving the identity of the suppressor unconfirmed. In addition to random screens, selective crosses between the Δ*ric8* mutant and mutants lacking genes regulated by G proteins in *N. crassa* and other species were performed to generate double mutants. This approach identified both Δ*pde1* (cAMP phosphodiesterase-1) and Δ*rgs-1* (regulator of G protein signaling-1) as suppressors of Δ*ric8*, consistent with their shared link to G protein signaling.

Introduction

While the RIC8 protein plays a critical role in G protein signaling, the defects caused by the loss of *ric8* can be corrected in some organisms by mutating other genes in pathways related to G protein signaling. In *C. elegans*, a mutation resulting in a constitutively active Gα protein is able to partially compensate for loss of *ric8* (Schade et al., 2005). Mutants lacking DGK-1 were found in a suppressor screen to partially correct for the loss of RIC8 (Miller et al., 2000). DGK-1 is known to function downstream of Gα proteins in neurons, and is involved in the regulation of cAMP signaling (Miller, Emerson, & Rand, 1999). Complementary to the *dgk-1* mutant result, a dominant active allele of the adenylyl cyclase gene *acy-1* corrects some of the defects of the Δ*ric8* mutant (Charlie, Thomure, Schade, & Miller, 2006).

In *N. crassa*, two types of suppressor mutations have been identified that partially correct for the loss of *ric8*. The introduction of an allele of *gna-1* or *gna-3* which mimics the GTP bound form of the Gα partially restores the growth and asexual defects of the Δ*ric8* mutant, but fails to complement the sexual defects (Wright et al., 2011). Similarly, the introduction of an allele of the regulatory subunit of Protein Kinase A (PKA), *mcb*, also partially corrects the asexual defects in the Δ*ric8* background (Wright et al., 2011). This gene is known to operate downstream of G proteins, and is a negative regulator of cAMP signaling. Therefore, down-regulation of *mcb* can compensate for loss of RIC8, a positive regulator of cAMP signaling (Wright et al., 2011).

As mentioned in Chapter 2, loss of the *ric8* gene induces a large number of severe defects in *N. crassa*. These include reduced growth rate, hyperconidiation on solid and in liquid medium, and female sterility. While female fertility requires multiple weeks to analyze, growth rate and conidiation are amenable to rapid suppressor screens (Wright et al., 2011). Both of

these defects can be scored 48 hours after inoculation, and mutants are macroscopically distinguishable from their Δ*ric8* neighbors. The ease of detection, combined with the slow growth rate of the Δ*ric8* mutant, form an ideal intersection for a suppressor screen.

Ultraviolet (UV) light is a well-established tool for inducing random genetic mutations in organisms that has been used for nearly a century (Stadler & Sprague, 1936). Based on the incomplete overlap in defects between the Δ*ric8* mutant and the Δ*gna-1* Δ*gna-3* double mutant, the role of RIC8 is predicted to expand beyond its G protein pathway control (Wright et al., 2011). Additionally, G proteins control a wide range of downstream pathways, and it is not known which of these are most closely intertwined with the function of RIC8 (L. Li et al., 2007). The use of a random mutagenesis method allows for novel mutants to be identified based on phenotype without the need to select in advance genes that might be of interest. UV mutagenesis most commonly involves the formation of a bond between adjacent thymines, and a change in nucleotide sequence occurring when the damaged DNA is repaired. This process typically results in a cytosine to thymine transversion, accounting for over three-quarters of all UV-induced mutations (Cohen-Fix & Livneh, 1992). Besides the cytosine to thymine transversion, other transversions do occur, though infrequently, and addition or removal of nucleotides is occasionally observed (Cohen-Fix & Livneh, 1992).

In *N. crassa*, UV mutagenesis has been utilized for decades to efficiently generate libraries of random mutants. Exposure of mature conidia to a controlled dosage of UV light that reduces the survival of spores to 20% to 50% has been experimentally determined to induce roughly one mutation per genome (R.H. Davis & de Serres, 1970). This optimized mutational rate makes follow-up simpler, as a single genetic change is likely the source of any derived phenotype.

The bulk segregant analysis method termed Single Nucleotide Polymorphism – Cleaved Amplified Polymorphic Sequence (SNP-CAPS) has been optimized for *N. crassa* to leverage SNP differences between strains for mapping mutations (Lambreghts et al., 2009). The Oak Ridge *N. crassa* strain has been used as the canonical wild type and has a fully sequenced genome (Galagan et al., 2003). The Mauriceville strain is morphologically indistinguishable from Oak Ridge, but is considered an exotic wild type and recent sequencing has mapped SNPS in this genetically distinct background (Dunlap et al., 2007). Leveraging this genetic diversity, obtaining 100 or more morphologically identical progeny from a cross between a strain possessing an unknown mutation in the Oak Ridge background and the exotic wild type Mauriceville, makes it possible to map the novel mutation to a region of a single chromosome using only three-96 well plates of PCR reactions and subsequent digests. This tool can be used on a mutant-by-mutant basis to reach greater precision in mapping novel mutations.

While mapping has become more precise and more efficient, the dramatic improvements in sequencing technologies has made the process of identifying mutations through direct sequencing more feasible. Illumina short HiSeq 2500 sequencers (Illumina, San Diego, CA) are now capable of generating over 10x coverage of the entire *N. crassa* genome in a single lane of sequencing (Smith, Phatale, Sullivan, Pomraning, & Freitag, 2011).

The existence of a completed genome sequence for *N. crassa* dramatically reduces the complexity of the sequencing & assembly task. The complete genome sequence has undergone multiple annotation revisions in recent years, but its underlying sequence is essentially the same as in its 2003 publication (Borkovich et al., 2004; Galagan et al., 2003). Using the Burrows-Wheeler Assembler with a reference genome, it is possible to assemble short read sequencing data into a complete genome in hours without specialized hardware (H. Li & Durbin, 2010).

With a reference genome and assembled mutant genome, it is a trivial task to identify differences, but identifying relevant difference requires more careful analysis. SNPs occur spontaneously in nature, and most are benign, representing extraneous discrepancies between mutant and reference genomes (Vignal, Milan, SanCristobal, & Eggen, 2002). Prioritization of mutations based on annotated genomes using Sequence Alignment/ Map Tools (SAM Tools) can display short read alignments and rapidly identify not merely changes between reference and mutant genomes, but also prioritize them based on proximity to a gene, proximity to exons or promoter regions, with the mutation being synonymous or non-synonymous. The output can also be queried to determine whether a resulting amino acid change is major (for example acidic to basic) or minor (for example acidic to other acidic) (H. Li et al., 2009). Rapidly obtaining this metadata about each variation relative to the reference genome allows for efficient characterization of mutations that are likely to be biologically relevant.

In this Chapter I isolate and map one suppressor mutation. Additionally, I cross a group of mutants lacking genes implicated in G protein signaling to the Δ*ric8* knockout mutant in order to assess the genetic relationship of these genes with *ric8*. These data combine to expand community knowledge of the functions of *ric8*.

Materials and Methods:

***N. crassa* strains and media**

The *N. crassa* strains used for this chapter are detailed in Table 3.1. Δ*ric8* strain #1811 was used for isolation of suppressors. The UV generated strain (Δ*ric8*, *sup*^{UV}) was named P3, and the strain with the *sup*^{UV} mutation purified away from the Δ*ric8 mat a* background was named P3-10. The Mauriceville wild type was used to generate a SNP map. Double mutants (Δ*ham-3*, Δ*ric8*; Δ*ham-4*, Δ*ric8*; Δ*ham-5*, Δ*ric8*; Δ*ham-7*, Δ*ric8*; and Δ*ham-9*, Δ*ric8*) were generated using sexual crosses with the Δ*ric8* heterokaryotic helper strain, Δ*ric8* +*a*^{m1} (Griffiths, 1982), as the female. Complementation of *ham-5* was attempted using the *sup*^{UV} mutant described above, and the wild type *his-3 mat A* (*his3*$^{-}$), as well as the Δ*ham-5 his-3 mat A* (*ham-5*, *his3*$^{-}$), and Δ*mus51*::*nat*^{R} *mat A*. For crosses to genes implicated in G protein signaling, Δ*rgs-1*, Δ*rgs-2*, Δ*rgs-3*, Δ*rgs-4*, Δ*rgs-5*, Δ*cr-1*, Δ*pde-1*, and Δ*pde-2* mutants were each crossed as males to Δ*ric8* + a^{m1}. Double mutants from these crosses (Δ*rgs-1*, Δ*ric8*; Δ*rgs-2*, Δ*ric8*; Δ*rgs-4*, Δ*ric8*; Δ*cr-1*, Δ*ric8*; Δ*pde-1*, Δ*ric8*).

All media recipes are described in Appendix A. For this chapter VM medium is used alone and with supplements of hygromycin B (+Hyg), Ignite (+ignite), inositol (+inl), and pantothenic acid (+pan). FGS and regeneration agar are used with the same supplements. For vector work in *E. coli*, LB medium supplemented with ampicillin (LB+Amp) is used. For yeast recombinational cloning YPDA and synthetic dropout medium minus uracil (SD-Ura) were used.

UV Mutagenesis

To generate suppressor mutants, conidia from the Δ*ric8* mutant were subjected to UV mutagenesis. Seven day old conidia from a Δ*ric8* mutant were harvested as described in Appendix B (Conidia Harvesting). Conidial suspensions were quantified using a hemocytometer (Appendix B, Cell Counting) and diluted in a sterile 0.1% agar solution at a concentration of $5x10^6$ conidia per mL. Aliquots containing 10 mL were dispensed into sterile petri dishes in a biosafety cabinet, where they were exposed to UV light using a 0.70 Amp, 60 Hz short wave UV lamp model XX-15G. Multiple iterations during control tests determined that a 15 second exposure from a distance of 20 cm induced a roughly 50% survival rate, previously associated with being an optimal dosage, corresponding to a single mutation per genome (R.H. Davis & de Serres, 1970; Giles, 1951).

After exposure to UV light, conidia were serially diluted to $5x10^2$ in ten-fold increments and 50 μL aliquots from each dilution were plated on VM+Hyg, FGS, and VM (Appendix A, Appendix B: Spread Plating). Samples were incubated at 25°C for two days. It was determined that plates bearing 2,500 to 250 conidia produced the optimal number of colonies (roughly 100 or fewer per plate). Multiple rounds of mutagenesis, comprising tens of thousands of colonies were plated on three different media: VM+Hyg, FGS, or VM (Appendix A, Appendix B). Any colonies displaying improved growth rate or suppressed conidiation were isolated using a sterilized Pasteur pipette and transferred to VM+Hyg slants (Appendix B, Colony Picking).

Strain Purification and Confirmation

Putative suppressors were first re-grown on VM plates to confirm the suppression observed in the small colony was a penetrant phenotype. Strains that grew better than the Δ*ric8*

mutant were selected for further analysis. Next, to confirm the mutant was a suppressor of the defects caused by the loss of *ric8* and not simply a contaminant, each purified mutant was subjected to Southern analysis. DNA from each putative suppressor strain, the Δ*ric8* mutant and the wild-type 74A strain was extracted according to the Puregene protocol (Appendix B). For each sample, 5 μL of genomic DNA was digested at 37°C for 12 hours with 5-10 units of *NcoI* in 1.5 μL of 10x NEB Buffer 3, with water to a total volume of 15 μL. Loading dye was added to 1x concentration, and the entire sample for each strain was electrophoresed alongside a λ-*Hind*III DNA ladder on a 1% agarose gel (Appendix B). The gel was then stained in ethidium bromide for 10 minutes, and bands visualized with UV light. The gel was then denatured by soaking it in a solution that contained 200 mM NaOH and 600 mM NaCl. The gel was then neutralized for 45 minutes in a solution containing 1 M TrisCl pH 7.4 and 1.5 M NaCl. The gel was then soaked in a 2x SSC (8.82 g $NaC_6H_7NaO_7$ and 17.52 g of NaCl in 1 L water) and transferred to a neutral charge nylon transfer membrane (GE Healthcare model #N00HY00010). The DNA was crosslinked on the membrane using a CL-100 Ultraviolet Crosslinker (UVP).

A radiolabeled probe was synthesized using random primer labeling (Promega, Madison, WI). A total volume of 26 μL containing 100 ng of DNA from the knockout cassette (Colot et al., 2006) was boiled for 5 minutes at 95°C to denature the DNA. The sample was cooled on ice and 10 μL 5x random primer buffer, 4 μL of 4 mg/mL bovine serum albumin (BSA), 3 μL 10x pooled dNTPs without dCTP, 1 μL Klenow DNA polymerase, and 5 μL (50μCi) ^{32}P-dCTP (MP biomedicals, Solon, OH). This probe hybridizes with 2.4 and 1.7 kb fragments in wild type, and 3.0 and 2.1 kb fragments in the Δ*ric8* mutant.

Hybridization solution was made by dissolving 1 mole Na_2HPO_4, 2 mL of 500 mM EDTA, and 70 g of SDS completely in 500 mL water with low heat and stirring. After cooling, 10 g of BSA

was dissolved in the solution, and it was brought to a 1 L final volume. The crosslinked membrane was placed in a hybridization tube with 20 mL of hybridization solution and incubated at 65°C for 1 hour. The radiolabeled probe was added, and the tube was incubated 65°C for an additional 10-14 hours. A wash solution was prepared containing 40 mM Na_2HPO_4, 1 mM EDTA, 5% SDS, and 0.5% PMSF in water, and 20 mL was used in each of two 15 minutes washes. A second wash solution was prepared with 40 mM Na_2HPO_4, 1 mM EDTA, and 5% SDS in water, and this was used to wash two additional times with 20 mL wash solution for 15 minutes with each. Finally, the membrane was exposed to film (BioMax XAR, Kodak Company, Rochester, NY) at -80°C.

Bulk Segregant Analysis

Bulk segregant analysis was performed according to a previous protocol (Lambreghts et al., 2009). The P3-10 strain in the Oak Ridge wild-type background was crossed to the exotic wild-type strain, Mauriceville. More than 200 progeny were picked, and morphologically sorted based on exhibition of the mutant or wild-type phenotype. DNA was extracted from the progeny, alongside Mauriceville and wild-type 74A according to the protocol described in Appendix B (*N. crassa* Phenol:Chloroform DNA Extraction). Aliquots of the DNA from the strains were quantified and checked for purity using 260/280 ratio, and were diluted to reach a concentration of 100 ng/μL (Appendix B). The normalized progeny DNA was then pooled in equal proportions by combining 10 μL of each progeny into a single tube of template DNA.

Analysis of the mutant progeny was performed using primers designed by Lambreghts et al (Lambreghts et al., 2009), and supplied by the Fungal Genetics Stock Center (Table 3.2, FGSC, Kansas City, Missouri). For each sample, 100 ng of genomic DNA was amplified in a 20 μL

standard TAQ PCR reaction with a 30 second 54^{o}C annealing time and a 1 minute extension time (Appendix B). This PCR reaction was performed using each of the primers in Table 3.2 with 74A, Mauriceville, and mutant pool DNA samples. 10 μL of the PCR product was digested with 1-5 units of the corresponding enzyme from Table 3.2, 2 μL of 10x of the appropriate buffer, 0.1 mg/mL BSA if required, and water to reach a final reaction volume of 20 μL. These samples were incubated for three hours at the temperatures indicated in the same table, and then separated on a 1% agarose gel (Appendix B, Gel Electrophoresis). Band intensity was visually compared to both Mauriceville and 74A. When the pooled PCR product for a given SNP displayed no bias or a bias towards the Mauriceville product, no linkage was implied. When the pooled PCR product was skewed in favor of the 74A wild type, a potential linkage with the UV mutation was inferred. Observation that the majority of SNPs on the same linkage group showed a strong Oak Ridge bias provided strong evidence that the linkage group bears the sup mutation.

SNP-CAPS individual mutant mapping.

Upon identification of a specific region for a given mutant, the SNP mapping primers designed by Lambreghts et al. (Lambreghts et al., 2009) were used to probe individual mutants from the pool. The result was not a relative band intensity, but an absolute quantification of what percent of mutants carried a Mauriceville SNP at each location. A reduction in the percentage of Mauriceville SNPs correlated with closer proximity to the mutation of interest.

Mutant-by-mutant analysis also made it possible to resolve the approximate location of individual crossover events. When assessing an individual mutant, a transition from an Oak Ridge form of a SNP to a Mauriceville form of a SNP identified a range in which a crossover

event occurred. These crossover events placed an absolute boundary on where the *sup*^{UV} mutation could exist.

Large Scale DNA & Illumina library preparation.

DNA was extracted using the large scale phenol-chloroform extraction method described in Appendix B. After multiple calibration runs, it was determined that optimal shearing was achieved when 200 μL of 24 μg/mL DNA solution was sonicated in a Biorupter with ice water for 10 minutes on high with a 30 second on/30 second off cycle. This optimal shearing was indicated by a smear of DNA fragments in the 300 to 500 bp range. Multiple tubes were pooled to give a final volume of 600 μL containing 15 μg of total DNA, and then concentrated using a Qiaex II column and re-suspended in 20 μL of water (Appendix B, QiaexII Concentrating). End repair was then performed in a PCR tube by mixing 20 μL DNA, 18.5 μL water, 4 μL 10x T4 DNA ligase buffer with 10 mM ATP, 2.5 μL T4 DNA polymerase from NEB (7.5 units), 0.5 μL of Klenow (exo+) DNA Pol I from NEB (5 units), and 2.5 μL T4 Polynucleotide Kinase from NEB. The mixture was incubated at 20^{o}C for 30 minutes, and then purified by the PCR Purification protocol, re-suspending in a final volume of 32 μL of EB buffer (Qiagen; Appendix B). Next, a poly-A overhang was added by adding 5 μL of 10x Klenow buffer, 10 μL of 1 mM dATP and 2 μL Klenow (exo-) to the tube of DNA, and incubating for 30 minutes at 37^{o}C. To purify this product, a Qiagen Minelute kit was used to remove salts and concentrate the volume down to 10 μL in EB buffer (Appendix B). Adapters (described in Table 3.3) were prepared by mixing the two in a 1:1 ratio (50 μL to 50 μL) and then boiled for 2 minutes, and frozen in aliquots after they had cooled to room temperature. These adapters were then ligated to the ends of the sheared and purified DNA by adding 7 μL of water, 5 μL of T4 ligase buffer, 1 μL of 5 μM adapters, and 2.5 μL of T4

Ligase from NEB to the 10 μL sample of A-tailed DNA. The product of this reaction was run on a 2% NuSieve agarose gel alongside a 100bp step ladder, and the range from 300-500 bp in length was cut out and extracted using the Qiaex II gel extraction kit, ending with a 10mL sample suspended in water. The sample was then amplified using 1 μL of DNA as template in a 25 μL total reaction volume with 0.75 μL of each 5 μM primer (Illumina_Primer_fw and Illumina_Primer_rv, Table 3.3), and run for 18 cycles with a 30 second 65°C annealing temperature, and a 30 second extension time (Appendix B, Phusion PCR). This was repeated multiple times, and five replicates were pooled into a single PCR purification, with a final volume of 20 μL of water (Appendix B). This sample was analyzed on a Nanodrop spectrophomoteter (Fisher Scientific, Wilmington, DE 19810), where it was checked for purity using a 260/280 ratio, and 15 μL of a 56 ng/μL sample was submitted for sequencing with its quantification to allow the sequencing center to dilute to meet their specifications. A 36 bp, unpaired run was performed using an HiSeq2500 sequencer (Illumina, San Diego, CA), and short read data was returned.

Bioinformatics analysis

The short reads generated from Illumina sequencing are output in a FASTQ file (Cock, Fields, Goto, Heuer, & Rice, 2010). The *N. crassa* genome build and the gene annotation files are available for direct download in FASTA format from the Fungal Genetics Stock Center website, www.fgsc.org (Galagan et al., 2003; Pearson, 2014).

The last 2 nucleotides of each read were expunged from the data in addition to any other base calls that exhibited a PHRED score of less than 20 (Ewing & Green, 1998). To assemble the sequenced genome relative to the published genome, the Burrows-Wheeler

Alignment tool (BWA) software was used (H. Li & Durbin, 2010). The output from the BWA algorithm was a Sequence Alignment/ Map (SAM) file, containing the final genome sequence, and an overlay for the reads used to determine each nucleotide in the sequence.

The variations between the Illumina sequenced and assembled genome and the published reference genome were compiled with BWA and output using its mpileup function. This output the locations of all mutations, the type of mutation, and allowed for sorting based on whether the mutation lay within a given gene, and whether it induced a synonymous or non-synonymous mutation. All non-synonymous mutations with PHRED scores greater than 20 in coding DNA in the genomic region established by SNP-CAPS were output, and checked.

Sequencing to confirm the mutation

The two putative mutations in *ham-5* were re-sequenced for confirmation. Primers were designed to amplify a region of 1,000 base pairs or less with the mutation in the center, and Phusion PCR was performed with a 30 second, 55^{o}C annealing temperature, and a 60 second extension time (Table 3.3, Appendix B). The product was amplified and submitted for sequencing in two tubes containing each of the forward and reverse primers (Appendix B). The sequences were aligned using CLC Sequence Viewer (Qiagen, Linburg, Netherlands).

Design and generation of the *ham-5* complementation vector

Complementation of the *sup*^{UV} mutant was initially attempted using a vector carrying the entire *ham-5* gene under its native promoter, designed to integrate ectopically in the *N. crassa* genome. The complementation construct included the pBlueScript II vector, the *bar* selectable marker (Pall, 1993), 1 kb of the promoter region, and the entire *ham-5* ORF.

The complementation construct was built from four distinct pieces. The first was a PCR product bearing 1 kb of the promoter and the first 1 kb of the *ham-5* gene, generated by primers ham-5_1_fw and ham-5_1_rv bearing digestion sites for *Not*I and *Eco*RI respectively. This was amplified from 2 μL of a 1:10 dilution of genomic DNA extracted above from wild type 74A, with an annealing temperature of 67°C for 1 minute, and extension time of 5 minutes using the Phusion PCR protocol with a 50 μL reaction volume (Appendix B). The resulting band was gel purified and subsequently TA-cloned into the pGEMT vector (Promega; Appendix B). DNA was extracted from the *E. coli* strain carrying the recombinant vector using the MiniPrep protocol (Appendix B). The fragment was then digested out of the vector using *Not*I and *Eco*RI enzymes in *Eco*RI buffer at 37°C, and a 4.0 kb fragment was gel extracted from a 1% agarose gel using the Qiaex II protocol (Appendix B). The second fragment was also a PCR product bearing the remainder of the *ham-5* gene, generated from primers ham-5_2_fw and ham-5_2_rv, with digestion sites for *Eco*RI and *Bam*HI, respectively. This fragment was cloned in the same manner as the first fragment, except that the digestion was carried out using *Eco*RI and *Bam*HI, and the final fragment size was 2.7 kb.

The third and fourth fragments came from pre-existing vectors. The pTJK1 vector contains the *bar* marker which confers resistance to Isgnite (Jones, Greer-Phillips, & Borkovich, 2007). The *E. coli* strain with this vector was cultured and DNA was extracted using the Qiagen MiniPrep kit (Appendix B). The vector was digested using *Xba*I and *Bam*HI in NEB buffer 4 at 37°C. The 1 kb fragment bearing the bar reporter gene and the *ccg-1* promoter was then gel purified using a 1% gel (Appendix B). Finally, the pBluescript II vector was extracted from an *E. coli* strain as was performed for pTJK1 (Alting-Mees & Short, 1989). This sample was digested

using *Xba*I and *Not*I in NEB buffer 3 at 37°C, and the 2.9 kb linearized vector fragment was purified after electrophoresis on a 1% agarose gel (Appendix B).

The four products were combined and ligated (Appendix B). The mixture was transformed into chemically competent DH5α *E. coli* cells (Appendix B). Transformants were extracted using boiling minipreps (Appendix B). Diagnostic digests using *Bam*HI, followed by gel electrophoresis resulted in a single 3 kb fragment if pBluescript II alone was present or a 12 kb fragment if all three fragments were combined into the vector (Appendix B). DNA from a transformant with a 12 kb vector was sequenced using BigDye sequencing and confirmed to bear the entire *ham-5* gene and promoter region (Appendix B). The vector was then transformed into the *sup*^{UV} strain, and transformants plated on Ignite medium. Transformants were picked 2-5 days later onto VM+Ignite slants. Transformants were scored for complementation based on whether the strain grew like the initial mutant or more similarly to wild type.

Design and generation of the *ric8*, *ham-5*, and *ham-5*^{trunc} tagged *N. crassa* strains

A vector system designed for high throughput protein-protein interaction testing was the last attempt made to complement the *ham-5* mutants. This system, designed by Colot and Borkovich, is comprised of two vectors with identical multiple cloning sites, bearing either the *inl* auxotrophic marker, S-tag, and RFP (pRS426-inl-S-Tag-RFP) or the *pan-2* auxotrophic marker, V5-tag, and GFP (pRS426-pan-V5-Tag-GFP). Three inserts were prepared to integrate into the vector system: *ham-5*, *ham-5* ^{trunc}, and *ric8*. All were prepared using Phusion PCR. For *ham-5*, primers ham-5-SO-fw and ham-5-SO-rv were used with a 20 second, 60°C annealing step and a 5 minute extension time using the *ham-5* ectopic complementation vector as template. For *ham-5*^{trunc},

primers ham-5-SO-fw and ham-5t-SO-rv were used with a 20 second, 60°C annealing step and a 2 minute extension time using the *ham-5* ectopic complementation vector as template. For *ric8*, primers ric8-SO-fw and ric8-SO-rv were used with a 20 second 60°C annealing step and 2 minute extension time using wild type 74A DNA for (Table 3.3). The *ham-5*, *ham-5*^{trunc}, and *ric8* products were expected to be 5.3, 1.8, and 1.6 kb respectively, and were confirmed by gel electrophoresis (Appendix B). These were gel extracted and quantified by comparison with λ-*Hind*III ladder (Appendix B). Vectors for RFP and GFP were digested using *Bam*HI and similarly gel extracted and quantified. Approximately 300ng of vector and 300ng of insert were used in six yeast recombinational cloning transformations with *URA*3 as the selectable marker: *ham-5* in pRS426-inl-S-Tag-RFP, *ham-5*^{trunc} in pRS426-inl-S-Tag-RFP, *ric8* in pRS426-inl-S-Tag-RFP, *ham-5* in pRS426-pan-V5-Tag-GFP, *ham-5*^{trunc} in pRS426-pan-V5-Tag-GFP, *ric8* in pRS426-pan-V5-Tag-GFP (Appendix B). The transformants were scraped from the plate with a microscope slide and DNA was extracted using the Yeast DNA extraction protocol. The purified DNA was transformed into electrocompetent DH5α *E. coli* (Appendix B).

DNA from transformants was extracted using the Boiling MiniPrep protocols, and diagnostic digests were performed and assessed using gel electrophoresis (Appendix B). All digests contained 5 μL of vector, 0.5 μL of each enzyme, 2.5 μL of NEB Buffer 3, 17 μL water. Digests were incubated for 4 hours at 37°C, and then 5 μL of 6x DNA Loading Dye was added to each sample. Transformants bearing *ham-5* in the GFP vector were digested with *Bgl*II, yielding a 10.6 kb fragment for vector alone, but 10.2, 3.6, 1.2, and 0.6 kb fragments if the vector contained the *ham-5* fragment. Transformants bearing *ham-5* in the RFP vector were digested with *Hind*III which yielded 8.8 and 1.3 kb fragments for vector alone, but 8.8, 3.9, and 2.5 kb fragments if the vector included the *ham-5* fragment. Transformants bearing *ham-5*^{trunc} in the

GFP vector were digested with *Bgl*II which yielded a 10.6 kb fragment for vector alone, but 10.2, 2.1 kb fragments if the vector bore the *ham-5*^{trunc} fragment. Transformants bearing *ham-5*^{trunc} in the RFP vector were digested with *Pst*I and *Xho*I, which yielded a 10.1 kb fragment for vector alone, but 8.4 and 3.5 kb fragments if the vector contained the *ham-5*^{trunc} fragment. Transformants bearing *ric8* in the GFP vector were digested with *Eco*RV, which yielded a 10.6 kb fragment for vector alone, but 8.0 and 4.2 kb fragments if the vector included the *ric8* fragment. Transformants with *ric8* in the RFP vector were digested with *Eco*RV, which yielded a 10.1 kb fragment for vector alone, but 7.7 and 4.0 kb fragments if the vector bore the *ric8* fragment. The full sequences for each of these vectors are presented in Appendix E.

Confirmed vectors were transformed into a *N. crassa mus-51*::*nat*^{R} strain using a voltage of 1800 and plated on VM plus Ignite plates also contained pantothenic acid (GFP) or inositol (RFP). Transformants were picked onto VM+Ignite slants for growth and conidia were then assessed for respective GFP or RFP fluorescence (Appendix B, Fluorescent Microscopy).

Generation of double mutants through sexual crosses

Double mutants between Δ*ric8* and *rgs* or cAMP-related genes were generated by crosses of knockout mutants to the Δ*ric8* Helper strain as described in above section titled "Generating of double mutants through sexual crosses". Genome project-generated primers were used to check progeny for possession of both the Δ*ric8* and second mutation. Over 100 progeny of each cross were picked and tested, and double mutants with Δ*cr-1*, Δ*pde-1*, Δ*rgs-1*, Δ*rgs-2* and Δ*rgs-4* were obtained. Despite picking over 200 ascospores for each of the other three crosses (Δ*rgs-3*, Δ*rgs-5* and Δ*pde-2*), no double mutants were obtained presumably due to linkage and/or viability issues.

Phenotypic analysis of double mutants

Three assays were performed to test the suppression of each double mutant. First, apical extension was assessed by inoculating a VM plate with conidia, and growing the mutant for 48 hours at 25^{o}C in the dark. The distance from the point of inoculation to the edge of the colony was measured for a minimum of three replicates, and the average and standard deviation were calculated. Second, the aerial hyphae growth was measured by inoculating a standing liquid culture containing two mL of liquid VM in an 18x100 mm tube, and incubating the culture for five days at 25^{o}C in the dark. The distance between the top surface of the VM and the top of the hyphae grown up the tube were recorded and the average and standard deviation of at least three replicates were calculated. Finally, female fertility was assessed as described above for the Δ*ham* mutants.

Results

Generation of putative Δ*ric8* suppressor mutants.

In order to generate a mutation which suppressed the defects of the Δ*ric8* mutation UV mutants were screened in high throughput. Tens of thousands of mutants were screened on petri dishes each bearing 20-100 colonies. From these, 46 colonies were picked which exhibited faster growth or less conidiation that the Δ*ric8* mutant alone. 33 of the mutants were picked from VM+Hyg plates, eight from VM plates, and four from FGS plates. From these initial 46, only eight showed improved growth rate when assessed on individual petri dishes for quantitative growth rate, four from FGS plates and four from VM plates.

A single suppressor of the Δ*ric8* mutation was obtained.

The eight mutants displaying hygromycin resistance and improved growth rate were next subjected to southern analysis. Only one mutant, P3 (Δ*ric8*sup^{UV}), displayed a positive Southern result for the Δ*ric8* knockout mutation in addition to the improved growth rate (Figure 3.2). This mutant was originally isolated from a VM plate, and none of the other fast growers from FGS or VM plates displayed the Δ*ric8* genetic background.

Suppressor mutation corrects growth rate and conidiation defects, but not fertility defects.

Upon confirmation that Δ*ric8*sup^{UV} bore the Δ*ric8* genetic background, more phenotypic testing was conducted. The growth rate of the mutant was measured and determined to be 2.5x that of the Δ*ric8* mutant (Figure 3.3). Additionally, hyperconidiation defects caused by the Δ*ric8* mutation (Wright et al., 2011) were over-corrected by the *sup*^{UV} mutation to the point that the

Δ*ric8 sup*^{UV} strain produces almost no conidia. The mutant successfully underwent a sexual cross as a male, but was female-sterile, indicating that the Δ*ric8* defects in the sexual cycle were not corrected by the suppressor mutation.

The *sup*^{UV} single mutant displays similar defects to the *sup*^{UV} Δ*ric8* strain.

To further analyze the mutation, the Δ*ric8 sup*^{UV} strain was crossed to wild type 74A as a male according to the protocol in Appendix B (Sexual Crosses). When picked on VM, four genetically distinct progeny were expected: wild type, Δ*ric8*, *sup*^{UV}, and Δ*ric8 sup*^{UV}. It was expected that wild type would display normal growth, Δ*ric8* extremely reduced growth, Δ*ric8 sup*^{UV} moderate growth, and while the phenotype of *sup*^{UV} alone was unknown and could pool with any of the others or exhibit a distinct fourth phenotype. The expected three classes of progeny were observed, and no fourth class was obtained. Hygromycin sensitivity was screened next, and the pool that grew like the initial Δ*ric8 sup*^{UV} could be subdivided into hygromycin resistant and hygromycin sensitive. The hygromycin sensitive class was the parental Δ*ric8 sup*^{UV}, while the hygromycin sensitive represented the individual *sup*^{UV} mutation.

SNP-CAPS general mapping implicates linkage group II as the location of the *sup*^{UV} mutation.

The isolated suppressor mutant, *sup*^{UV}, was crossed to the exotic wild type, Mauriceville. 250 progeny were picked from this cross, and were divided into wild-type-like and suppressor-like classes. 125 displayed wildtype-like growth, while 120 displayed suppressor-like growth, and five were unviable. DNA was extracted from 115 of the 120 suppressor-like progeny, as well as Oak Ridge and Mauriceville controls, and the samples had an average 260/280 ratio of > 1.7. This purity was sufficient to proceed with PCR and DNA was then amplified and subsequently

digested for each of pool, Mauriceville, and Oak Ridge DNA, and subsequently separated by gel electrophoresis.

The nature of the pooled DNA was compared to both Oak Ridge and Mauriceville DNA for each SNP on each linkage group. As explained above, any bias towards wild type would indicate a possible linkage between the mutation of interest and the SNP assayed. On linkage group one, only one of the 12 SNPs tested exhibited a bias towards wild type, indicating the mutation was not on linkage group one (Figure 3.4). On LGII, six of ten SNPs tested exhibited a bias towards the wild type form of the SNP, strongly suggesting the mutation was on linkage group two (Figure 3.5). On linkage group three none of the nine tested SNPS displayed any bias towards wild type, strongly suggesting that the mutation was not on linkage group three (Figure 3.6). On linkage group four only two of the eight test SNPs displayed any bias towards wild type, making it unlikely linkage group four was linked to the mutation (Figure 3.7). On linkage group five 16 SNPs were tested, but only two displayed a bias towards wild type, indicating that it was probably not linked to the mutation. Analysis of linkage group six revealed that none of the six tested SNPs have any wild type bias, making it highly improbable that the mutation is on linkage group six (Figure 3.8). Finally, linkage group seven only two of eight tested SNPs show a wild type bias, making linkage group seven an unlikely candidate for the location of the mutation (Figure 3.9).

With the SNP-CAPS results providing a strong indication that LGII bore the mutation of interest, all SNPs on LGII were retested in duplicate, and the band intensity was quantified. The relative intensity of the bands was quantified, and results were a stronger indication that LGII was responsible as six of ten again displayed a strong bias towards wild type, one displayed a weak bias towards wild type, one no bias, and only two slight bias towards Mauriceville (Figure

3.12). This information was sufficient to implicate LGII, and rule out a mutation near either of the telomeres based on the unbiased crossover rates near those ends, but no further clarification could be obtained from the pooled DNA.

SNP-CAPS mutant-by-mutant mapping identifies central third of linkage group two as bearing the *sup*^{UV} mutation.

To more precisely map the location of the *sup*^{UV} mutation it was necessary to assay large numbers of individual strains rather than simply a large pool of DNA. The first 44 of the 115 mutant progeny were individually assayed at eight of the SNPs present near the middle of linkage group. As the distance between the mutation and the SNP assayed shrank, it was expected that the frequency of possessing the Mauriceville form of the SNP would decrease as well. The ratios in Table 3.4 show that SNP NC.II.0000226 displayed only a slight bias with 24 of 40 mutants possessing the Oak Ridge form of the SNP. Moving to SNP NC.II.0000185 though resulted in only 7% of the SNPs exhibiting wild type assortment. Looking across the entire chart, it is possible to observe where each crossover event must have taken place based on the transition from a wild type (WT) SNP to a Mauriceville (MV) SNP. This would indicate that progeny number 15 experienced a crossover event between SNP NC.II.0003555 and NC.II.0000381, and thus that the mutation must lie to the right of SNP NC.II.0003555 for the progeny to exhibit both the mutant phenotype and the Mauriceville form of the SNP at that position and all positions further to the left. Conversely, both progeny six and progeny 36 exhibited Mauriceville forms of SNPs at SNP NC.II.0000011, while they exhibit the wild type form of the SNP at NC.II.0000160, indicating a crossover event between these two SNPs. This, combined with the knowledge that the progeny display mutant phenotypes, indicate that the

mutation must lie to the left of SNP NC.II.000001. Putting the data together from both sides, the mutation of interest was thus determined to lie between SNPs NC.II.0003555 and NC.II.0000011 on linkage group II (Table 3.4).

Illumina sequencing identified an insertion leading to a premature stop codon in *ham-5* in the *sup*^{UV} mutant.

Illumina sequencing combined with BWA assembly and SAM Tools visualization efficiently revealed variations between the sequenced genome and the genome of the *sup*^{UV} mutant. Unfortunately, 14521 mutations were observed between the two genomes, far in excess of what could be processed manually. Rough mapping had revealed LGII as the region containing the SNP, but that left 1653 mutations to test. Using the mutant-by-mutant mapping data from SNP-CAPS, this group was rapidly culled to 308. Requiring that mutants exist within exons brought the number down to 51. Finally, requiring the mutation be non-synonymous brought the number to a manageable 25. Of these, 12 were single base transversions, while 13 were insertions or deletions.

Manual analysis of each mutation was then conducted to determine which should be pursued. When viewed in SAM Tools, many called mutations were only substantiated by multiple instances of exactly the same read, suggesting they were derived from a single mistake in PCR at an early cycle, and merely repeated, and reads originating from other positions agreed with the sequenced genome. Others were only supported by the last few nucleotides of various reads, and reads bearing the nucleotide in question near the beginning or middle of the read matched with the reference genome (Table 3.5). Both of these types were presumed to be sequencing or assembly errors and not pursued further. This left only two mutations. The first

was a valine to leucine mutation at residue 1407. It was re-sequenced using Sanger sequencing, and found to result from a sequencing error. The second was the insertion of an adenine base at codon 586 resulting in a premature stop codon less than half way through the gene (Table 3.5, Figure 3.12A). This area was sequenced using the Sanger method, and validated by both forward and reverse sequencing of the gene. Furthermore, re-sequencing of the reference genome revealed that the adenine insertion absent from the initial genetic background (Figure 3.12B).

Hyphal anastomosis in *N. crassa* is a distinct mechanism of sharing genetic information.

Hyphal anastomosis is a cell fusion process in *N. crassa* thatallows adjacent hyphae to join and permits cytoplasmic flow between the two neighboring colonies (Aldabbous et al., 2010; Roca, Arlt, Jeffree, & Read, 2005). When a sexual cross is not feasible because of mutation or growth conditions, this is the only remaining way for *N. crassa* to share genetic information between adjacent colonies. Many mutants have been identified that are unable to perform this kind of cell fusion, and the family of genes responsible has been named "*ham*", in reference to hyphal anastomosis.

Hyphal anastomosis can be categorized into a few groups. One group is those involved in the formation and regulation of the striatin-interacting phosphatase and kinase (STRIPAK) complex (Goudreault et al., 2009). In humans, this group regulates cellular differentiation, but the exact mechanism of control is not fully understood (Kean et al., 2011). This regulation is conserved from human to fungi, where in *S. macrospora*, PRO-22 and PRO-11 function as scaffolds within the STRIPAK complex (Bloemendal et al., 2012). The *N. crassa* homolog for *pro-22* is *ham-2*, and loss of this gene has been shown to induce pleotropic defects, including the fusion defect for which it was named (Xiang, Rasmussen, & Glass, 2002). Similarly, the *pro-11*

homolog in *N. crassa* is *ham-3*, which exhibits defects akin to the *ham-2* mutant, consistent with these functioning together as essential parts of the STRIPAK complex (Simonin, Rasmussen, Yang, & Glass, 2010).

While not linked to the STRIPAK complex, there are other hyphal anastomosis genes that have been associated with signaling activity. HAM-4 possesses a forkhead domain known to bind phosphoproteins (Simonin et al., 2010). The exact role of *ham-5* is somewhat unclear, as experiments in *N. crassa* failed to identify a role in MAPK signaling, while a more thorough analysis in the fungus *Podospera anseria* found links to regulation of MAPK localization (Aldabbous et al., 2010; Jamet-Vierny, Debuchy, Prigent, & Silar, 2007). Finally, hyphal anastomosis genes *ham-6*, *ham-7*, and *ham-8* have been theorized to act in regulating the fusion event itself in *N. crassa* (Fu et al., 2011). The *ham-9* gene is hypothesized to be involved in signaling, due to its possession of a SAM domain, typically associated with protein-protein interactions (Fu et al., 2011). Taken together, this group of hyphal anastomosis mutants represents a diverse family of regulatory genes that exhibit control over the ability of *N. crassa* to undergo fusion through various regulatory pathways.

Morphology of the Δ*ham-5* mutant is consistent with that of Δ*ric8 sup*^{UV}.

Upon identification of the early stop in *ham-5* in the suppressor mutant, the knockout mutant was obtained from the Fungal Genetics Stock Center. The Δ*ham-5* mutant exhibits all the same phenotypic defects as the *sup*^{UV} mutant. The defects include reduced apical extension rate, repressed conidiation, and female infertility. The other defects known of the Δ*ham-5* mutant were also assessed in the *sup*^{UV} mutant. As *ham-5* is a gene essential for hyphal anastomosis, the formation of CATs was analyzed. The *sup*^{UV} mutant mimicked the Δ*ham-5*

mutant in being unable to form CATs, consistent with the hypothesis that the *sup*^{UV} mutant was defective for *ham-5* (Figure 3.13).

Δ*ham-5* and other hyphal anastomosis gene mutations do not suppress the Δ*ric8* defects.

Once *ham-5* was implicated as the possible Δ*ric8* suppressor gene, the immediate question was whether suppression was specific to *ham-5* or a generic trait of hyphal anastomosis mutations. To answer this question, double mutants were made with Δ*ham-5* and other hyphal anastomosis mutants. With *ric8* present on LGI, crosses between a Δ*ric8* strain and another mutant on LGI would require a crossover event in order to generate the double mutant. The *ham-6* and *ham-8* genes are closest to *ric8*, each mapping about 0.1 Mb away.The *ham-4*, *ham-7*, and *ham-9* genes are on LGI, but are all ~1 Mb or more away from *ric8,* making them difficult but feasible to obtain with recombination. The *ham-5* and *ham-3* genes are on LGII, making obtaining double mutants for these genes efficient.

The Δ*ric8* Δ*ham-5* double mutant was generated through sexual crosses between the Δ*ric8* helper strain and Δ*ham-5*. In the cross between Δ*ric8* helper and Δ*ham-5*, the progeny segregated themselves into the three expected phenotypic classes: Δ*ric8*-like, Δ*ham-5*-like, and wild type. PCR analysis of progeny identified two Δ*ric8* Δ*ham-5* double mutants, both from the Δ*ric8*-like phenotypic class. Further phenotypic analysis revealed no correction of defects in the Δ*ric8* background by the loss of Δ*ham-5*, indicating that deletion of *ham-5* does not suppress Δ*ric8* defects.

Simultaneously, Δ*ric8*, Δ*ham-3*; Δ*ric8*, Δ*ham-4*; Δ*ric8*, Δ*ham-7*; and Δ*ric8*, Δ*ham-9* double mutants were generated by sexual crosses between the Δ*ric8* helper strain and the

respective hyphal anastomosis mutant. Similar to the Δ*ric8* Δ*ham-5* strain, three classes of progeny were obtained in each of these mutants (Δ*ric8*-like, wild type strain, and similar to the respective hyphal anastomosis mutant). Also, like the Δ*ham-5* Δ*ric8* double mutant, these mutants did not display any suppression of the Δ*ric8* defects.

Attempts to complement *sup*^{UV} with *ham-5* in *trans* were unsuccessful.

In order to prove that *ham-5* was allelic with *sup*^{UV}, complementation of the initial suppressor mutation was attempted using ectopic integration of the complete *ham-5* gene in the *sup*^{UV} genetic background. A complementation construct containing *ham-5* tightly linked to the Ignite resistance gene *bar* was transformed into Δ*ham-5* and *sup*^{UV} strains. Of more than 100 transformants that displayed ignite resistance none exhibited any evidence of successful complementation of the suppressor defects.

Attempts to generate tagged HAM-5 and HAM-5^{trunc} were unsuccessful.

Constructs were made for *ham*-5 and *ham*-5^{trunc} that would allow for easy integration at the *pan2* or *inl* loci with an epitope and fluorescently tagged form of the protein, amenable to subsequent microscopy and coimmunoprecipitation (Ouyang, Colot, Dunlap, and Borkovich, unpublished). Three independent rounds of transformations were attempted to generate each of the six possible combinations of *ham-5*, *ham-5^{trunc}*, and *ric8* in each GFP and RFP vector. Transformation with vectors bearing *ham-5* and *ham-5^{trunc}* did not produce any transformants with GFP or RFP fluorescence or phenotypic variation. In contrast, transformation with vectors bearing *ric8* produced a strain with GFP fluorescence. This strain displayed diffuse cytoplasmic localization of GFP.

The loss of *pde-1* or *rgs-1* partially suppresses the Δ*ric8* mutant.

Previous studies have demonstrated that regulators of G protein signaling (*rgs*) genes negatively regulate Gα proteins, accelerating the hydrolysis of Gα-GTP back to Gα-GDP (Hollinger & Hepler, 2002). As RIC8 is known to fascilitate GDP for GTP exchange on the Gα subunit, it was expected that the loss of *rgs* would compensate for the loss of *ric8* by allowing Gα-GTP to persist longer in the cell. As there are five RGS proteins with only three Gα subunits, a high degree of redundancy was expected. Thus, when it was observed that only Δ*rgs-1* suppressed the Δ*ric8* defects, it was consistent with RIC8 acting opposite an RGS protein, and the inability of other RGS proteins to suppress indicates either redundancy or regulation unrelated to RIC8 (Figure 3.15).

Apical extension analysis (Figure 3.14A) revealed that Δ*pde-1*, Δ*ric8* grew 25% better than Δ*ric8*. The same assay also showed that the Δ*rgs-2*, Δ*ric8* grows slightly faster than Δ*ric8*, but the difference was not statistically significant. *cr-1* was the only mutation that inhibited growth of Δ*ric8* by more than 50%. Δ*rgs-1*, Δ*ric8* and Δ*rgs-4*, Δ*ric8* both grew slower than the Δ*ric8* mutant. Measurement of aerial hyphae (Figure 3.14B) demonstrated Δ*ric8*, Δ*rgs-1* was the only mutant that grows significantly better than Δ*ric8*. Δ*cr-1*, Δ*ric8* was the only mutant which grew more poorly than Δ*ric8*. All other mutants displayed identical aerial hyphae height to that of Δ*ric8*. Female fertility was assessed for the same five double mutants, and none of the introduced mutations were able to restore female fertility in the Δ*ric8* background.

Discussion

Generation of the *sup*^{UV} mutation using UV mutagenesis was accomplished without selection.

The process of generating suppressor mutants required screening a large number of mutants, and incurred a large number of false positives. The sparseness of suppressors is not unexpected, as mutations must 1) exist in coding or regulator regions of genes, 2) affect a gene related to the initial mutant, and 3) elicit an effect on the organism that corrects the defects of the initial mutation. Given the ease of culturing *N. crassa* and of obtaining spores, scale was not an issue from a materials side, but it increased the possibility of contamination. *N. crassa* spores are easily dispersed, and cultures cannot survive without air flow, requiring that even in closed boxes containers cannot be completely sealed. With a mutant as sick as Δ*ric8*, any other laboratory strain, most of which do carry hygromycin resistance, would grow on any media used for this assay, and grow better than Δ*ric8*, presenting itself as a false positive. There is more labor involved in ruling out one of these false positives than there is in mutating and assaying thousands more spores, making minimizing false positives the most important step in optimizing the protocol. To reduce contamination, the entire project was conducted in a biosafety cabinet rather than a laminar flow hood, and the cabinet was UV sterilized for at least 20 minutes prior to use in addition to the typical ethanol wipe-down to ensure no contamination could come from the hood. Boxes were also ethanol sterilized, and as our incubators are stationary, these boxes were closed before leaving the hood, and then placed at the top of the incubator. Samples were preferentially mutated at times when incubators were in the least use, to minimize the possibility of cross contamination. All of these precautions reduced, but did not eliminate, the presence of contaminants.

The other source of false positives is minor natural variation. The germination of the Δ*ric8* mutant is delayed on average, but spores germinate anywhere from 4 to 8 hours after inoculation, and then can proceed to grow at slightly variable rates. It is not uncommon for a colony of RIC8 to grow asymmetrically because of minor variations, but despite picking dozens of these suppressors, even when these fast-growing regions of an old colony were picked, the phenotype was not carried along to the new plate. It is unclear what the exact mechanism or mechanisms for these variations are, but these phenotypes were not penetrant, as they displayed on one culture, but upon collection, no longer displayed the defect for which they were selected. With a strain as sick as Δ*ric8*, it does not take a significant variation for a mutant to be suspected, but these false suppressors were easier to score by simply regrowing them on a VM plate and comparing them to Δ*ric8*. Thus, efforts to optimize the protocol focused more on eliminating contaminants than addressing the minor natural variations.

The Δ*ric8 sup*^{UV} strain exhibits improved asexual development relative to Δ*ric8*.

Introduction of the *sup*^{UV} mutation in the Δ*ric8* background provides significant but incomplete suppression of the Δ*ric8* defects. As was typical of all previously identified suppressors, asexual defects were corrected, but sexual defects were not. The growth rate improvement was significant, similar to that of the *mcb* mutation. The aerial hyphae defect was actually corrected to the point of displaying a very fluffy morphology, distinct from any of the previous Gα activating mutations. The phenotype was somewhat similar to, but more severe than, the *mcb* mutant, suggesting there could possibly be a link with cAMP metabolism. Additionally, the mutant is essentially aconidial, similar to the *mcb* mutant. Phenotypic data also identified that the *sup*^{UV} mutant could not undergo hyphal anastomosis (Figure 3.13).

Merging of mapping and sequencing produced an optimal balance for mutant identification.

SNP-CAPS mapping was highly effective at narrowing the region containing the *sup*^{UV} mutation. One interesting false trail came from the SNP Nc.II.0004338, which upon further analysis, was found to not be located on LGII. This SNP was originally mapped to the middle of the region suspected to contain the *sup*^{UV} mutant, giving a roughly unbiased result, while its neighbors were almost exclusively of the Oak Ridge form. Once this discrepancy was discovered, it was obvious that LGII bore the mutation. Unfortunately, simply comparing band intensity was of little more use than even more classical mappings, which simply implicate a linkage group. Fortunately, the primers used on a mutant-by-mutant basis were able to reveal a region a little over a Megabase in the middle of the linkage group where the mutation was predicted to reside. The two step process brought the region of interest from an entire 42 Mb genome to about 4 MB of a 4.2 Mb linkage group, to finally only about 1 Mb, reducing the window to less than 3% of the genome.

This narrowing was of great value when sequencing was performed. Having a reference genome, the assembly was not difficult, and the quality of reads obtained was quite good. Unfortunately, it was evident from the over 14,000 predicted variations that targeted analysis was in order. Combining the annotation data with the mapping data reduced this set to a mere 25, which was very manageable. Omitting the mapping would have yielded hundreds, if not a thousand variations, which would require manual follow-up. The one observation from the manual analysis was that an additional piece of data would have been useful from the SAM Tools analysis – how many of the reads used as evidence for a variation were derived from reads with identical start points? These presumably originate from a single early PCR error, and the

small imperfections added up to 23 of the 25 mutants called being easily dismissed manually. In the future, adjusting the algorithm to account for these variations could make whole genome sequencing directly for a single change more practical. In my analysis, only two merited follow up, and assuming a linear scaling, this would mean only 60-70 would require re-sequencing, which might prove less work than the initial SNP-CAPS mapping if the bioinformatics analysis could be sufficiently optimized to reach such a level of accuracy. This however would expose the project to one more possible area of error – not considering the existence of amino acid changes that were both non-synonymous and of insignificant biological effect. It is not unreasonable to think that there could be another amino acid or two that is genuinely mutated somewhere in the genome, but these may have no biological effect, and SNP-CAPS effectively eliminates any that are not in the immediate proximity of the mutant of interest, while a purely bioinformatics approach would give no such guidance. For this reason, the merging of a mapping technique with a sequencing technology and subsequent bioinformatics workup appears to have yielded the ideal balance of rapid data generation, with some biological evidence to narrow the search region.

Hyphal anastomosis gene knockout mutations do not suppress the defects of Δ*ric8*.

Most surprisingly, the implicated Δ*ham-5* knockout mutation failed to suppress the defects of Δ*ric8* in the Δ*ham-5* Δ*ric8* double mutant. The inability to complement any of the Δ*ric8* defects when the *sup*^{UV} mutation complemented growth rate, aerial hyphae production, and conidial production contradicted the initial hypothesis that the *sup*^{UV} mutation presumed to be *ham-5*^{trunc} mimicked a *ham-5* null mutant. At the same time, the *sup*^{UV} mutant was tested for its ability to undergo hyphal fusion and found to behave like the Δ*ham-5* mutant in its inability

to form the hyphal fusion structure of conidial anastomosis tubes (CATs) (Figure 3.13) It was suggested that Δ*ric8* could be a hyper-fusion mutant, which is reasonable, considering it grows and germinates slowly, yet forms CATs normally (Eaton et al., 2012). Testing of the Δ*ric8 sup*^{UV} mutant revealed that it still produced CATs, consistent with Δ*ric8* suppressing the inability of a *ham* mutant to undergo fusion. Unfortunately, the Δ*ric8* Δ*ham-5* mutant was unable to form CATs, similar to the published results for Δ*ham-5* (Aldabbous et al., 2010). A new hypothesis was that the truncated form of the gene may have a dominant effect in *trans* to the wild-type allele. Testing of this hypothesis requires further study.

The majority of hyphal anastomosis genes reside on LGI with *ric8*, making many of the crosses impractical. Nonetheless, mutants from each loosely affiliated group were able to be tested in relation to Δ*ric8*. From the STRIPAK complex, Δ*ham-3* Δ*ric8* did not grow any better than the Δ*ric8* mutant, suggesting that disrupting the STRIPAK complex could not suppress Δ*ric8* defects. Similarly, loss of the forkhead domain containing *ham-4* did not correct any defects in the Δ*ric8* background. The loss of *ham-7* was also not able to correct any of the Δ*ric8* defects. Finally, removing the SAM domain gene *ham*-9 did not correct Δ*ric8* defects. Putting all these results together, it would be expected that while RIC8 has a functional role linked to *ham-5*, its role is not intertwined with general hyphal anastomosis, as none of the null mutants unable to undergo hyphal anastomosis were capable of correcting the Δ*ric8* defects.

Failed ectopic complementation with *ham-5* suggests a size limitation or dominant *sup*^{UV} allele.

The inability to complement the *sup*^{UV} mutation could stem from an issue of dominance. Because the mutant was obtained by UV mutagenesis of harvested macroconidia, it is probable

the mutation occurred in a cell that was multinucleate. There is a possibility that a few microconidia were formed as well, or that a conidium experienced the statistically unlikely event of having a single nucleus, but it is far more probable that the mutation occurred in a single nucleus, and exhibited a dominant phenotype. This would lead to the hypothesis that it may not be possible to complement the *ham-5* mutation by simply inserting a complete copy alongside the existing mutated copy. Whatever the underlying cause may be, complementation using ectopic integration proved unsuccessful, making it necessary to pursue alternative methods to validate the identity of the *sup*^{UV} mutation.

Results from attempts to produce strains with tagged *ham-5*, *ham-5trunc*, and *ric8* replicated RIC8 localization data, but was uninformative regarding the relationship between *ham-5* and *ric8*.

To eliminate the variable regarding whether *ham-5*^{trunc} was a dominant allele, a different approach was used that would also expand the possible follow-up experiments. Both full length and truncated *ham-5* were transformed into a wild-type genetic background. The system allows for colocalization and coimmunopreciptation experimentation, so full length *ric8* was also integrated into the same vector system. No successful transformants were obtained for any form of *ham-5*, making it impossible to prove or disprove the hypothesis of *sup*^{UV} being *ham-5*. The system had successfully been used in other experiments, and even in this study a strain bearing *ric8* tagged with GFP was obtained, indicating the system was functional. This strain was analyzed and found to confirm the previous data that RIC8 is localized throughout the cytosol.

Suppression of Δ*ric8* by Δ*pde-1* and Δ*rgs-1* further validate the role of *ric8* in regulating Gα-GTP levels and cAMP levels.

cAMP signaling has been shown to be positively regulated by RIC8 proteins, so it is expected that the loss of *ric8* would have effects reflecting a reduction in cAMP. Consistent with this theory, loss of *cr-1*, the adenylylcyclase that converts AMP to cAMP, exacerbated the defects of the Δ*ric8* mutant, presumably by bringing low levels of cAMP down to zero. Conversely, loss of phosphodiesterases, which degrade cAMP would allow the cellular levels in *ric8* mutants to increase back towards those in wild type. This effect was not as dramatic as that of the *rgs* suppressor, but there was a positive effect on growth rate in the Δ*pde-1*, Δ*ric8* mutant, consistent with the model in Figure 3.15.

Future Directions

The primary objective of this aim was to identify suppressors of Δ*ric8*, and three were successfully identified. The subsequent hypothesis that *ham-5* functions in conjunction with *ric8*, remains inconclusive and is a point of ongoing research. The SNP-CAPS, Illumina sequencing, Sanger sequencing, and morphological character of the mutant all strongly point the *sup*^{UV} mutant being a mutation within the *ham-5* gene and relating functionally to hyphal anastomosis. The inability of the Δ*ric8* Δ*ham-5* double mutant to grow any better than the Δ*ric8* mutant indicate that if such a relationship exists, it must be related to an at least partially functional truncated form of *ham-5* rather than a total loss of the *ham-5* function. One attempt to prove this was undertaken, but it is possible that the protein is significantly affected by the addition of an epitope and fluorescent tag. Testing of a *ham-5*^{trunc} construct in a different vector system without any tags could be used to test this hypothesis. Furthermore, the relationship

between RIC8 and HAM-5 could be assessed for direct interaction using the yeast two hybrid system and this approach is already underway. The use of tagged vectors was intended to be used to assess any interaction between the two proteins, but as the tag may be what prevented the protein from functioning, other means may be necessary where the viability of the strain is not contingent on the function of the protein. Additionally, a yeast two hybrid screen using the HAM-5 protein as bait could establish what proteins are functionally interacting with it. The results from double mutants demonstrated that RIC8 is involved with both cAMP regulation and Gα-GTP regulation. The redundancy of the RGS proteins would suggest that making double mutants of these in the Δ*ric8* genetic background could reveal additional *rgs* genes genetically related to *ric8*. Also, given the proximity of *ric8* and some *rgs* genes, transformation with a *nat*^{ri} or *bar*^{r} knockout construct could be more effective at obtaining the other mutants. With respect to cAMP metabolism, it is now evident that the next step would be to measure cAMP levels in Δ*ric8* mutants. This signaling molecule is strongly implicated by literature on G protein regulation, and by evidence from this study and others regarding cAMP related and regulated genes.

Table 3.1: *N. crassa* strains used in Chapter 3.

Strain	Relevant genotype	Comment(s)	Source or Reference
74A-OR23-1A (74A)	Wild type, *mat A*	FGSC[a] #987	FGSC
74a-OR8-1a (74a)	Wild type, *mat a*	FGSC #988	‘’
Δ*ric8*	Δ*ric8*::*hph*$^{+}$, *mat a*		Wright 2011
Δ*ric8* Helper	Δ*ric8*::*hph*$^{+}$, *his3*::*a*^{m1}, *mat A*		Wright 2011
Δ*ric8 sup*^{P3}	Δ*ric8*::*hph*$^{+}$, *sup*^{UV}, *mat a*		This study
P3-10	*sup*^{UV}, *mat A*		“
Mauriceville	Wild type, *mat A*		FGSC
Δ*ham-3*	Δ*ham-3*::*hph*$^{+}$, *mat a*	FGSC #11300	“
Δ*ham-4*	Δ*ham-4*::*hph*$^{+}$, *mat a*	FGSC #12080	“
Δ*ham-5*	Δ*ham-5*::*hph*$^{+}$, *mat a*	FGSC #15045	“
Δ*ham-7*	Δ*ham-7*::*hph*$^{+}$, *mat a*	FGSC #13775	“
Δ*ham-9*	Δ*ham-9*::*hph*$^{+}$, *mat a*	FGSC #19549	“
Δ*ric8* Δ*ham-3*	Δ*ric8*::*hph*$^{+}$, Δ*ham-3*::*hph*$^{+}$, *mat a*		This Study
Δ*ric8* Δ*ham-4*	Δ*ric8*::*hph*$^{+}$, Δ*ham-4*::*hph*$^{+}$, *mat a*		“
Δ*ric8* Δ*ham-5*	Δ*ric8*::*hph*$^{+}$, Δ*ham-5*::*hph*$^{+}$, *mat a*		“
Δ*ric8* Δ*ham-7*	Δ*ric8*::*hph*$^{+}$, Δ*ham-7*::*hph*$^{+}$, *mat a*		“
Δ*ric8* Δ*ham-9*	Δ*ric8*::*hph*$^{+}$, Δ*ham-9*::*hph*$^{+}$, *mat a*		“
Δ*ham-5 his3*$^{-}$	Δham-5::hph^{+}, his3, *mat A*		“
Δ*mus51*	Δ*mus-51*::*nat*$^{+}$		Ouyang, Unpublished
Δ*cr-1*	Δ*cr-1*::*hph*$^{+}$, *mat a*	FGSC #11514	FGSC
Δ*pde-1*	Δ*pde-1*::*hph*$^{+}$, *mat a*	FGSC #11432	“
Δ*pde-2*	Δ*pde-2*::*hph*$^{+}$, *mat a*	FGSC #11430	“
Δ*rgs-1*	Δ*rgs-1*::*hph*$^{+}$, *mat a*	FGSC #12372	“
Δ*rgs-2*	Δ*rgs-2*::*hph*$^{+}$, *mat a*	FGSC #21981	“
Δ*rgs-3*	Δ*rgs-3*::*hph*$^{+}$, *mat a*	FGSC #11421	“
Δ*rgs-4*	Δ*rgs-4*::*hph*$^{+}$, *mat a*	FGSC #12406	“
Δ*rgs-5*	Δ*rgs-5*::*hph*$^{+}$, *mat a*	FGSC #13651	“
Δ*ric8* Δ*cr-1*	Δ*ric8*::*hph*$^{+}$, Δ*cr-1*::*hph*$^{+}$, *mat a*		This study
Δ*ric8* Δ*pde-1*	Δ*ric8*::*hph*$^{+}$, Δ*pde-1*::*hph*$^{+}$, *mat a*		“
Δ*ric8* Δ*rgs-1*	Δ*ric8*::*hph*$^{+}$, Δ*rgs-1*::*hph*$^{+}$, *mat a*		“
Δ*ric8* Δ*rgs-2*	Δ*ric8*::*hph*$^{+}$, Δ*rgs-2*::*hph*$^{+}$, *mat a*		“
Δ*ric8* Δ*rgs-4*	Δ*ric8*::*hph*$^{+}$, Δ*rgs-4*::*hph*$^{+}$, *mat a*		“

[a]FGSC, Fungal Genetics Stock Center, Kansas City, MO

Table 3.2: SNP-CAPS primers.

Well	SNP ID	LG	Enzyme	Well	SNP ID	LG	Enzyme
A2	Nc.I.0000746	1	Tsp509I	G6	Nc.III.0000161	3	MseI
A4	Nc.I.0000153	1	Tsp509I	G7	Nc.III.0000492	3	MseI
C2	Nc.I.0000801	1	BstUI	A12	Nc.IV.0000694	4	Tsp509I
C4	Nc.I.0000801	1	BstUI	E5	Nc.IV.0000722	4	NlaIII
C5	Nc.I.0000087	1	ApoI	E6	Nc.IV.0000048	4	NlaIII
D2	Nc.I.0000200	1	AluI	E12	Nc.IV.0003963	4	MspI
D8	Nc.I.0001959	1	MboI	F5	Nc.IV.0000408	4	RsaI
D10	Nc.I.0001959	1	MboI	G8	Nc.IV.0000607	4	MseI
E1	Nc.I.0000792	1	NlaIII	G9	Nc.IV.0000686	4	MseI
E10	Nc.I.0000006	1	MspI	G10	Nc.IV.0000252	4	MseI
F10	Nc.I.0001098	1	MseI	B7	Nc.V.0000834	5	TaqI
F12	Nc.I.0000118	1	MseI	B8	Nc.V.0001366	5	TaqI
A6	Nc.II.0000185	2	Tsp509I	B9	Nc.V.0000052	5	TaqI
A8	Nc.II.0000480	2	Tsp509I	B10	Nc.V.0000691	5	TaqI
C9	Nc.II.0000160	2	HaeIII	D7	Nc.V.0000273	5	MboI
E3	Nc.II.0000355	2	NlaIII	D9	Nc.V.0000438	5	MboI
E4	Nc.II.0000381	2	NlaIII	E7	Nc.V.0000509	5	NlaIII
F2	Nc.II.0000802	2	Eco0109I	F6	Nc.V.0000012	5	RsaI
F4	Nc.II.0004341	2	HhaI	G2	Nc.V.0000200	5	MseI
F9	Nc.II.0003253	2	MseI	H1	Nc.V.0005860	5	MseI
G1	Nc.II.0000226	2	MseI	H2	Nc.V.0006254	5	MseI
G3	Nc.II.0004338	2	MseI	H3	Nc.V.0006252	5	MseI
G4	Nc.II.0003921	2	MseI	H4	Nc.V.0000200	5	MseI
A9	Nc.III.0003985	3	Tsp509I	H5	Nc.V.0000600	5	MseI
A10	Nc.III.0000331	3	Tsp509I	B5	Nc.VI.0000161	6	Tsp509I
C3	Nc.III.0000072	3	BstUI	D6	Nc.VI.0000168	6	AluI
C7	Nc.III.0000262	3	ApoI	D12	Nc.VI.0000421	6	MboI
C10	Nc.III.0000445	3	HaeIII	E8	Nc.VI.0000039	6	NlaIII
D5	Nc.III.0000020	3	AluI	H6	Nc.VI.0000095	6	MseI
F3	Nc.III.0000238	3	AccI	H7	Nc.VI.0000005	6	MseI
G5	Nc.III.0000409	3	MseI				

Table 3.3: General primers used in Chapter 3.

Gene	Primer Name	Sequence (5'-3')	Template
Generic	*Illumina_Adapter_1*	GATCGGAAGAGCTCGTATGCCGTCTTCTGCTTG	
Generic	*Illumina_Adapter_2*	ACACTCTTTCCCTACACGACGCTCTTCCGATCT	
Generic	*Illumina_Primer_fw*	AATGATACGGCGACCACCGAGATCTACACTCTTTCCCTACACGACGCTCTTCCGATCT	P3-10 gDNA*
Generic	*Illumina_Primer_rv*	CAAGCAGAAGACGGCATACGAGCTCTTCCGATCT	P3-10 gDNA
ham-5	ham-5_VL_fw	CCGAAGTCGATCCAGTGTCTCC	P3-10 gDNA
ham-5	ham-5_VL_rv	ATGGTTCCTGGCAGGGGGTGAG	P3-10 gDNA
ham-5	ham-5_A_fw	GTTCACCAAAAGCCGTCTGC	P3-10 gDNA
ham-5	ham-5_A_rv	ACGTAGATCTCAATCGCATCG	P3-10 gDNA
ham-5	ham-5_1_fw	GCGGCCGCTGCTACCATTGACACACATCGATGC	wt 74A gDNA
ham-5	ham-5_1_rv	GGTAATAAGCTTAAGGGCCGAATTCTTCG	wt 74A gDNA
ham-5	ham-5_2_fw	CGAAGAATTCGGCCCTTAAGCTTATTACC	wt 74A gDNA
ham-5	ham-5_2_rv	GGATCCTTAGATCATCTCACTATGATGCAAC	wt 74A gDNA
ham-5	ham-5-SO-fw	ACCCCTCACATCAACCAAATCTAGAATGTCGGTCCCCGGACACATCTCGA	wt 74A gDNA
ham-5	ham-5-SO-rv	TCCGCCGCCTCCGCCCTTAATTAAGATCATCTCACTATGATGCAACCCC	ham-5 ectopic vector
ham-5	ham-5t-SO-rv	TCCGCCGCCTCCGCCCTTAATTAAGACGATGTCATGTTCTCTGATCCCA	ham-5 ectopic vector
ric8	ric8-SO-fw	ACCCCTCACATCAACCAAATCTAGAATGGCCTCAATAGGAGTTTCTGGGC	wt 74A gDNA
ric8	ric8-SO-rv	TCCGCCGCCTCCGCCCTTAATTAAGTCCGAATCCTCTTCGTAGTCGTCG	wt 74A gDNA
hph	hph_end_fw	CGCCCCAGCACTCGTCCGAGGGC	cross progeny
ric8	ric8_1kb_5UTR	GGGAGAGCTACACTAGATGG	cross progeny
ham-3	ham-3_1kb_5'	CTGCATCGCAATCCCGTCGC	cross progeny
ham-4	ham-4_1kb_5'	CAGGGGCGGGGACTACCAGT	cross progeny
ham-5	ham-5_1kb_5'	GGGCAACTAGGCCCCGAAATC	cross progeny
ham-7	ham-7_1kb_5'	GACGGTCCCCCGACTTTGGC	cross progeny
ham-9	ham-9_1kb_5'	TCGAGGACACCATCCGGGCT	cross progeny
cr-1	cr-1_1kb_5'	GGCCCTGGCAGTCAGGTTGC	cross progeny
pde-1	pde-1_1kb_5'	AAGAGGGTGTGAGAACTTGG	cross progeny
pde-2	pde-2_1kb_5'	AGAGTGGGCGGGTTTGCTGC	cross progeny
rgs-1	rgs-1_1kb_5'	CCCGGCTCTTTGTCAGGCCC	cross progeny
rgs-2	rgs-2_1kb_5'	CCACCACACCACAACACAACACG	cross progeny
rgs-3	rgs-3_1kb_5'	TACTCGCGGGCGACAACGTC	cross progeny
rgs-4	rgs-4_1kb_5'	GCCCTGCGTGTACAAAACGAGGA	cross progeny
rgs-5	rgs-5_1kb_5'	GGATGTCACCCCCGCAAAGCA	cross progeny

*gDNA = genomic DNA

Table 3.4: Fine mapping of linkage group two.

		SNP ID (Nc.II.000___)							
		0226	**0185**	**3253**	**3555**	**0381**	**0160**	**0011**	**3921**
Oak Ridge		26	25	42	34	43	43	39	40
Mauriceville		14	2	1	1	0	0	2	3
Total		40	27	43	35	43	43	41	43
% Oak Ridge		**65%**	**93%**	**98%**	**97%**	**100%**	**100%**	**95%**	**93%**
	1	MV	-	OR	-	OR	OR	OR	OR
	2	MV	-	OR	-	OR	OR	OR	OR
	3	MV	-	OR	OR	OR	OR	OR	OR
	4	MV	-	OR	OR	OR	OR	OR	OR
	5	MV	-	OR	OR	OR	OR	OR	OR
	6	MV	MV	MV	MV	OR	OR	OR	OR
	7	MV	MV	OR	OR	OR	OR	MV	MV
	8	MV	OR	OR	-	OR	OR	-	OR
	9	MV	OR	OR	OR	OR	OR	MV	MV
	10	MV	OR	OR	OR	OR	OR	OR	MV
	11	MV	OR	OR	OR	OR	OR	OR	OR
	12	MV	OR	OR	OR	OR	OR	OR	OR
	13	MV	OR	OR	OR	OR	OR	OR	OR
	14	MV	OR	OR	OR	OR	OR	OR	OR
	15-40	OR	OR	OR	OR	OR	OR	OR	OR

Each SNP number in row two completes the name from row one (i.e. 0226 is SNP Nc.II.0000226). The Oak Ridge row is the count of mutants displaying the Oak Ridge form of the given SNP, while the Mauriceville row is the count of the mutants displaying the Mauriceville form of the SNP. The % Oak Ridge gives the bias of the SNP towards Oak Ridge, with anything over 50% indicating a linkage. 26 of the mutants displayed Oak Ridge SNPs for this entire region, and are summarized in the bottom line with OR to indicate Oak Ridge designating each SNP. All mutants possessing at least one Mauriceville SNP are arbitrarily numbered 1 to 14 and displayed individually. For these, the yellow highlighted MV indicates the existence of a Mauriceville form of a SNP, while a – indicates an inconclusive PCR reaction. SNP Nc.II.0000185 proved to be less reliable, as nearly a full third of PCR reactions failed, but SNPs on either side had revealed the mutation lied to the right of this SNP, rendering re-amplification of this region unnecessary. Ultimately, the crossover event in each of these progeny can be observed to have taken place between any adjacent OR and MV SNPs, indicating that the mutation must lie between SNPs Nc.II.0003555 and Nc.II.0000011.

Table 3.5: Mutations identified by Illumina sequencing

LG	Position	Type	Orig	Mut	Phred Score	Seq Error	NCU	Change?	Conclusion
2	1671665	TV	A	T	33.1	Yes			
2	1938883	TV	C	T	34.8	Yes*	6786	V → L	seq. error
2	2167941	TV	A	G	28.5	Yes			
2	2851597	TV	T	C	46.3	Yes			
2	2851670	TV	T	C	24.5	Yes			
2	2852620	TV	C	G	209	Yes			
2	2853702	TV	C	G	122	Yes			
2	2853708	TV	G	T	134	Yes			
2	2853779	TV	C	A	148	Yes			
2	2853789	TV	A	G	84	Yes			
2	2899026	TV	A	T	190	Yes			
2	3222710	TV	T	C	139	Yes			
2	1727884	InDel	AT	ATT	156	Yes			
2	1798140	InDel	CTTT	CTTTT	214	Yes			
2	2057920	InDel	ATT	ATTT	214	Yes			
2	2176793	InDel	T	TC	129	Yes			
2	2279714	InDel	AT	ATT	103	Yes			
2	2281764	InDel	CTTT	CTTTT	214	Yes			
2	2435866	InDel	GA	GAA	215	NO	1789	Early Stop	validated
2	2642712	InDel	A	AG	146	Yes			
2	2720297	InDel	C	CG	70.5	Yes			
2	2760741	InDel	AG	AGG	214	Yes			
2	2835635	InDel	G	GT	214	Yes			
2	2852552	InDel	AGGGGGG	AGGGG	214	Yes			

The LG column indicates the Linkage Group that contained the variation. Position identifies the location within that linkage group. The two types of mutations analyzed were transversions (abbreviated TV) and insertions or deletions (abbreviated InDel), all located within exons. The Phred score is the output of the confidence of the assembly being accurate for each mutation. Any score over 20 is considered a decent quality call, and all here display Phred qualities in excess of the minimum threshold. Upon identification of a mutation, each was checked against mRNA data and the latest build of the genome, and only two were identified as mutations, while all others were found to be assembly or PCR errors. When the C to T transversion at position 1938883 was analyzed for its translational effect, it was found to result in a change from valine to leucine. While unlikely to induce a significant functional change, the region was sequenced, and in this instance the variation was found to arise from a sequencing error in the Illumina sequencing. This was not entirely unexpected, as the Phred score was significant enough to pursue, but not nearly as high of confidence as most other observed putative variations. The insertion of an extra A at position 2435866 was analyzed and determined to induce an early stop shortly after the mutation. Upon sequencing, this mutation was confirmed by traditional sequencing methodology, consistent with the high Phred score for the mutant identification.

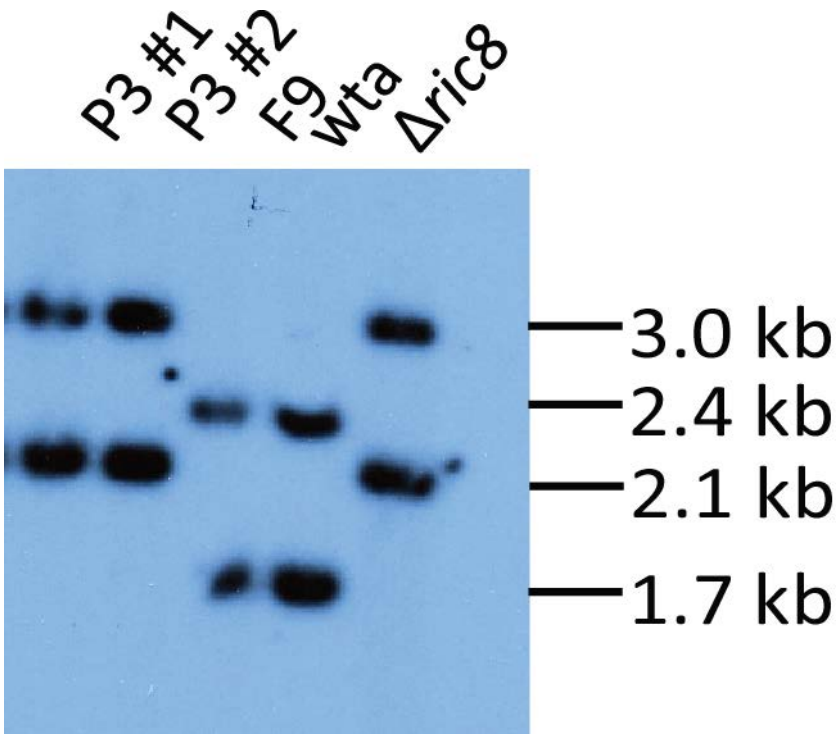

Figure 3.1: Southern analysis confirms *sup*^{UV} is a homokaryon in the Δ*ric8* genetic background. Two independent samples from the *sup*^{UV} named P3 were run alongside another putative mutant F9 as well as wild type and Δ*ric8* controls. The Southern gives 2.4 and 1.7 kb bands for wild type and 3.0 and 2.1 bands for Δ*ric8*. The P3 mutant was confirmed as a homokaryon of Δ*ric8*, while F9 was revealed to be a contaminant bearing the wild-type form of the *ric8* gene.

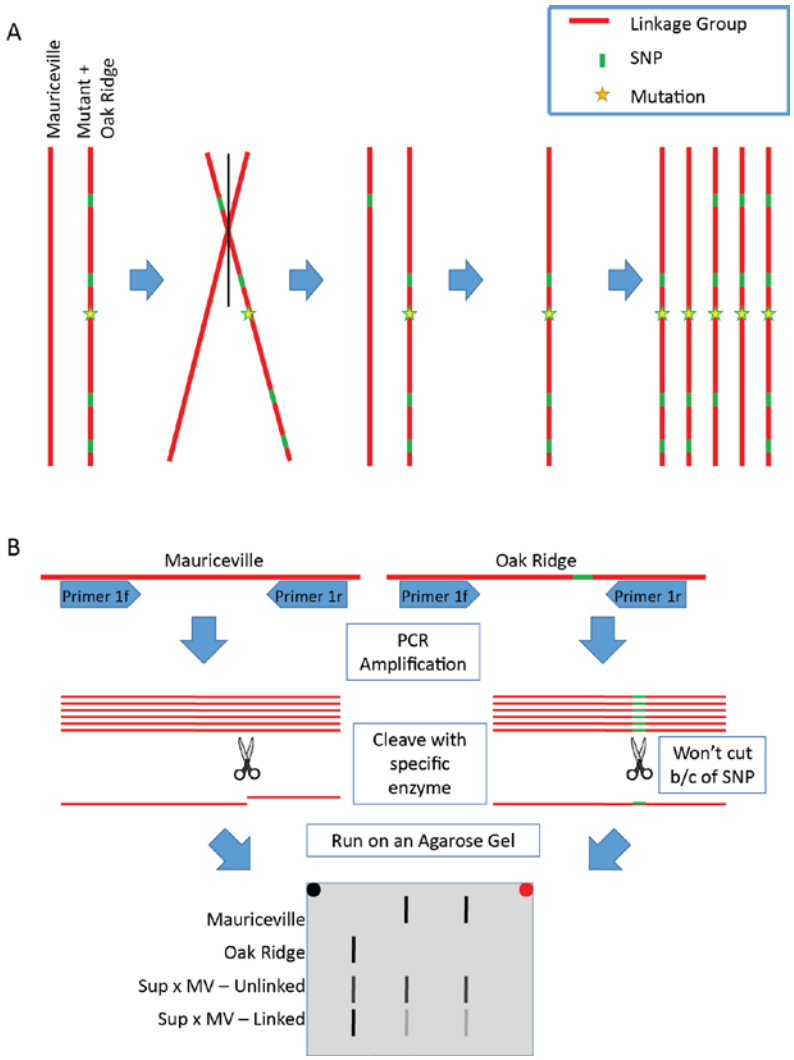

Figure 3.2: Summary of the SNP-CAPS method to map mutations. A: An Oak Ridge *N. crassa* strain bearing a mutations is crossed to the exotic wild-type strain Mauriceville, which is morphologically identical to Oak Ridge, but carries numerous distinct SNPs (shown by green bars) in its background. Crossover events occur naturally throughout the genome during meiosis. With the mutation (star) being selected, SNPs which occur on unlinked linkage groups (red line) will exist in equal quantities for both SNP forms. SNPS on the same linkage group as the selected mutation will show a bias towards the Oak Ridge form over the Mauriceville form, and the degree of the bias will be directly proportional to the distance between the SNP and the mutation responsible for the phenotype. B: After pooling more than 100 of the progeny with the mutant phenotype, unique primers surrounding individual SNPs are used to amplify 96 different loci, and then a digestion enzyme that targets the site of the SNP is used. These are chosen in such a way that one form of the SNP will be cleaved by the digestion enzyme, while the other will not, resulting in distinct banding patterns. The ratio of intensities between the Mauriceville and Oak Ridge products can be used to identify any bias in the products, and with the crossover rates described in A, can be used to identify whether the SNP is linked to the mutation, and if so, the degree of linkage.

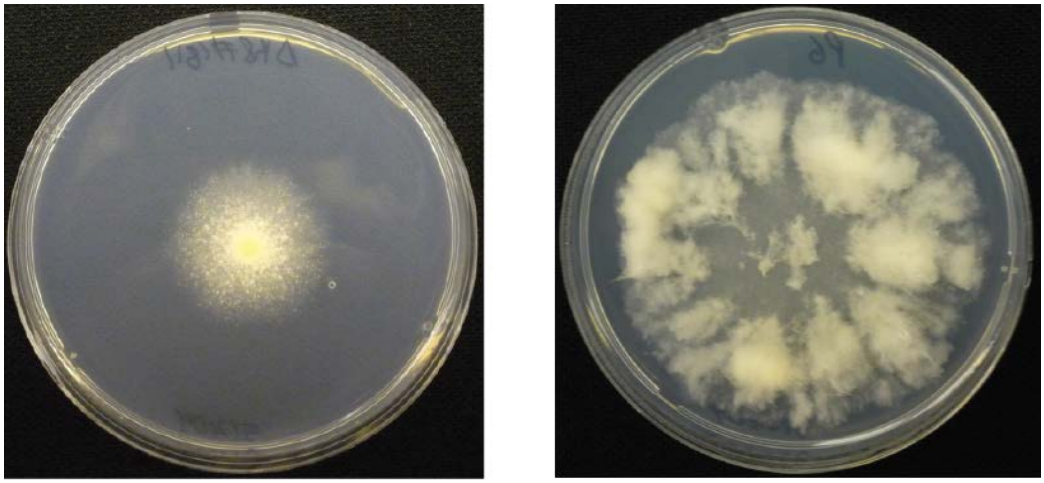

Figure 3.3: The UV generated mutant *sup*^{UV} suppresses the defects of the Δ*ric8* background. Both panels are 96 hour cultures on VM plates grown at 25°C. The Δ*ric8* mutant is on the left and the *sup*^{UV} mutation in the Δ*ric8* background on the right. The *sup*^{UV} mutation causes a 2.5x increase in growth rate in the Δ*ric8* background. Additionally, the hyperconidiation defects of the Δ*ric8* mutant are corrected by *sup*^{UV}. Finally, production of aerial hyphae is restored by the *sup*^{UV} mutation.

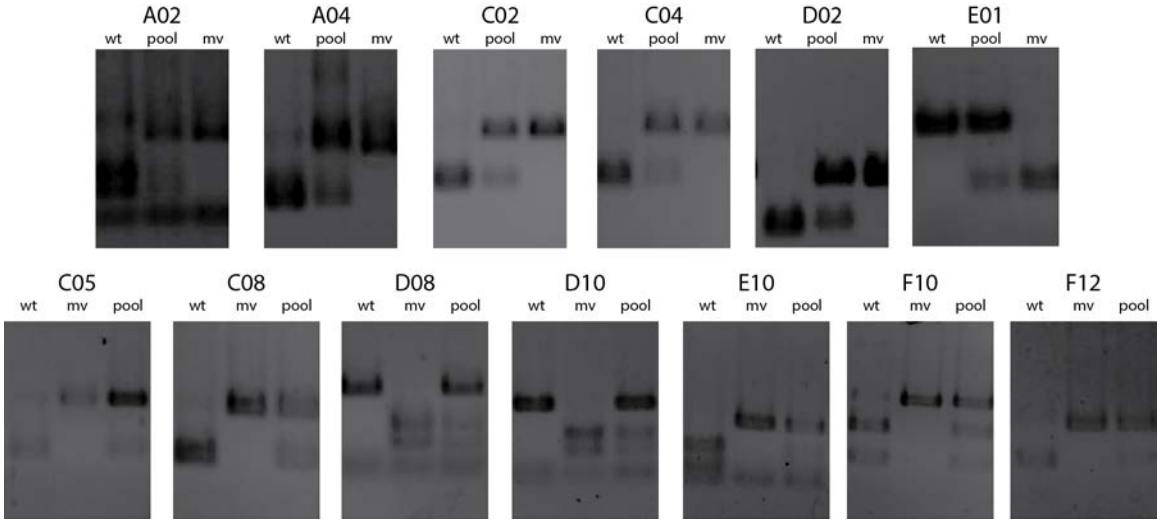

Figure 3.4 SNP-CAPS analysis of LGI of *sup*^{UV} relative to wild type 74A and Mauriceville. PCR was performed on all samples, with the same quantity of template DNA, annealing temperature, annealing time and extension time. Samples were separated on a 1% agarose gel. Samples in the top panel have lanes arranged in the wild type 74A (wt), pool, and Mauriceville (mv) order, while the bottom panel is arranged wild type 74A (wt), Mauriceville (mv), and pool. If the mutation selected for in the pooled DNA was on LGI a bias towards the wild type PCR product will be evident. SNPs A02, A04, C02, D02, C05, C08, D08, D10, E10, F10, and F12 all display either no bias or slight bias towards the Mauriceville product. Only SNP E01 displayed bias towards wild type. The observation that 11 out of 12 samples did not display a bias towards wild type is consistent with the mutation not being located on LGI.

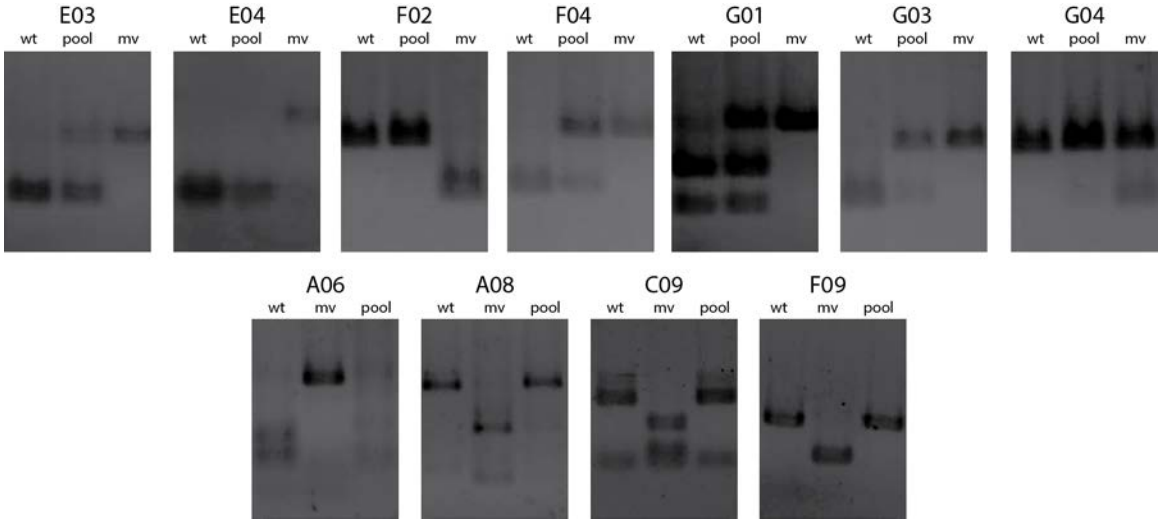

Figure 3.5 SNP-CAPS analysis of LGII of *sup*^{UV} relative to wild type 74A and Mauriceville. PCR was performed on all samples, with the same quantity of template DNA, annealing temperature, annealing time and extension time. Samples were separated on a 1% agarose gel. Samples in the top panel have lanes arranged in the wild type 74A (wt), pool, and Mauriceville (mv) order, while the bottom panel is arranged wild type 74A (wt), Mauriceville (mv), and pool. SNPs F04, G01, G03, and A06 either display no bias or a bias towards Mauriceville. Conversely, SNPs E03, E04, F02, A08, C09, and F09 all display strong bias towards wild type. This ratio of 60% of mutants displaying a strong bias towards wild type is consistent with the *sup*^{UV} mutation present on LGII.

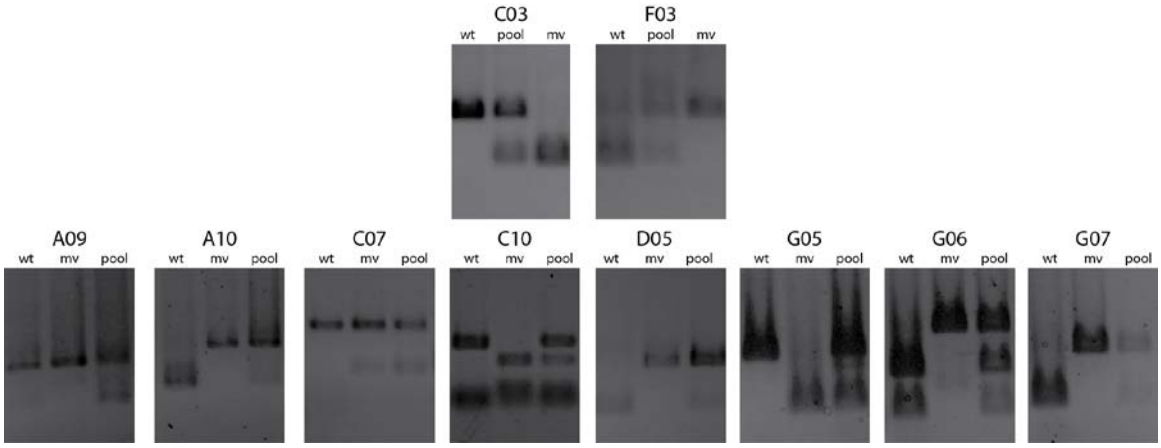

Figure 3.6 SNP-CAPS analysis of LGIII of *sup*^{UV} relative to wild type 74A and Mauriceville. PCR was performed on all samples, with the same quantity of template DNA, annealing temperature, annealing time and extension time. Samples were separated on a 1% agarose gel. Samples in the top panel have lanes arranged in the wild type 74A (wt), pool, and Mauriceville (mv) order, while the bottom panel is arranged wild type 74A (wt), Mauriceville (mv), and pool. SNPs C03, F03, A10, C07, C10, D05, G05, G06 and G07 all display either no bias or a bias towards Mauriceville. No SNPs display strong bias towards wild type. With a 100% of SNPs not displaying any bias towards wild type it is a reasonable conclusion that the *sup*^{UV} mutation is not located on LGIII.

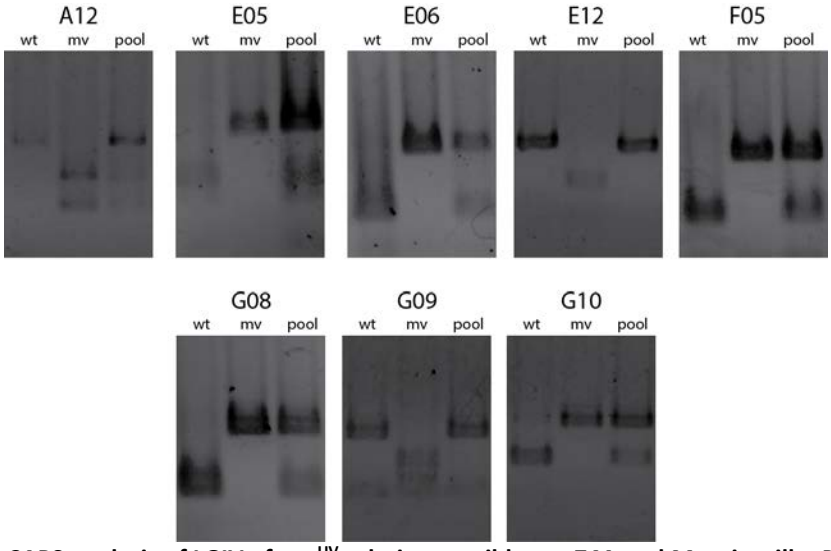

Figure 3.7 SNP-CAPS analysis of LGIV of *sup*^{UV} relative to wild type 74A and Mauriceville. PCR was performed on all samples, with the same quantity of template DNA, annealing temperature, annealing time and extension time. Samples were separated on a 1% agarose gel. Samples in the top panel have lanes arranged in the wild type 74A (wt), pool, and Mauriceville (mv) order, while the bottom panel is arranged wild type 74A (wt), Mauriceville (mv), and pool. SNPs A12, E05, E06, F05, G08, and G10 either display no bias or a bias towards Mauriceville. Conversely, SNPs E12 and G09 all display strong bias towards wild type. With 75% of mutants displaying no bias towards Wild Type it is expected that the *sup*^{UV} mutation is independent of LGIV.

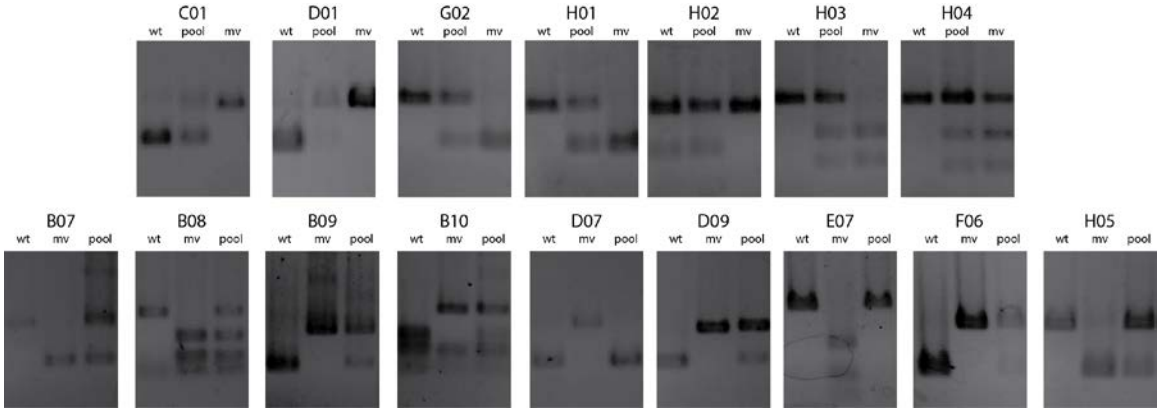

Figure 3.8 SNP-CAPS analysis of LGV of *sup*^{UV} relative to wild type 74A and Mauriceville. PCR was performed on all samples, with the same quantity of template DNA, annealing temperature, annealing time and extension time. Samples were separated on a 1% agarose gel. Samples in the top panel have lanes arranged in the wild type 74A (wt), pool, and Mauriceville (mv) order, while the bottom panel is arranged wild type 74A (wt), Mauriceville (mv), and pool. SNPs C01, D01, G02, H01, H02, H03, H04, B07, B08, B09, B10, D09, F06, and H05 all either display no bias or a bias towards Mauriceville. Only SNPs D07 and E07 display strong bias towards wild type. With 87.5% of mutants displaying no bias towards wild type it is unlikely that LGV is linked to the *sup*^{UV} mutation.

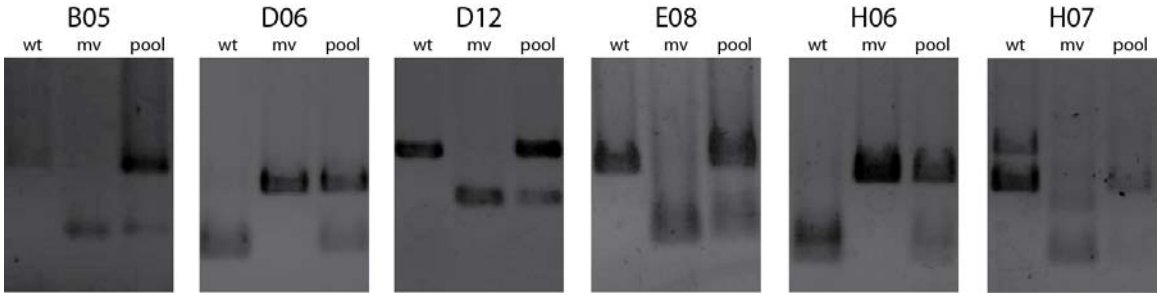

Figure 3.9 SNP-CAPS analysis of LGVI of *sup*^{UV}. Samples in the top panel have lanes arranged in the wild type 74A (wt), Mauriceville (mv), and pool order. SNPs B05, D06, D12, E08, H06 and H07 all either display no bias or a bias towards Mauriceville, with none showing a strong bias towards wild type. This ratio of 100% of mutants displaying a strong bias towards wild type is consistent with the mutation selected for not being present on LGVI.

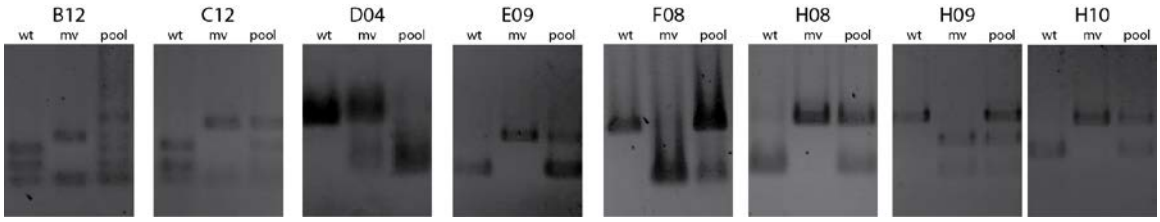

Figure 3.10 SNP-CAPS analysis of LGVII of *sup*^{UV} relative to wild type 74A and Mauriceville. Samples in the panel have lanes arranged in the wild type 74A (wt), Mauriceville (mv), and pool order. SNPs B12, C12, D04, H08, H09 and H10 all display either no bias or a bias towards Mauriceville. Only SNPs E09 and F08 display slight biases towards wild type. With 75% of mutants displaying no bias towards wild type, and the rest only showing a slight bias, it is unlikely that LGVII is linked to the *sup*^{UV} mutation.

Figure 3.11: Band intensities quantified on LGII. The SNPs across LGII were analyzed a second time in duplicate, and band intensity was quantified. They are arranged across linkage group, and the scale indicates the corresponding Megabases. This strongly confirms the *sup*^{UV} mutation was located on LGII, and that it does not reside near the left end of the LG.

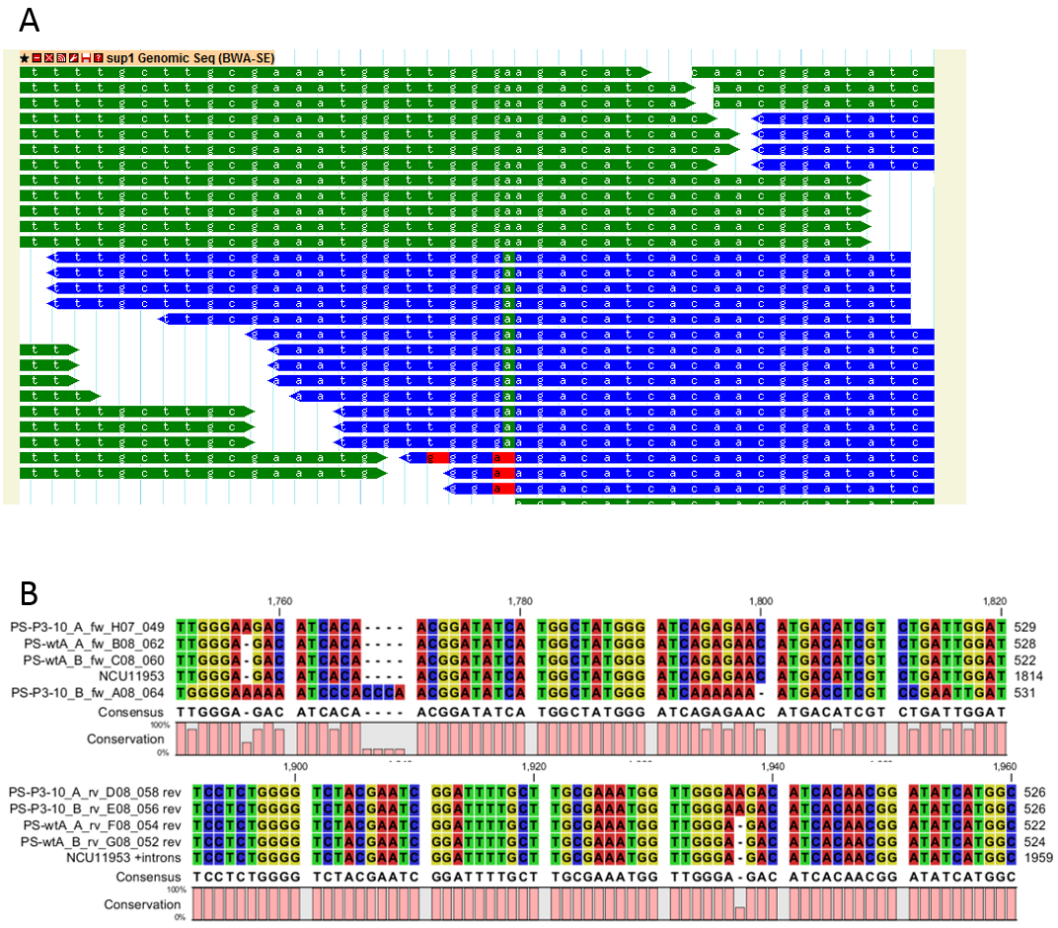

Figure 3.12 Alignment of *sup*^{UV} DNA to the reference genome reveals insertion of an adenine base. Part A: The evidence for the mutation from Illumina sequencing is strong with 26 of 28 reads confirming the insertion. Part B: Re-sequencing of the region reveals that the insertion is present in independent DNA sequencing runs (PS-P3-10_...), both in forward and reverse, and the insertion is absent from the parental wild type (PS-wtA_...). This confirms that the mutation is unique to the genome of the *sup*^{UV} strain.

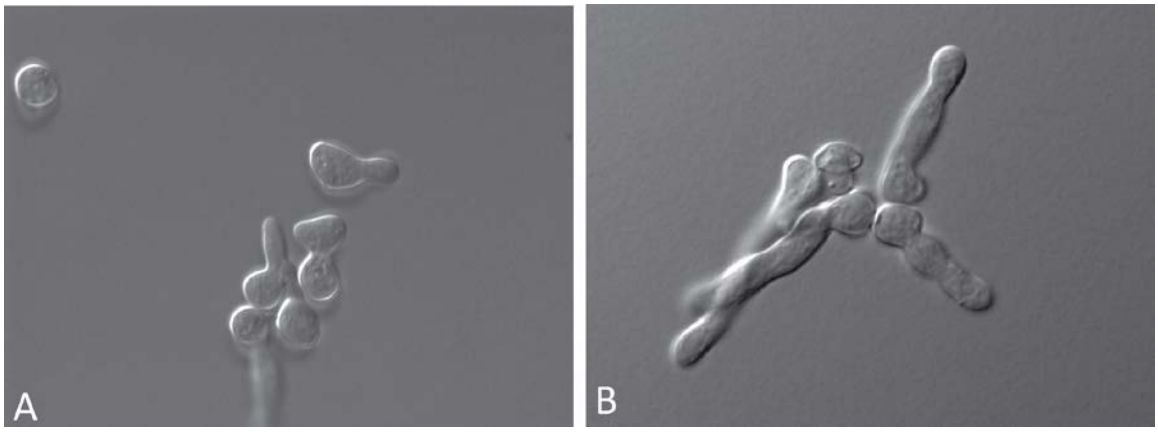

Figure 3.13: The *sup*^{UV} mutant is unable to produce CATs. Conidia were incubated for six hours at 30^{o}C in the dark. Images were taken at 60x magnification using DIC. Panel A displays wild type, which readily forms Conidial Anastomosis Tubes (CATs), the most easily analyzed form of hyphal anastomosis. They are the small connections between adjacent cells. Panel B displays a representative image of the *sup*^{UV} mutant, which does not form CATs, even among tightly associated conidia.

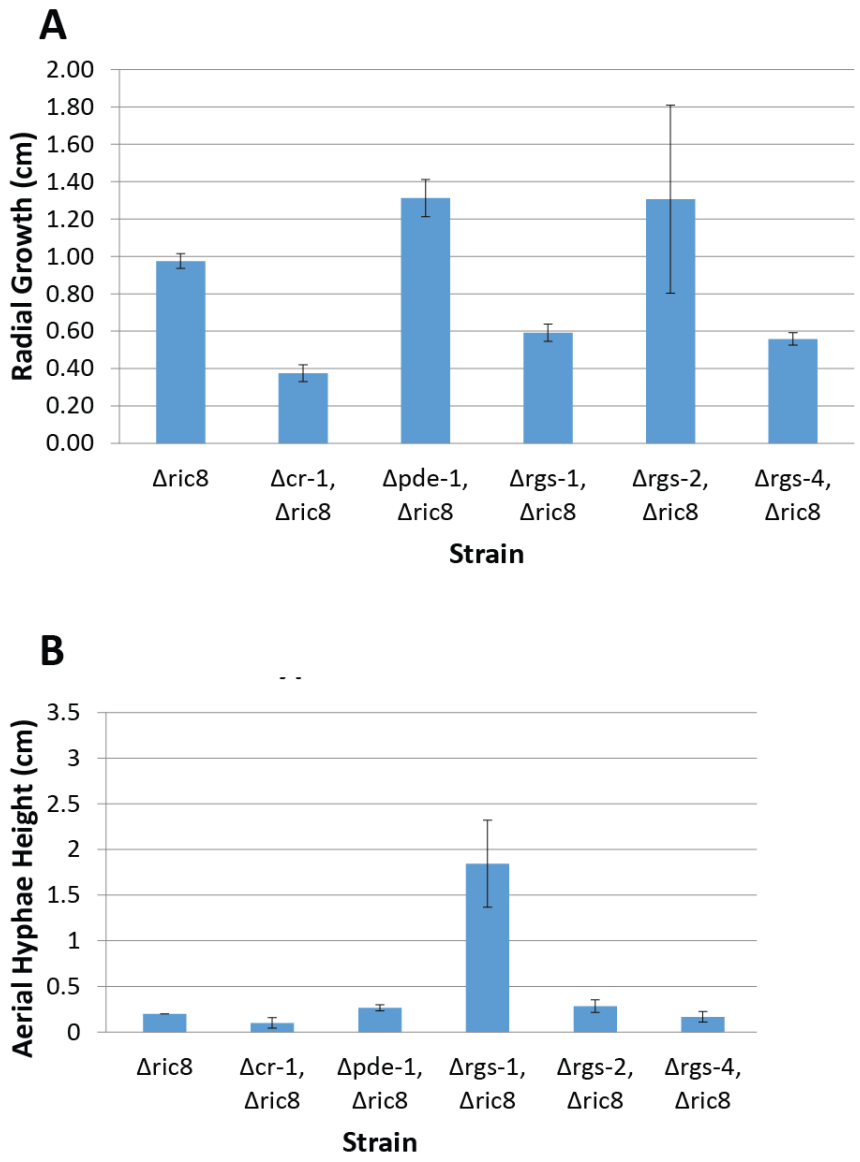

Figure 3.14: Phenotypes of crossed suppressor mutants. A. The apical extension assay was performed on VM plates at 25°C in the dark for 48 hours. Only Δ*pde-1* Δ*ric8* displayed a statistically significant growth rate improvement relative to Δ*ric8*. B. Aerial hyphae growth was tested using a standing liquid culture grown for 5 days in the dark at 25°C. Only Δ*rgs-1* displays a significant improvement of Δ*ric8*.

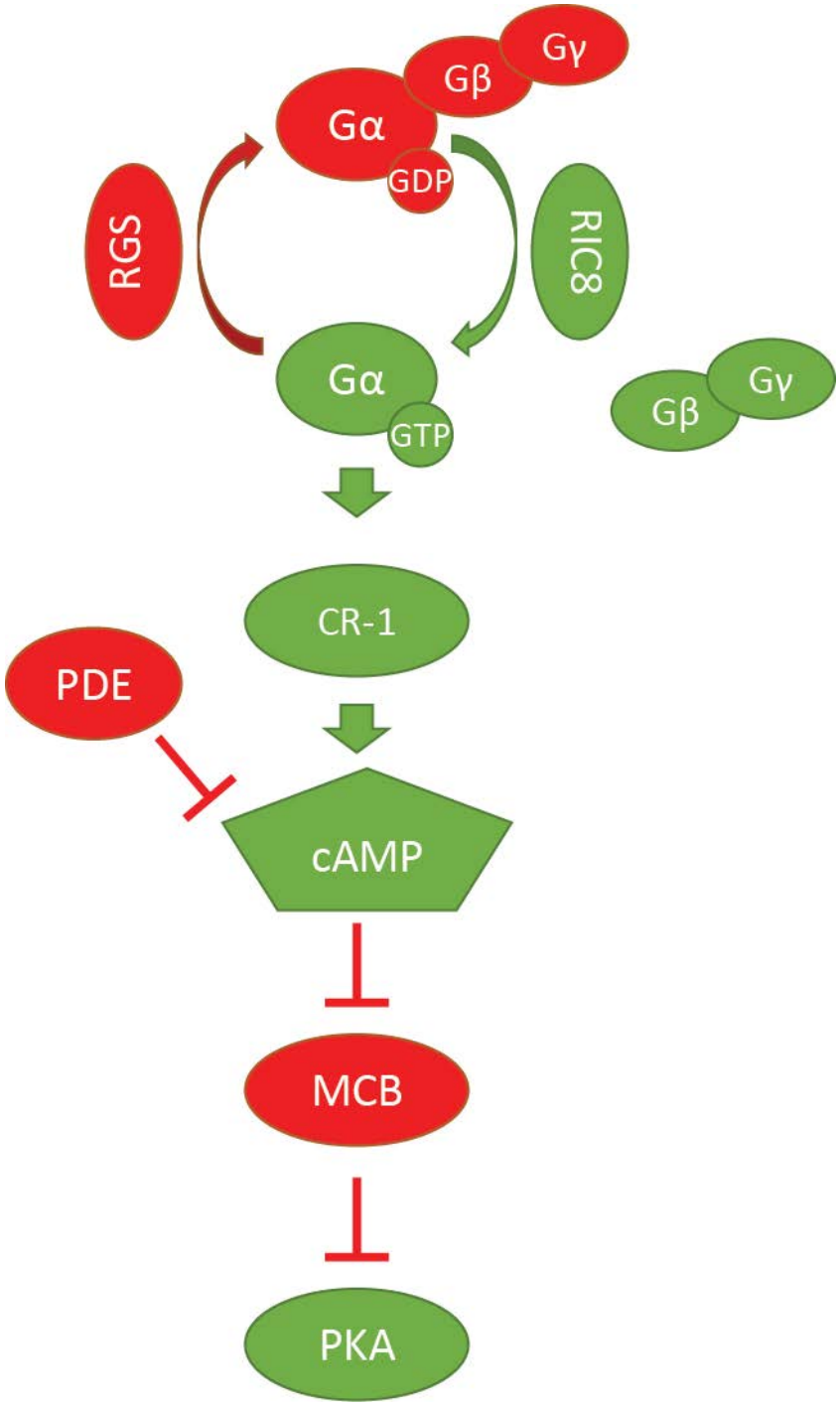

Figure 3.15: Proposed pathway of RIC8 regulation of Gα proteins and cAMP signaling. All proteins proposed to be positively regulated by RIC8 are displayed in green, while those negatively regulated are in red. The loss of *rgs-1* or *pde-1* was found to suppress the defects of the Δ*ric8* mutant, similar to effects of the *mcb* mutation. Mutation of *cr-1* worsens the defects in the Δ*ric8* mutant, while the introduction of hyperactive Gα also suppresses the loss of Δ*ric8*, consistent with both of these being positively regulated by RIC8.

Chapter 4

Structural analysis of RIC8

Abstract

To ascertain the structure-function relationship of regions of the RIC8 protein, yeast two hybrid and guanine nucleotide exchange factor (GEF) assays were performed using RIC8 truncation and glycine substitutions. Analysis of truncations revealed that the N-terminal 132 amino acids are essential for interaction with GNA-1, while binding is observed in a truncation lacking the C-terminal third of the protein (amino acids 344-480). Loss of either the C-terminal or N-terminal portions of the protein completely eliminated GEF activity of RIC8 towards GNA-1 and GNA-3. To better distinguish the structure-function relationship, 21 RIC8 proteins bearing engineered glycine mutations at individual conserved amino acids were analyzed for GEF activity in *in* vitro assays. The results indicate that a few residues dispersed throughout the N-terminus are essential for GEF activity, presumably due to their involvement in Gα protein binding. Furthermore, a large number of residues in the C-terminus, predicted to cluster on the top face of the C-terminus, show greater control of GEF activity. Some of the C-terminal mutant RIC8 proteins exhibit two-fold or more acceleration or reduction of GEF activity. Taken together, the data support a role for the N-terminus of RIC8 in binding Gα proteins, while the C-terminus is required for GEF activity. These results provide the first demonstration of functional domains for RIC8 in eukaryotes.

Introduction

G protein signaling involves a chain of events, beginning with a ligand binding a G Protein Coupled Receptor (GPCR), which in turn stimulates the exchange of GDP for GTP on the Gα subunit (Oldham & Hamm, 2008). RIC8 has been shown to function as a GEF for Gα proteins, similar to GPCRs (Wilkie & Kinch, 2005). This regulation results from direct interaction between RIC8 and Gα proteins. In humans, RIC8 was shown to directly interact with $G\alpha_s$ and $G\alpha_q$ (Klattenhoff et al., 2003). In *N. crassa*, RIC8 has been shown to bind GNA-1 and GNA-3 in the yeast two hybrid system (Wright et al., 2011). RIC8 has been observed to display GEF activity towards mammalian Gα proteins in *in vitro* assays. In rat, Ric8-A protein functions as a GEF for a subset of Gα proteins, including $G\alpha_q$, $G\alpha_{i1}$, and $G\alpha_o$ (Tall et al., 2003). In *N. crassa*, RIC8 exhibits GEF activity *in vitro* towards purified Gα proteins GNA-1 and GNA-3. Thus, RIC8 has been shown to function as a positive regulator of Gα proteins through a direct interaction and by exhibiting GEF activity towards them *in vitro*.

The crystal structure of RIC8 has not been solved, but some general biochemical methods have been coupled with computer-aided modeling to produce a predicted structure of the protein. Computer-modeling predicts a RIC8 is composed of a superhelix of α-helices, termed armadillo folds (Figueroa et al., 2009). This has been partially validated by circular dichroism analysis and thermostabilty tests, which indicate a structure containing 80% α-helices (Figueroa et al., 2009).

The role of RIC8 in regulating GTP binding of Gα proteins is conserved in species as diverse as *N. crassa* and *H. sapiens*, but the sequences are quite divergent($E = 5e^{-8}$). Alignments of *N. crassa*, *X. tropicalis*, *C. elegans*, *D. melanogaster*, and *H. sapiens* reveals only 26 amino acids that are conserved across all species (Wright et al., 2011). Given the limited conservation,

the working hypothesis is that these conserved amino acids are the most important for the Gα binding and GEF activity of the RIC8 protein.

Materials and Methods

Yeast two hybrid strain generation

Yeast two hybrid strains were made as a derivative of the RIC8 yeast two hybrid vector used in Chapter 2 for chemical screening (Wright et al., 2011). The *E. coli* strain carrying the RIC8-GAD yeast two hybrid vector was grown from freezer stock on a LB+Amp plate (Appendix B), and a colony was used to inoculate 5 mL of liquid LB+Amp medium, grown overnight at 37°C with shaking, and DNA was extracted by MiniPrep (Appendix B).

A 1:10 dilution of the purified DNA was prepared in sterile water. Truncated forms of *ric8* were amplified according to the "Phusion PCR" protocol (Appendix B) with an annealing temperature of 65°C for 30 seconds, and an extension time of 2 minutes, using primer pairs described in Table 4.1. Fragments were generated lacking 132 amino acids from the N-terminus (Δ132N), 136 amino acids from the C-terminus (Δ136C), 54 amino acids from the C-terminus (Δ54N), or a combination of truncations of both N- and C-termini (Δ132N Δ136C and Δ132N Δ54C), as shown in Figure 4.1. Each of these fragments was subjected to gel electrophoresis on a 1% agarose slide gel and the amplified product was purified according to the "Gel Extraction" protocol (Appendix B). Recipient GAD and GBK vectors were prepared as described above. They were linearized by digestion with *Xba*I and *Eco*RI enzyme 37°C overnight, and gel extracted as described above.

Vectors containing each of the truncated forms of RIC8 were produced using "Yeast Recombinational Cloning", as described in Appendix B. In this instance, 6 μL of recipient linearized GAD or GBK vector was mixed with 30 μL of insert DNA and transformed into yeast after which transformants were plated on SD-Leu or SD-Trp plates. After 2-3 days of growth at

30°C, all colonies were scraped from the surface of the plate, and DNA was extracted from them as described below in "Yeast DNA Extraction" (Appendix B). This pool of DNA was transformed into chemically competent DH5α *E. coli* and plated on LB+Amp or LB+Kan medium for GAD or GBK vectors respectively (Appendix B). Five colonies from each transformation were spotted on a fresh plate containing the appropriate medium, and DNA was extracted as described above for the initial vector.

To confirm the truncations, the transformants were digested with *Eco*RI and *Bam*HI to separate the vector from the insert. For GAD, the vector was expected to be 8.0 kb, and for GBK the vector was expected to be 7.3 kb. The insert size was checked as well: Δ132N (1.0 kb), Δ54C (1.3 kb), Δ136C (1.0 kb), Δ132N Δ54C (0.9 kb), and Δ132N Δ136C (0.6 kb). Once the vectors were confirmed, they were transformed into the AH109 yeast strain for use in the Matchmaker yeast two hybrid system. Diploids of each RIC8-GAD strain were made by mating with the GNA-1-GBK containing yeast two hybrid strain (Appendix B). Diploids with GNA-3-GAD were made with each of the RIC8-GBK strains.

Yeast two hybrid assays

Diploids were assayed for interaction on media lacking nutrients supplied by the reporter genes (histidine or adenine). To accomplish this, a single colony was picked with a sterile toothpick from a SD-Trp-Leu plate and used to inoculate an assay plate. Assay plates included a SD-Trp-Leu plate for a positive control, and three interaction test plates: SD-Trp-Leu-Ade, SD-Trp-Leu-His, and SD-Trp-Leu-Ade-His. Each plate also included Clontech positive and negative control strains. Strains that grew on SD-Trp-Leu-Ade-His were classified as having a strong interaction (two reporter genes activated). If the strain grew SD-Trp-Leu-Ade or SD-Trp-

Leu-His but did not grow on SD-Trp-Leu-Ade-His the interaction was classified as weak (only one reporter gene activated). If the diploid only grew on the SD-Trp-Leu control plate, the result was scored as no interaction.

Generation of *ric8* glycine substitutions

In order to generate *ric8* alleles that contained single amino acid replacements, a series of vectors were designed by and generated in collaboration with Dr. Asharie Campbell that substituted glycine for different conserved amino acids. First, DNA containing the entire *ric8* ORF without introns was extracted (Appendix B) from an *E. coli* strain carrying the *ric8*-GBK yeast two hybrid vector (Wright et al., 2011). The plasmid was cut using *Eco*RI and *Sal*I in Buffer 3 (NEB) with BSA at 37^{o}C for 4 hours, and the resulting 1.4 kb fragment bearing *ric8* was gel extracted using the Qiaex II protocol (Appendix B). The vector pGEM4z (Promega) was also extracted from *E. coli* and digested with enzymes *Eco*RI and *Sal*I in Buffer 3 at 37^{o}C for 4 hours, and finally gel purified (Appendix B). These two pieces were ligated, transformed into chemically competent DH5α cells, and cells were plated on LB+Amp plates (Appendix B). Transformants were confirmed by sequencing with SP6 and T7 primers (Appendix B). This vector was then used as the template for site-directed mutagenesis.

For site-directed mutagenesis, specialized overlapping primers (described in Table 4.2) were used to amplify the entire *ric8*-pGEM4z vector. The protocol used a hot start Phusion PCR protocol: 1.5 μL of 1:10 diluted template was mixed with 5x Phusion buffer, 1 μL of 10 mM dNTPs, 2.5 μL of each 10 pm/μL forward and reverse primer, and 32 μL of water. The reaction was started at 98^{o}C for 60 seconds, and then 0.5 μL of Phusion was added to the mixture. The reaction then proceeded for 18 cycles of 30 seconds at 98^{o}C, 60 seconds of 53^{o}C and 90 seconds

at 72°C, and then a final 10 minute extension at 72°C. The product was digested with *Dpn*I for 1 hour at 37°C to cleave the original, methylated vector, and the remaining amplified vector was transformed into chemically competent DH5α *E. coli* with ampicillin for selection (Appendix B). These vectors were sequenced using the same T7 and SP6 primers as above, and those containing an exact copy of *ric8* mutated only in the desired codon were selected. Finally, 20 μL of the vector was digested with *Nde*I and *Bam*HI in Buffer 4 for 4 hours at 37°C, and a 1.4 kb fragment for each mutant was gel-purified. The recipient vector, pET-16b, was prepared by also digesting with *Nde*I and *Bam*HI in Buffer 4 at 37°C overnight, and this time a 5.7 kb linearized vector was gel purified. Each mutant *ric8* fragment was ligated into the recipient vector and transformed into chemically competent DH5α cells. These were checked using colony PCR with R8_check fw and rv primers (Table 3.2), and then plasmid DNA was extracted using the Qiagen miniprep kit (Appendix B). The resulting vectors included *ric8* under an inducible promoter, with an N-terminal 6xHIS tag to facilitate protein purification.

Overexpression and purification of Gα proteins

Gα proteins were overexpressed and purified in collaboration with Dr. Asharie Campbell using a protocol previously used in our laboratory (Wright et al., 2011). Four tubes containing 5 mL of LB+ amp were each inoculated with a colony of the 6H-Gα expressing *E. coli* strain. The tubes were grown with shaking at 225 RPM overnight at 37°C. The four tubes were combined to inoculate 1 L of LB+Amp in a 2.8 L Fernback flask, which was incubated with shaking at 225 RPM at 37°C for 2 hours. 10 μM IPTG was then added to induce protein expression, and the culture was grown for 6 more hours at 25°C with shaking at 100 RPM. The cells were pelleted at 5000 RPM for 10 minutes at 4°C, and pellets were frozen at -20°C. The pellet was re-suspended in 10

mL His-Pur Lysis buffer (50 mM NaH_2PO_4 pH 7.4, 300 mM NaCl, 10 mM imidazole, 10% glycerol, 0.1 mM PMSF) with 0.2 mg/mL lysozyme, and incubated on ice for 20 minutes. The suspension was then sonicated 6 times for 15 seconds each time at 30% power with 60 second rests between each sonication using a Fisher Scientific Sonic Dismembrator Model 500. The sample was then pelleted at 20,000 RPM for 20 minutes at 4°C. The supernatant was transferred to a 3 mL bed volume of His-Pur Cobalt beads and incubated for 1 hour at 4°C on a rotating shaker. The mixture was centrifuged at 2,000 RM for 2 minutes at 4°C, and the supernatant was removed. The beads were re-suspended in 5 mL lysis buffer, and the suspension was transferred to a poly-prep column. The column was washed with 5 mL lysis buffer, and then protein was eluted with 4 mL of each 60, 80, 100, 120, and 140 mM imidazole, pooled, and concentrated to 1 mL using Amicon Ultra-4 Centrifugal filter Units concentrator column with a 4,000 xg spin (Millipore, Darmstadt, Germany).

Overexpression and purification of RIC8 proteins

RIC8 proteins were overexpressed and purified in collaboration with Dr. Asharie Campbell using a modified form of the protocols established by Wright and Borkovich (Wright et al., 2011). One colony of each HIS-RIC8 mutant was inoculated into each of two 5 mL LB+Amp cultures, and grown overnight with shaking at 225 RPM at 37°C. A 1 L flask with 500 mL of LB+Amp medium was inoculated with the 10 mL combined from the two overnight cultures, and grown with shaking at 225 RPM for 2.5 hours at 37°C. IPTG was added to reach 100mM and the culture was incubated with shaking at 150 RPM for 5 hours at 30°C to induce RIC8 protein expression. The cells were pelleted at 4000 RPM in an Avanti J-26 XP Beckman floor centrifuge using rotor JS-4.0 for 10 minutes at 4°C. Pellets were frozen at -20°C.

The pellet was re-suspended by pipetting in 10 mL of His-Pur Lysis buffer (50 mM NaH_2PO_4 pH 7.4, 300 mM NaCl, 10 mM imidazole, 10% glycerol, 0.1 mM PMSF). The solution was brought to 0.2 mg/mL lysozyme and incubated on ice for 20 minutes. The suspension was sonicated 4 times at 30% power for 30 seconds with 1 minute rests on ice between each sonication, using a Fisher Scientific Sonic Dismembrator Model 500. The sonicated suspension was centrifuged at 25,000 RPM with rotor JA-25.5 at 4^{o}C for 20 minutes. The supernatant was removed and pipetted onto 2 mL of His-Pur Cobalt beads (Thermo Scientific, Rockford, IL) in a 50 mL conical tube and incubated for 1 hour at 4^{o}C on a nutator. This mixture was centrifuged at 700 g for 30 seconds at 4^{o}C in a Centra CL3 centrifuge with an IEC 243 rotor. The supernatant was discarded and the pellet was re-suspended in 5 mL of wash buffer (Lysis buffer plus 20 mM imidazole) and transferred to a poly-prep column. A volume of 15 mL of wash buffer was used to wash the column, and then RIC8 was eluted using 3 mL of each 75, 100, 120 and 140 mM. The elutions were pooled and concentrated to 500 μL using Amicon Ultra-4 Centrifugal filter Units concentrator column with a 4,000 xg spin (Millipore, Darmstadt, Germany). The concentrated protein was quantified first using a Bradford assay, and then by band quantification on a Coomassie stained gel (Appendix B).

GEF assays

GEF assays were performed with assistance from Dr. Asharie Campbell according to a previously published protocol (Wright et al., 2011). All assays were performed in 20 μL sample volumes of exchange buffer. A 10 μL of Gα with 20 mM $MgSO_4$ was prepared in Gα exchange buffer in one tube. A second tube with 10 μL of 400 nM RIC8 with 4 μM GTPγS and 1 μL of 1μCi/μL GTPγ^{35}S (Perkin Elmer, Waltham, MS) in exchange buffer was prepared. Reactions were

initiated by mixing the components in these two tubes. The reaction was allowed to progress for up to 60 minutes at 30°C. Reactions were quenched using 100 μL of cold stop solution (20 mM Tris-Cl pH 8.0, 100mM NaCl, 2 mM MgSO4, 1 mM GTP). For the zero time point, the stop solution was added to the Gα tube prior to addition of the RIC8 mixture. After adding stop solution, the solution was filtered on a 0.45 mM HA mixed cellulose membrane (Millipore) using vacuum, and filters washed three times with 5 mL of cold wash solution (50 mM Tris Cl pH 8.0, 100 mM NaCl, and 2 mM $MgSO_4$). Filters were allowed to dry, and then transferred to scintillation vials containing 4-5 mL of scintillation fluid (Scintiverse BD cocktail, Fisher Scientific). Bound GTPγS CPM were quantitated by scintillation counting for 1 minute (Beckman LS 6500 Multi-Purpose Scintillation Counter).

Data analysis for GEF assays

Data analysis was performed using Excel (Microsoft, Redmond, Washington). To begin, the raw counts for each time point were input from the scintillation counter readout. Averages and standard errors were calculated for each set of replicates at each time point. If two of three data points were near identical (within 10% of each other) and the third differed by 50% or more from the other two data points, it was rejected as an outlier. The zero time point counts were then subtracted from each time point. The average and standard error for each time point was finally divided by the counts for reactions containing wild-type RIC8 at 10 minutes in the same experiment, and reported as a percentage, displayed in a graph (Figure 4.4, Figure 4.5). Experiments involved triplicates of each sample, and each data point is a representative example from at least two independent experiments.

Results

The N-terminus of RIC8 is essential for interaction with GNA-1.

Strains were successfully generated for all five truncations of RIC8 in both GAD and GBK vectors. Diploids with RIC8-GAD and GNA-1-GBK were generated for all five, as were diploids for RIC8-GBK and GNA-3-GAD. These orientations were consistent with previous experiments displaying interaction (Wright et al., 2011). As a control, the full length RIC8 GAD and GBK vectors were crossed with each set of five truncations, and tested alongside each mutant.

Testing the RIC8/ GNA-1 diploids revealed that all strains that were Δ132N displayed no interaction with GNA-1, as deduced from the lack of growth on medium lacking histidine and/or adenine. Both diploids of GNA-1 with C-terminal truncations, Δ54C and Δ136C, grew on SD-Trp-Leu-Ade, but not the more stringent SD-Trp-Leu-Ade-His. Finally, the double truncation diploids with GNA-1, Δ132N Δ54C and Δ132N Δ136C did not grow on any of the three media that would suggest an interaction between the two proteins.

Attempts to replicate the RIC8 GNA-3 interaction in the yeast two system proved unsuccessful. Diploids with GNA-3 were generated for all truncation mutants and with full length RIC8, but every one of these strains was unable to grow on anything more stringent than SD-Trp-Leu, even when cultured for five days. This interaction appears to be very weak, and will likely need to be attempted again.

Analysis of GEF activity for RIC8 truncations revealed that loss of the N-terminus or C-terminus eliminates activity.

GEF activity was assessed for each of the three RIC8 truncation forms (Δ132N, Δ54C, and Δ136C) and compared to controls (Figure 4.4). Data was collected for GNA-1 alone, GNA-1 with full length RIC8, and GNA-1 with each truncation at zero and ten minutes.

The presence of full-length RIC8 induced a seven-fold increase in GTP binding of GNA-1 at ten minutes relative to reactions containing only GNA-1 (Figure 4.4). None of the three truncations were able to stimulate GTP binding to GNA-1, as the GTP binding for these three assays was statistically indistinguishable from the minus RIC8 control.

Full-length RIC8 increased GNA-3 GTP binding by eight-fold at ten minutes relative to GNA-3 alone. Similar to GNA-1, all truncation mutants failed to increase binding of GTP to GNA-3 after ten minutes.

Glycine substitutions near the N-terminus primarily elicit an inhibitory effect, while ones from the C-terminus elicit both inhibitory and excitatory effects and substitutions in the center of the protein have little effect on GEF activity.

GEF activity was tested for each of the 21 RIC8 glycine substitution mutant proteins, each carrying a mutation in a conserved residue (Table 4.5). Mutant proteins were considered have low GEF activity if the value was 60% or lower than observed in reactions containing wild-type RIC8. Mutant proteins were considered to be hyperactive if GEF activity was 140% or greater than wild type.

Four main results were observed: no change, increased Gα-GTP binding, decreased Gα-GTP binding, and differential effects on GNA-1-GTP and GNA-3-GTP. Mutations that decreased

activity were exclusively located in the N-terminus and C-terminus. Mutations L40G, K44G, N87G, N409G, E435G, and L439G all exhibited decreased GEF activity relative to RIC8. Only one mutation, L83G, increased the GEF activity of RIC8.

Mutants that showed differential effects on GNA-1 or GNA-3 were all located in the middle and C-terminal regions of RIC8. Among them, proteins bearing E182G, P314G, P410G, K432G or E433G all displayed increased GEF activity towards GNA-1, but normal GEF activity towards GNA-3. The S398G mutation resulted in reduced GEF activity towards GNA-1, but normal GEF activity towards GNA-3. The L184G mutation resulted in increased GEF activity towards GNA-3, and decreased GEF activity towards GNA-1.

Discussion

The less conserved N-terminal portion of RIC8 is essential for binding GNA-1.

I originally hypothesized that the most highly conserved region of the protein, the C-terminus, would be essential for binding to the Gα protein. The most conclusive piece of the yeast two hybrid data, however, showed that the C-terminus of the RIC8 protein is dispensable for binding of GNA-1. This result led to a new hypothesis – that the variation between Gα proteins across species might require a more variable binding region, but the region required for GTP binding and GEF activity might require a site that was conserved across diverse species. Furthermore, loss of the N-terminus of RIC8 is sufficient to eliminate binding to GNA-1. This was not affected by either C-terminal truncation (Δ136N Δ54C or Δ136N Δ132C), suggesting there is not an auto-inhibitory function for the C-terminus that could be removed to compensate for the loss of the N-terminus. There does remain the possibility that the change in the start site induced larger structural changes that continued into the central portion of the protein. However, considering the data for the C-terminus, it can be concluded that the binding domain for GNA-1 lies in the N-terminal two-thirds of the protein, and is most likely at least partially contained in the N-terminal third of the protein.

Loss of even a modest portion of RIC8 completely abates the GEF activity of the protein.

The N-terminus of RIC8 was established above as being important for the binding of GNA-1. From this, it was expected that a form of RIC8 which could not bind to GNA-1 could not act as a GEF. This hypothesis was confirmed when it was seen that the Δ132N RIC8 did not exhibit GEF activity towards GNA-1. Though the yeast two hybrid assay could not be performed

using truncated RIC8 and GNA-3, it was expected that GNA-3 would bind a similar region as GNA-1, and that the loss of the N-terminus would also eliminate GEF activity towards GNA-3. This was observed to be the case, as there was no increase in GTP binding to GNA-3 when Δ132N RIC8 protein was added to the reaction. This is consistent with the N-terminus being involved in GNA-3 binding, but proof will require additional experiments.

More interestingly, it was found that any truncation of the C-terminus completely eliminated GEF activity. This fits with the modified hypothesis that this more highly conserved region of the protein is involved in the GEF activity of RIC8.

GEF activity of most RIC8 proteins with a mutation along the front face of the N-terminus is low.

The analysis of 21 mutant RIC8 proteins for GEF activity towards two different Gα proteins revealed a number of interesting trends, especially in relation to the truncation data. The yeast two hybrid data showed that the N-terminus was very likely involved in binding Gα proteins. The truncation used included residues L40, K44, L83, N87, and L141. The mutation of any of L40G, K44G, or N87G resulted in a total loss of GEF activity towards GNA-1 (consistent with loss of binding of GNA-1), and also a significant reduction in GEF activity towards GNA-3. This would be consistent with GNA-1 and GNA-3 binding similar places in the N-terminus of RIC8, though the partial activity towards GNA-3 suggests the binding may be somewhat different for the two proteins. Interestingly, these all fall on the front face of the N-terminus of RIC8, with residues L40 and K44 adjacent to N87. Only the L83G mutant, which also falls in the same face, displays a modest increase in GEF activity for both GNA-1 and GNA-3.

Mutations in the central third of RIC8 elicit the least effect on GEF activity.

The central third of the protein has the fewest residues that affect GEF activity, but the two out of five tested that do, elicit increased activity when mutated. Mutations L141G, H207G, R305G, R309G and R185G spread throughout the middle region of the protein elicit no effect on the GEF activity of RIC8. The most biologically active residues are the pair of E182 and L184 which would appear to play a role in specificity, as mutating E182G increases the GEF activity towards GNA-1, while the L184G mutation increases GEF activity towards GNA-3. These mutations fall on the front face of the central third of the protein. They are not immediately adjacent to, but are near the N-terminal cluster of amino acids essential for GEF activity. The fact none of the other three residues in the region significantly alters GEF activity is consistent with the hypothesis that the middle third of RIC8 is not required for GEF activity, apart from the one cluster in an alpha helix that folds back towards the N-terminus.

Mutations arranged on the top face of the C-terminus form a cluster with spatially adjacent residues that greatly affect GEF activity.

The last third of RIC8 which bears the most conserved residues (12) also contains the most biologically active amino acids (7). Of the five assayed residues in the Δ54C truncation mutant region (E430G, K432G, E433G, E435G, L439G), four exhibit effects on GEF activity. The mutation of either of the adjacent residues K432G or E433G results in hyperactive GEF activity towards GNA-1, roughly two times that of wild-type RIC8. Moving just a few residues down to E435G and L439G, the mutation results in a two-fold or greater decrease in GEF activity for both Gα proteins. The severity of the effect of mutations in this narrow ten amino acid window suggests that this may be the region responsible for GEF activity. Furthermore, these residues

when mapped to the predicted structure fall in close proximity to residue P314, all existing on the top face of the last few super helices. The modeled tertiary proximity and the commonality of conservation and activity lend credence in both directions – both towards affirming the predicted structure, and supporting the importance of this region of the protein for GEF activity. Not surprisingly, residues N409 and P410 also fall on the same top face of the protein, and N409G and P410G display the greatest GEF activity of any protein. The only exception to this trend is that while residue S398 is on the bottom of face of this part of the protein, it exhibits a modest effect on GEF activity towards GNA-1. It is surprising to see so many hyperactive mutations in this region, but given the dispensable nature of the C-terminus with respect to binding, it is expected these still point to the portion of the protein which is responsible for GEF activity.

Conclusions regarding RIC8 structure function

The exact structure of RIC8 is still unknown, but integrating data from this chapter with the predicted models presents many interesting hypotheses about its structure-function relationship. First, the data support a scenario which the C-terminus is dispensable for binding of GNA-1, and possibly Gα proteins in general, while the N-terminus is responsible for Gα binding. The minimally conserved central quarter of the protein appears to be the least required for binding and GEF activity, functioning primarily as a bridge between the N-terminal and C-terminal regions. This is further validated by the high degree of conservation in the C-terminus, where residues spread across the primary structure of RIC8 cluster together to form what is presumably a region directly responsible for GEF activity.

Future Directions

The use of truncation and glycine substitutions has been pushed nearly to its maximal effect, and there may be little more progress to be made without an actual crystal structure which would be a priority in any future research on RIC8 structure-function. Some additional information could be gleaned from a yeast two hybrid analysis of the same set of glycine substitutions, as knowing exactly which mutants are able to bind Gα proteins, and correlating that data with GEF activity would further clarify exactly which regions and residues are essential for binding or GEF activity. It is expected the N-terminal, but not C-terminal residues will be essential for binding. Finally, introducing mutations with effects on Gα binding or GEF activity into *N. crassa* would provide valuable phenotypic data to couple with the biochemical assay results.

Table 4.1: Primers used to generate RIC8 truncations

Name	Sequence (5'-3')
R8_fw	CACTAGTGAATTATGGCCTCAATAGGAGTTTCTG
R8_Δ132N_fw	CACTAGTGAATTCGGCACCACTGTTGACCTTGCCAA
R8_rv	GAAGAGGATTCGGACTGAAATTTGAGTCGACCATATG
R8_Δ54_rv	CATATGGTCGACTCAGGGCATATCCGGGAACGTCTCGGT
R8_Δ136_rv	CATATGGTCGACTCACGGGAGCAATGGGGTTGGTCATGTT

Table 4.2: Primers used to generate glycine substitutions.

Residue	AA	Sequence (5'-3')
40	L	GAGACAAGGCCGGGGAGGAACTCAAG CTTGAGTTCCTCCCCGGCCTTGTCTC
44	K	CTGGAGGAACTCGGGGTGTATGGCCG CGGCCATACACCCCGAGTTCCTCCAG
83	L	CGGAATGCCCTCGGTGTGCTCTGCAAC GTTGCAGAGCACACCGAGGGCATTCCG
87	N	GTGTGCTCTGCGGCGCCATGCTCCTC GAGGAGCATGGCGCCGCAGAGCACAC
141	L	GACCTTGCCAAGGGCATCGATGAGC GCTCATCGATGCCCTTGGCAAGGTC
182	E	CATGGCCCTGGGAGGGACACTACGGCTCC GGAGCCGTAGTGTCCCTCCCAGGGCCATG
184	L	GCCCTGGGAGAGACAGGACGGCTCCTG CAGGAGCCGTCCTGTCTCTCCCAGGGC
185	R	GAGACACTAGGGCTCCTGTTCAATGTCAC GTGACATTGAACAGGAGCCCTAGTGTCTC
207	H	GCTGCGGTCCCGGGTATAGTGACCCTTC GAAGGGTCACTATACCCGGGACCGCAGC
305	R	GCCGACTCTCCCGTTGGTGACTTCATCCGCAAGAG CTCTTGCGGATGAAGTCACCAACGGGAGAGTCGGC
309	R	CGTTCGTGACTTCATCGGCAAGAGCCTGCTC GAGCAGGCTCTTGCCGATGAAGTCACGAACG
314	P	GCAAGAGCCTGCTCGGCTCAGAAGAGGAGC GCTCCTCTTCTGAGCCGAGCAGGCTCTTGC
363	K	GACAAGGACGCAAACGGGTTTGTCGAAAAC GTTTTCGACAAACCCGTTTGCGTCCTTGTC
398	S	GGGCGAAAGTGGCCAGGCTGGTCAAAG CTTTGACCAGCCTGGCCACTTTCGCCC
409	N	GAGGGCGGTCGGCCCCATTACTGGCCAG GTCCGACACGTTGCCCAGAAGGTGGGACAC
410	P	GGAGGGCGGTCAACGGCATTACTGGCCAGTTCTTG CAAGAACTGGCCAGTAATGCCGTTGACCGCCCTCC
430	E	GAGATGACCATGGGGGAGAAGGAGCGTGAGGCCG CGGCCTCACGCTCCTTCTCCCCCATGGTCATCTC
432	K	GACCATGGAGGAGGGGGAGCGTGAGGCCGAGAG CTCTCGGCCTCACGCTCCCCCTCCTCCATGGTC
433	E	CATGGAGGAGAAGGGGCGTGAGGCCGAGAGAC GTCTCTCGGCCTCACGCCCCTTCTCCTCCATG
435	E	GGAGGAGAAGGAGCGTGGGGCCGAGAGACTGTTTG CAAACAGTCTCTCGGCCCCACGCTCCTTCTCCTCC
439	L	GCGTGAGGCCGAGAGAGGGTTTGTCTTGTTTGAGAG CTCTCAAACAAGACAAACCCTCTCTCGGCCTCACGC

Amino Acids above the green line fall in the region removed in the Δ132N truncation. Amino acids below the red line fall in the region removed in the Δ136C mutant RIC8 protein. The codon in the forward sequence resulting in glycine is highlighted in yellow.

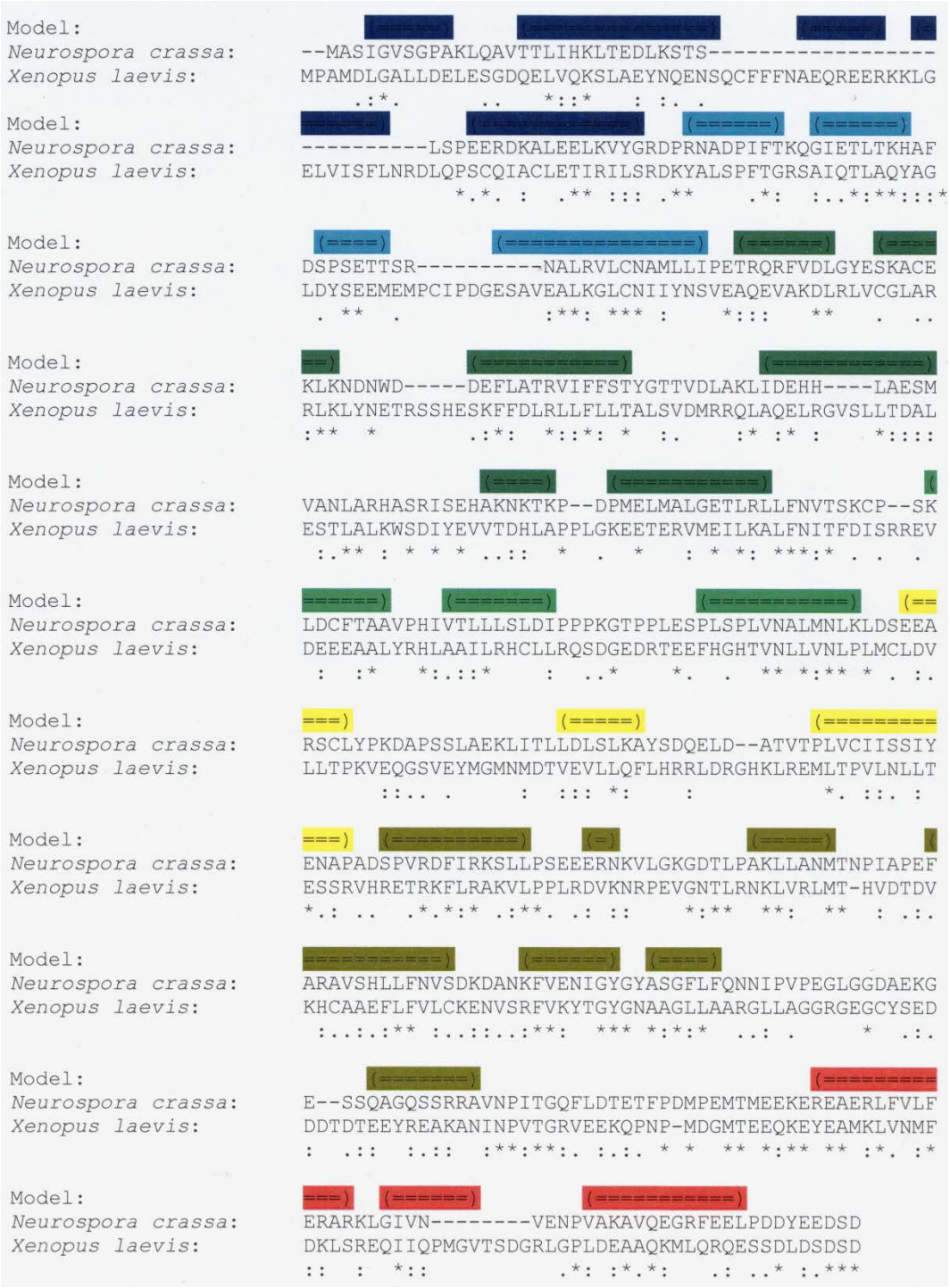

Figure 4.1: Alignment of *N. crassa* RIC8 to computational structure. The structure of RIC8 was modeled computationally in a previous study (Figueroa et al., 2009). This alignment displays an overlay of exactly which residues were used to form each of the alpha helices in the super helix, and color coded to correspond with the colorized 3D structure in the study.

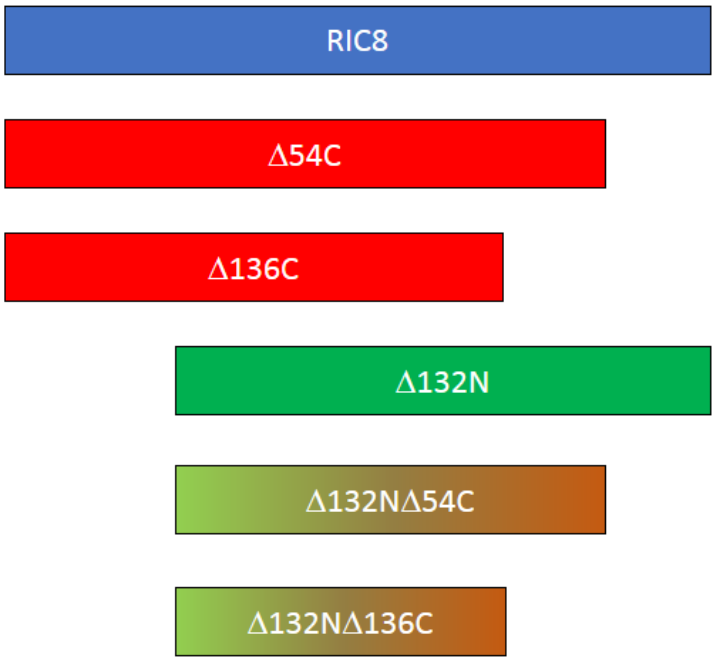

Figure 4.2: Truncations of RIC8. Five truncated forms of RIC8 were generated for this experiment. In red are the two C-terminal truncations, Δ54C and Δ136C, lacking 54 and 136 amino acids from the C-terminus respectively. In green is Δ132N, lacking 132 amino acids from the N-terminus. Finally, in the green to red transition are the double truncations, lacking 132 amino acids from the N-terminus, and missing either 54 (Δ132N Δ54C) or 136 (Δ132N Δ136C) amino acids from the C-terminus.

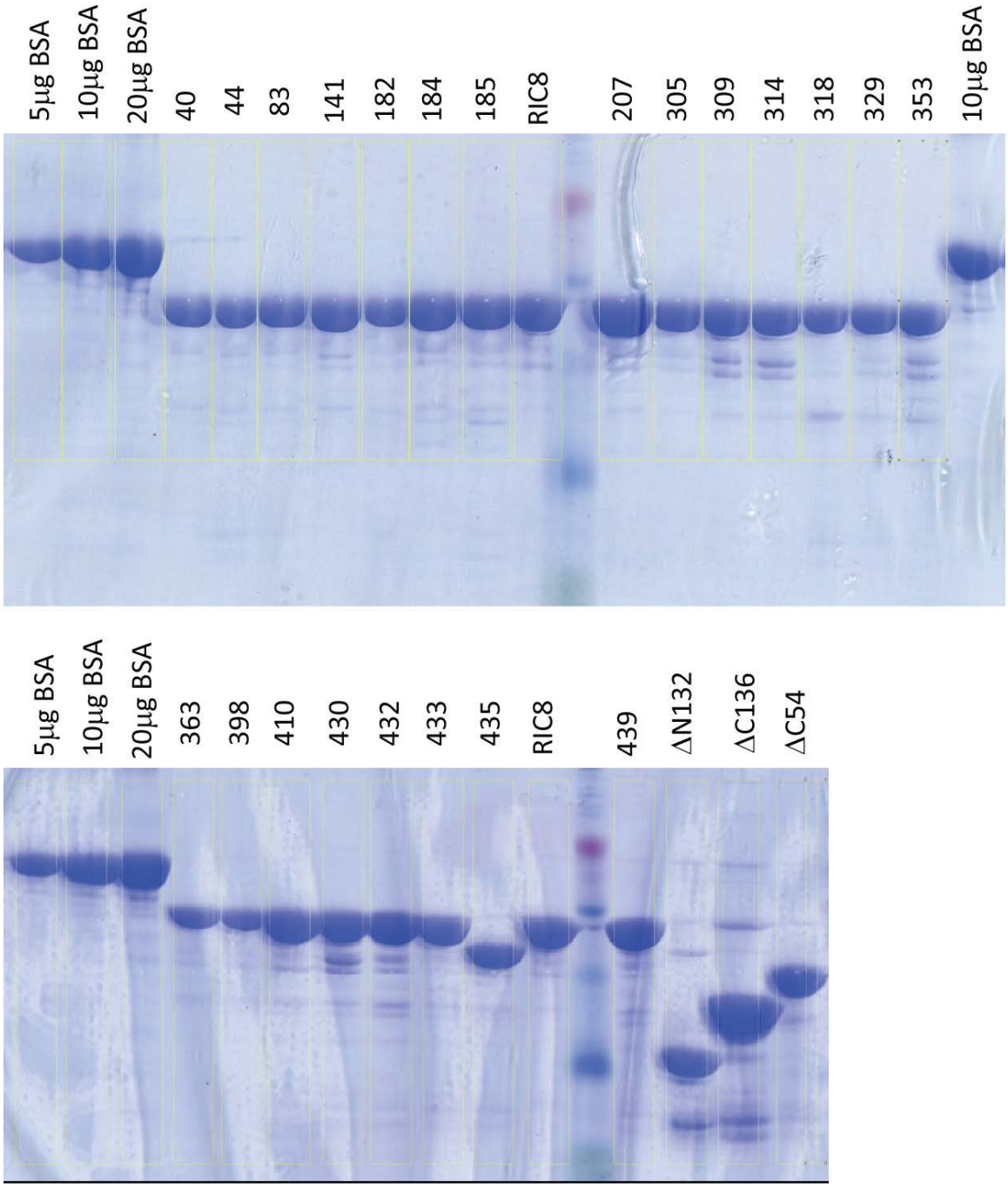

Figure 4.3: Calibrating concentrations for GEF assays. Protein concentrations were initially checked by Bradford assay, and then samples run on an SDS-PAGE gel and Coomassie-stained to confirm concentrations and protein integrity. Bands were quantified, and volume of protein adjusted to achieve equal amounts for each sample in GEF assays.

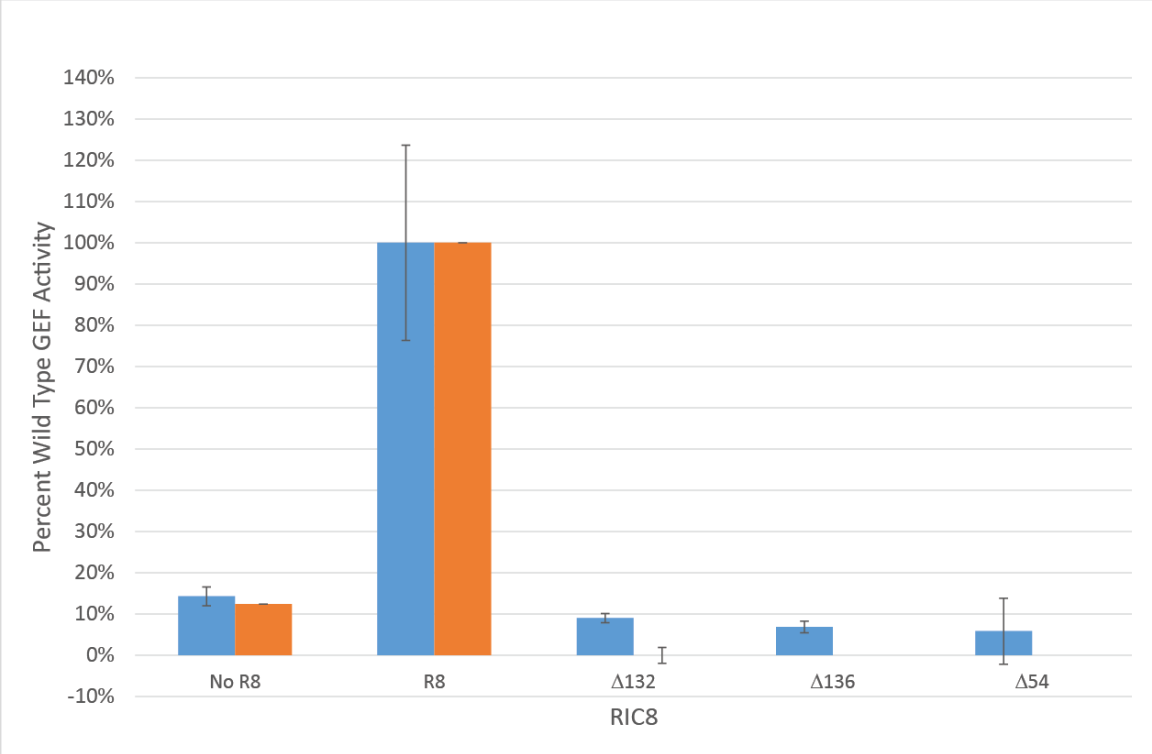

Figure 4.4: GEF activity of RIC8 truncation mutants towards Gα proteins. GEF activity was measured by detecting GTPγ^{35}S bound to Gα for each truncation mutant at 0 and 10 minutes. The difference is reported here, scaled to wild type RIC8 at 10 minutes. The blue bars indicate GEF activity towards GNA-1, and the orange bars indicate GEF activity towards GNA-3.

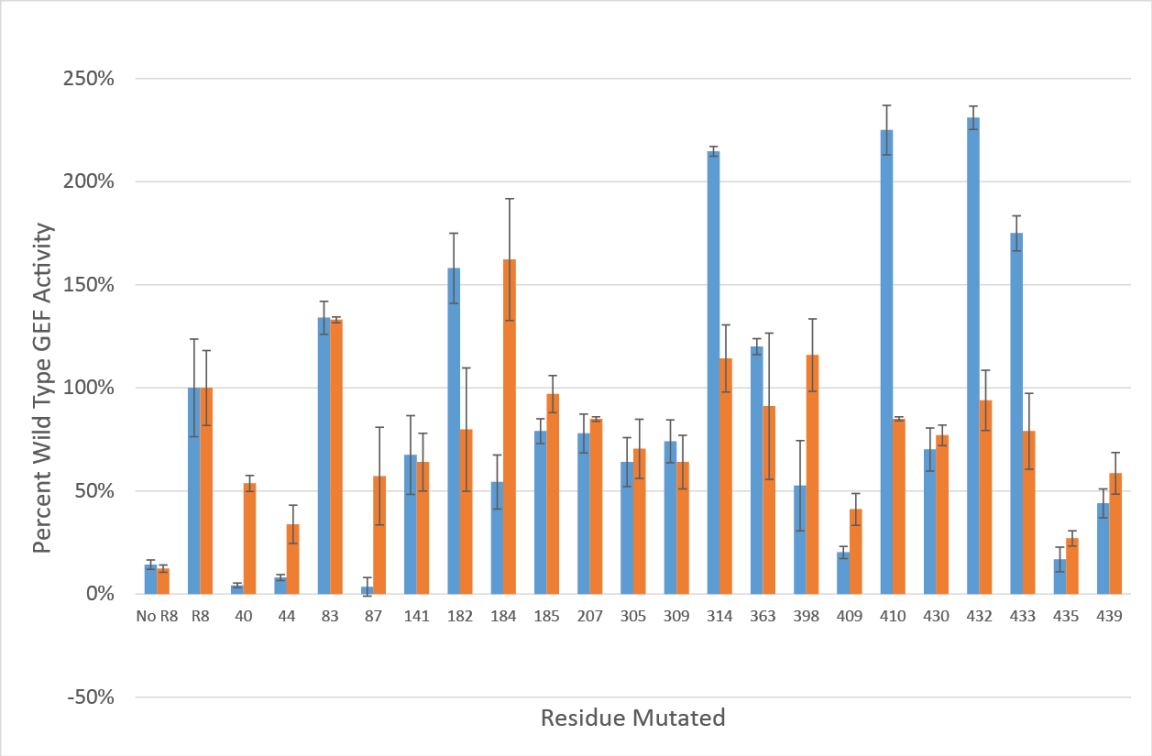

Figure 4.5: GEF activity of RIC8 glycine substitutions towards Gα proteins. GEF activity was measured by detecting GTPγ^{35}S bound to Gα for each glycine substitution mutant at 0 and 10 minutes. The difference is reported here, scaled to reactions with wild type RIC8 at 10 minutes. The blue bars indicate GEF activity towards GNA-1, and the orange bars indicate GEF activity towards GNA-3.

Appendix A: Media Recipes

***N. crassa* Media**

All *N. crassa* media can be made in either a solid or a liquid form. The recipes below describe the liquid form of each medium. To create a solid medium, Agar-Agar can be added to a recipe to a concentration of 1%. For microscopy involving fluorescence, Agar-Agar is substituted with agarose. All media is autoclaved 20-40 minutes on a liquid cycle to sterilize the solution, unless otherwise noted. Additionally, all media can be supplemented with nutrients or antibiotics at concentrations described in Table A.1. Exceptions to these considerations are noted as they occur. For any medium for where Ignite is used, 0.5% proline was added, and stock solutions without nitrogen (50x VM without NH_4NO_3) were used. After autoclaving, 400 μg/mL of Ignite was added to the medium. For hygromycin containing media, 200 μg/mL hygromycin B was added after autoclaving.

FGS: For 1 L of medium, 20 mL of VM stock salt solution (see VM recipe) and 20 g of agar-agar was added to 880 mL of water and autoclaved. The media was allowed to cool to 60°C in a water bath, and then 100 mL of 10x FGS stock solution (20% sorbose, 0.5% sucrose, and 0.5% fructose, filter sterilized) was added to the media and mixed thoroughly before pouring.

Regeneration Agar: For 600 mL regeneration agar, 12 mL 50x VM, 109.2 g sorbitol, 12 g yeast extract and 6 g of agar are dissolved in 504 mL water.

SCM: For 800 mL 0.8 g KNO_3, 0.54 g K_2HPO_4, 0.40 g KH_2PO_4, 0.40g $MgSO_4 \cdot 7H_2O$, 0.08g $CaCl_2$, 0.08 g NaCl, 80 μL biotin stock solution, 80 μL trace elements solution, 12 g sucrose, and 8 g agar were dissolved in water. Biotin stock solution was bade by dissolving 5 mg of biotin in a mixture of 25 mL water and 25 mL ethanol, and stored at 4°C. Trace elements were made by dissolving 5

g citric acid·1H_2O, 5 g $ZnSO_4$·7H_2O, 1 g $Fe(NH_4)_2(SO_4)_2$·6H_2O, 0.25 g $CuSO_4$·5H_2O, 0.05 g $MnSO_4$·1H_2O, 0.05g H_3BO_3, and Na_2MoO_4·2H_2O were dissolved in distilled water and stored at 4^oC until used.

VM: Vogels Minimal Medium is the most common *N. crassa* culturing medium. It consists of 1.5% sucrose, and 20 mL per liter of a 50x VM stock salt solution. The salt solution is composed of 755 mL water, 125 g sodium citrate dehydrate, 250 g KH_2PO_4, 100g NH_4NO_3, 10g $MgSO_4$·7H_2O, 5 g $CaCl_2$·2H_2O, 5 mL trace element solution, and 2.5 mL biotin stock solution, and preserved with 5 mL chloroform at room temperature.

Yeast Media

All media can be made as liquid form as described below or solid form by addition of 1.5% Agar-Agar. All media is autoclaved for 20-40 minutes on a liquid cycle to sterilize the solution and melt agar unless otherwise noted.

SD-Trp-Leu (Synthetic dropout minus tryptophan and leucine): 20 g dextrose, 6.7 g YNB (yeast nitrogen base), 2 g drop-out mix (without YNB, with AAs, without Trp, Leu), (15 g Agar-Agar for solid media), 1 L water, and 1 mL 1 M NaOH (to reach pH 5.8).

SD-Trp (Synthetic dropout minus tryptophan): SD-Trp-Leu media plus 10 mL/L of filter sterilized 10 mg/mL leucine stock solution.

SD-Leu (Synthetic dropout minus leucine): SD-Trp-Leu media plus 10 mL/L of filter sterilized 10 mg/mL tryptophan stock solution.

SD-Trp-Leu-Ade-His: 20 g dextrose, 6.7 g YNB, 2 g drop-out mix (without YNB, with AAs, without Trp, Leu, His, or Ade), (15 g Agar-Agar for solid media), 1 L water, and 1 mL 1 M NaOH (to reach pH 5.8).

SD-Trp-Leu-Ade (Synthetic dropout minus tryptophan, leucine and adenine): SD-Trp-Leu-Ade-His media plus 10 mL/L of filter sterilized 5 mg/mL histidine stock solution.

SD-Trp-Leu-His (Synthetic dropout minus tryptophan, leucine and histidine): SD-Trp-Leu-Ade-His media plus 10 mL/L of filter sterilized 1 mg/mL adenine hemisulfate stock solution.

SD-Ura (Synthetic dropout minus uracil): 20 g dextrose, 6.7g YNB, 2 g drop-out mix (without YNB, with AAs, without Ura), (15 g Agar-Agar for solid media), 1 L water, and 1 mL 1 M NaOH (to reach pH 5.8).

YPDA: 8 g yeast extract, 16 g dextrose, 16 g peptone, 80 mg adenine hemisulfate, (12 g Agar-Agar for solid media), and 1 L water.

Bacteria Media

General notes:

All bacteria media can be made as either a solid or liquid medium. The recipes below describe the liquid form of each medium. To create a solid medium Agar-Agar can be added to a recipe to a concentration of 1.5%. All media is autoclaved for 20-40 minutes on a liquid cycle to sterilize the solution and melt agar unless otherwise noted. Bacterial media can be supplemented with 100 μg/mL ampicillin or 50 μg/mL kanamycin after autoclaving as needed.

LB: For 1 liter 10 g tryptone, 5 g yeast extract and 10 g NaCl are dissolved in 1 L of water.

Appendix B: Protocols

Sterile technique – *N. crassa* is a vigorous grower and easily disperses its conidia. All culturing of *N. crassa* and other microorganisms in a lab that works with *N. crassa* must be performed with appropriate sterile technique. Any protocol designated sterile will presume standard sterile technique (working near a flame, only using autoclaved or filter sterilized solutions and supplies, and other industry standard practices) and in the case of *N. crassa* and yeast protocols, all sterile protocols are also to be performed in a hood – either laminar flow or biosafety cabinet – unless otherwise noted. In the case of bacteria, samples can be worked with near a flame outside a hood unless otherwise noted.

Species Independent Protocols

Cell Counting: Harvested cells of *E. coli*, yeast, or *N. crassa* were diluted in 1:10, 1:100, 1:1,000, and 1:10,000. 10 μL of the 1:1,000 dilution was loaded onto a clean hemocytometer. The hemocytometer was observed on a compound microscope with a 60x objective. The cells in each of four 0.04 mm^2 squares are counted. If more than 100 or less than 10 cells were observed in a square, a higher or lower dilution was used respectively. The count from 4 cells was averaged, and divided by its volume (4 nL) to obtain a concentration.

Spread Plating: A suspension of cells is pipetted onto an agar plate. A bent glass rod is dipped in 90% ethanol, and ignited in a Bunsen burner. After the flame burns out the rod is allowed to cool for a few seconds, and then the suspension of cells is spread by swiping the bent rod back and forth across the plate with one hand as the plate is rotated with the other hand until the suspension of cells has been absorbed into the plate.

Streak plating: Streak plating is accomplished by collecting cells on a sterile loop, stick, or toothpick and streaking it back and forth 2-3 times on one side of a plate. A fresh stick or toothpick, or a sterilized loop was used to drag from the corner of the initial inoculation, and streaked 2-3 more times across the plate. This was repeated twice more to spread cells across the entire plate.

***N. crassa* Protocols**

Colony Picking Plates with colonies to be picked were grown until distinct colonies 1 mm or more in diameter were visible, but not overlapping. Distinct colonies were picked using a sterile 5¾ inch Pasteur pipette. A bulb was placed on the Pasteur pipette and slightly depressed, and the tip was pushed into the agar surrounding the center of the colony. Light suction was applied by partially releasing the bulb, and the Pasteur pipette was removed from the plate with the agar plug in the tip of the pipette. This was transferred to a slant with appropriate nutrients and antibiotics by depressing the bulb rapidly to expel the agar plug.

Conidia Harvesting: 50 mL of sterile water was added to a flask of *N. crassa* (Flask Growth), and the flask was vortexed ~30 seconds to dislodge conidia. For Δ*ric8* mutants and others which produce conidia dense to the surface of the agar, a sterile stick was scraped across to dislodge conidia and the sample was vortexed again. The conidial suspension was poured through a handiwipe into a sterile flask, and transferred to a 50 mL conical tube. The conidia were pelleted in a Centra CL3 centrifuge with a 5 minute, 2,500 RPM spin in a 243 rotor, and re-suspended in 25 mL fresh sterile water. This was stored on ice until used.

Flask Growth: 40 mL of VM agar in a sterile 125 mL flask was inoculated with conidia or hyphae from a *N. crassa* slant. This was grown 2 days in the dark at 30°C, and then 3-5 days at 25°C in the light.

DNA Extraction – Phenol:Chloroform 5 mL of VM media in an 18x150 sterile tube with all necessary nutrients but no antibiotics was inoculated with *N. crassa* conidia using a wood stick. This was grown in a 30°C shaker at 200 RPM for 2-5 days (wild type-type typically 2, Δ*ric8*-like typically 4-5 days). The hyphae are collected by vacuum filtration on 2.5 cm Whatman filter paper and washed with sterile water. The cell pad is transferred to a 2.0 mL screw cap tube and pulverized under liquid nitrogen with a glass rod. 500 mL of lysis buffer (50 mM TrisCl pH 7.5, 250 mM NaCl, 0.5% SDS, 50 mM EDTA, 100 μg/mL Proteinase K) was added to the cell pulverized tissue and the sample was placed in a 55°C water bath for 1-4 hours. The sample was then centrifuged at 14,000 RPM for 5 minutes in a microfuge, and the supernatant was transferred to a new eppendorf tube, and supplemented with TE to reach 500 μL. The sample was mixed with 500 μL of 1:1 Phenol-Chloroform, centrifuged for 5 minutes, and then the supernatant (avoiding the interface) was transferred to a new tube. This was repeated once more, and then a last time with 24:1 Chloroform-Isoamyl alcohol. The final supernatant was mixed gently by inversion with 1 mL of 100% ethanol, and placed at -20°C for 20 minutes. The sample was then pelleted for 15 minutes at 4°C in a microfuge at 14,000 RPM. The supernatant was discarded and the pellet was washed with 500 μL of cold 70% ethanol, and centrifuged for 10 minutes at 4°C. The supernatant was poured off again, and the pellet was dried in a speed vacuum until dry. Finally, the pellet was re-suspended in 50 μL of TE buffer and stored at -20°C.

DNA Extraction – Phenol:Chloroform Large Scale: A condial suspension is used to inoculate a 250 mL flask with 50 mL of VM (plus any necessary supplements). This is grown at 30°C with 200

RPM shaking for 2 days in the dark. The flask is swirled to dislodge any hyphae stuck to the side of the flask, and vacuum filtered through 2 layers of handiwipes in a Buchner funnel. The hyphal mass was squeezed between paper towels to remove excess liquid, and then frozen at -80°C. They hyphae were then ground with mortar and pestle under liquid nitrogen, and the pulverized tissue was added to 10 mL of *N. crassa* SDS buffer (0.15 M NaCl, 0.1 M EDTA, 2% SDS, pH 9.5, 10 μg/mL) in a 125 mL flask. It was incubated at 37°C for 24 hours mixing intermittently. 10 mL of sterile water was added, and the suspension was centrifuged at 10,000 RPM for 10 minutes at 4°C. The supernatant is transferred to a fresh tube, and 2.5 volumes of 100% ethanol is added to precipitate DNA. The sample is centrifuged for 60 seconds at 10,000 RPM, and the supernatant is removed. The pellet is air-dried briefly, and re-suspended in 1 mL TE buffer by gentle mixing. 80 mg of proteinsase K is added once the DNA is dissolved and the sample is incubated at 37°C for 2 hours. This 1 mL solution is extracted 3 times with phenol and twice with chloroform by adding 1 mL of the organic liquid, mixing, and briefly centrifuging, transferring the clean top layer to a fresh tube after each extraction. 2.5 volumes of 100% ethanol are added to the sample and it is centrifuged 60 seconds at 14,000 RPM. The supernatant was removed, the pellet was dried briefly, and finally the sample was re-suspended in up to 2 mL of TE buffer.

DNA Extraction – Puregene: 5 mL of VM media in an 18x150 sterile tube with all necessary nutrients but no antibiotics was inoculated with *N. crassa* conidia using a wood stick. This was grown in a 30°C shaker at 200 RPM for 2-5 days (wild type-type typically 2, Δ*ric8*-like typically 4-5 days). The hyphae are collected by vacuum filtration on 2.5 cm Whatman filter paper and washed with sterile water. The cell pad is transferred to a 2.0 mL screw cap tube and pulverized under liquid nitrogen with a glass rod. 600 μL of Cell Lysis Solution (Gentra, Minneapolis, MN) and 3 μL Proteinsase K Solution (20 mg/mL) was added to the pulverized tissue and briefly

vortexed. The sample was incubated 1-12 hours at 55°C. The sample was cooled to room temperature and 200 μL Protein Precipitation Solution (Gentra) was added and placed on ice for 10 minutes. The mixture was vortexed and then centrifuged for 5 minutes at 14,000 RPM. The supernatant was transferred to a clean tube, and 600 μL isopropanol was added. The sample was mixed by inverting, and then centrifuged for 10 minutes at 14,000 RPM. The supernatant was poured off, and the pellet was washed with 1 mL cold 70% ethanol and centrifuged for 10 minutes at 14,000 RPM. The ethanol was discarded, and residual ethanol was removed by pipetting. The sample was then dried in a vacuum centrifuge, and re-suspended in 100 μL of TE and if desired 1 μL RNase.

Microscopy – Germination Assays: A 5-10 mm by 20-40 mm piece of agar was excised from a petri dish with germinating conidium, and inverted on a few drops of VM liquid on a cover slip. Germinating conidia were imaged using DIC on an Olympus IX71 inverted microscope (Olympus America, Center Valley, PA) with a 60x oil immersion objective. A QIClickTM digital CCD camera (QImaging, Surrey, British Columbia, CA) was used to collect images which were analyzed using Metamorph (Molecular Devices Corporation, Sunnyvale, CA).

Sexual Crosses: For a sexual cross, the strain to be used as the female is inoculated on a SCM slant. This is grown 7 days in continuous light at 25°C. The slant is then cleaned of aerial hyphae and conidia with a sterile swab dipped in sterile water. Then, a conidial suspension of the strain to be used as a male is prepared by inoculating a sterile stick with conidia into an eppendorf tube with 500 μL of sterile water. The suspension is washed two times by centrifuging at 3,000 RPM for 1 minute, aspirating the supernatent, and re-suspending the conidia in 500 μL of sterile water. A sterile swab is then dipped in this conidial suspension, and rubbed over the surface of the slant. The slant is then returned to the light for at least 2 weeks for ascospores to be ejected

and mature. Ascospores are collected using a wet sterile swab, and re-suspended in sterile water. The spores can be stored on the glass at 4°C for years, or in water at 4°C for a few months.

To isolate progeny, a 50 μL aliqot of spores is heat shocked in a 60°C water bath for 45 minutes, and then cooled to room temperature. Spores are plated on FGS with appropriate antibiotics and nutrients according to the Spread Plating protocol, using a one-time use spreader made from a 9 inch Pasteur pipette sealed by heating in a Bunsen burner at the tip, and bent to a 90° angle by heating in a Bunsen burner about 5 cm from the tip. The spores are incubated 1-2 days, and then picked next to a Bunsen burner using a flame sterilized flattened platinum wire, and transferred to a VM slant with appropriate antibiotics and nutrients.

Slant Growth: A slant was poured by adding 3 mL molten agar to a 10x100 mm tube, and then adding it to a rack at a 20-40° angle above horizontal. After cooling, the solid slant was inoculated with conidia or hyphae and incubated 2 days at 30°C in the dark, followed by 3 days at 25°C in the light.

Transformation: Electroporation: 8 day old conidia is harvested according to the Conidia Harvesting protocol, and washed in 25 mL water then 25 mL cold 1M sorbitol, with 2,500 RPM spins in a 50 mL conical tube in a clinical CL3 centrifuge, and finally re-suspended in 0.5 mL of the same cold 1M sorbitol solution. The conidia are quantified according to the Cell Counting protocol, and diluted/ concentrated with 1M sorbitol to reach a concentration of 2.5×10^9 conidia per mL. 40 mL aliquots are made and placed on ice in eppendorf tubes, and 1-10 μL bearing 1-2 μg of DNA are added to the tube (or the equivalent volume of TE for a negative control). The sample is transferred to the bottom of an electroporation cuvette, by pipetting and tapping the cuvette. The cuvette is dried and inserted into an Eppendorf 2510 Electroporator is

set to 2000 volts, where it is electroporated (the time constant should be above 5.0 to indicate a successful electroporation). Immediately after electroporation, 1 mL of cold 1 M sorbitol is added to the cuvette and mixed with a pastuer pipette. The sample is then returned to its eppendorf tube, and 100 μL and 940 μL are added to 10 mL of regeneration agar (containing appropriate antibiotic and nutrients), mixed by inverting 2-3 times, and then poured on top of a FGS plate containing appropriate nutrients and antibiotics. This plate is allowed to solidify, and then incubated 2-5 days before picking colonies using the Colony Picking protocol.

Yeast Protocols

Yeast Crosses: Diploids of yeast were obtained by a cross between mating type a and mating type α yeast haploids. The a and α strains were inoculated by streaking in opposite, overlapping directions onto a YPDA plate. This plate was incubated 24-48 hours, at which time a sterile toothpick was used to collect cells from multiple of the intersections of the two strains. These diploids were inoculated onto a SD-Trp-Leu plate by streak plating and incubated 48-72 hours.
Yeast Smash and Grab DNA Miniprep: Inoculate 5 mL of appropriate media with a single yeast colony and grow for 2 days at 30^{o}C with 200 RPM shaking. The cells were pelleted in an Eppendorf tube for 1 minute at 14,000 RPM and the supernatant was discarded. 0.3 mL of 425-600 micron glass beads (Sigma G-9268), 0.2 mL of lysis buffer (1- mM Tris, pH 8.0, 1 mM EDTA, 100 mM NaCl, 1% SDS, 2% Triton X-100) and 0.2 mL of a 1:1 phenol/chloroform mix were added to the pellet and the tube was vortex vigorously for 2 minutes. 0.2 mL of TE (10 mM Tris, 1 mM EDTA, pH 8.0) was added and the sample was vortexed for a 10 more seconds. The tubes were spun for 5 minutes at room temperature at 14,000 RPM. The upper (aqueous) phase was transferred to a fresh Eppendorf tube. 2 volumes of 100% ethanol and thoroughly mixed by

inverting. The sample was centrifuged 3 minutes at 14,000 RPM and the supernatant was discarded. The pellet was washed with 0.5 mL cold 70% ethanol and centrifuged for 5 seconds. The supernatant was removed, and excess ethanol was blotted on a paper towel. After spinning on a vacuum centrifuge to dry and the pellet was re-suspended in 50 μL TE.

Yeast Transformation: 5 mL of YPDA is inoculated with a single yeast colony and grown overnight at 30°C with 200 RPM shaking. This was transferred into a 250 mL baffle flask with an additional 50 mL of YPDA, and grown for 3-6 hours at 30°C with 200 RPM shaking until the OD_{600} reaches 1. This was pelleted in a 50 mL conical tube at 4,000 RPM in a Centra CL3 Centrifuge with a 243 rotor for 5 minutes. The supernatant was discarded and the pellet was washed with 25 mL of sterile water and pelleted as before. The pellet was re-suspended in 1 mL 100 mM LiOAc and transferred to a microfuge tube. This was pelleted for 15 seconds at 14,000 RPM in a microcentrifuge, the supernatant was discarded, and the pellet was re-suspended in 400 μL 100 mM LiOAc. The mix was vortexed, and 50 μL aliquots were pipetted into separate sterile Eppendorf tubes. These were spun 15 seconds at 14,000 RPM and the supernatant was removed. 326 μL of transformation mix (240 μL 50% polyethylene glycol 3350, 36 μL 1 M LiOAc, 50 μL of previously boiled salmon sperm DNA) was added to each tube, and then 34 μL of DNA plus water was added. The mix was vortexed to re-suspend the pellet, and incubated at 30°C for 30 minutes. The sample was inverted 2-3 times, and then heat shocked in a water bath for 30 minutes at 42°C. This was pelleted for 15 seconds at 14,000 rpm, and the pellet was re-suspended in 1 mL of sterile water. This entire sample was spread plated on a single plate of the appropriate selective medium.

Bacteria Protocols

DNA Extraction – Boiling Miniprep: 1.5 mL of an overnight *E. coli* culture is transferred to an eppendorf tube. The tube is centrifuged in a microfuge at 6,000 RPM for 30 seconds, and the supernatant is aspirated. 300 mL of STET (8% sucrose, 50 mM TrisCl pH 8.0, 50 mM EDTA, 5% Triton X-100, filter sterilized) is added, the pellet is dislodged with a toothpick, and vortexed to completely re-suspend cells. 20 μL of lysozyme is added, the tube is vortexed, and the tube is incubated in a 100^{o}C heating block for 2 minutes. The sample was centrifuged for 5 minutes at 6,000 RPM, and the loose pellet is removed using a toothpick leaving the supernatant in the tube. 300 μL of ammonium acetate/ isopropanol (5 volumes 8 M ammonium acetate: 12 volumes isopropanol) is added and the tube is vortexted. The sample is centrifuged for 5 minutes at 14,000 RPM, the supernatant is poured off, and the open tube is blotted on a paper towel. The pellet is re-suspended in 500 μL of 70% ethanol by vigorous vortexing. The suspension is centrifuged at 14,000 RPM for 5 minutes, and the supernatant is again poured off and the tube blotted on a paper towel. The residual ethanol is evaporated in a Speed-Vac, and the pelleted DNA is re-suspended in 50 μL of TE by vortexing.

Making Chemically Competent Cells: A tube with 2 mL of LB is inoculated with a colony of DH5α and grown overnight at 37^{o}C with 225 RPM shaking. 1 mL of this is added to each of 2 baffle flasks containing 100 mL of LB medium. The flasks are grown for ~2.5 hours, until the OD_{600} reaches 0.6-0.8. Once the desired OD is reached, samples are pelleted in 8 – 35 mL oak ridge tubes in a SA600 rotor at 4,500 RPM at 4^{o}C for 10 minutes. The supernatant is discarded, and the pellet is re-suspended in a total of 15 mL Solution A (2.1% MOPS pH 7.0, 1.2% RbCl), and centrifuged as before. The supernatant is again removed, and the pellet is re-suspended in 15 mL of Solution B (2.1% MOPS, 1.2% RbCl, 7.3% $CaCl_2$). This is left on ice for 30 minutes, and then

centrifuged as above. The supernatant is removed, and the pellet is re-suspended in 12 mL of Solution C (2.1% MOPS, 1.2% RbCl, 7.3% $CaCl_2$, 1.5% glycerol). Immediately, this aliqoted in 200 μL portions into eppendorf tubes, and flash frozen with liquid nitrogen. The cells are stored at -80°C until they are used.

Making Electrocompetent Cells: Two tubes each containing 5 mL of LB are inoculated with DH5α and grown overnight at 37°C with 225 RPM shaking. This is used to inoculate 1 liter of LB media in a Fernbach flask, which is grown at 37°C with 225 RPM until the OD_{600} reaches 0.5 to 0.8. The flask is placed on ice for 15 minutes, and then cells are pelleted at 4,000 xg for at 4°C for 15 minutes. The cells are re-suspended in 1 L of cold sterile water, and centrifuged as before. The pellet is re-suspended in 500 mL cold sterile water, and centrifuged again with the same parameters. The cells are re-suspended in 20 mL of 10% glycerol, and centrifuged as before for a final time. The pellet is re-suspended in 2-3 mL of 10% glycerol relative to the OD_{600}, and stored in 40 μL aliquots at -80°C.

TA Cloning: 1-7 μL of purified PCR product is mixed with 1 μL 10x Taq buffer, 0.2mM dATP, and 5 units of standard Taq polymerase brought to 10 μL with distilled water. This is incubated at 70°C for 20 minutes. 2 μL of the product is mixed with 1 μL pGEMT, 1 μL T4 DNA ligase, 1 μL 10x ligase buffer, 5 μL water, and incubated at 16°C overnight.

Transforming Chemically Competent Cells: An aliqot of chemically competent cells is thawed from -80°C storage on ice. 1 to 10 μL of DNA is added to 200 μL of cells, and incubated on ice for 20 minutes. The tube is then incubated in a 42°C heating block for 2.5 minutes. 1 mL of LB medium is added to the tube, and the sample is incubated for 30-60 minutes at 37°C with shaking. 100 μL is Spread Plated on a plate containing the appropriate antibiotic, and the remainder is concentrated with a 60 second spin at 600 RPM, and the remainder is re-supended

and Spread Plated on a single plate. These are incubated overnight at 37°C. For plasmids amenable to Blue-White color selection, 40 mL of 0.1 M IPTG and 40 mL of 20 mg/mL XGAL are spread with a sterilized glass spreader on the plate a few minutes prior to spreading the cells.

Transforming Electrocompetent Cells: a cuvette is chilled on ice while a 40 μL aliqot of electrocompetent cells is thawed on ice. The electroporator is set to 2,500 volts, and 1 to 5 μL (~25 ng) of DNA is added to the cells. The cell mixture is transferred to the cuvette, which is electroporated, ideally resulting in a 4 to 5 millisecond time constant. The sample is re-suspended in LB medium, transferred to a sterile eppendorf, and grown at 37°C with 225 RPM shaking for 1 hour. Cells are plated on appropriate medium and grown overnight to obtain colonies.

DNA Extraction – Qiagen Miniprep: All buffers and materials for this protocol are made by Qiagen. A 5 mL volume of LB was inoculated with a single bacterial colony and grown overnight at 37°C with 225 RPM shaking. The cells were pelleted with 60 second spins at 14,000 in a microfuge, and re-suspended in 250 μL of Buffer P1. 250 μL of Buffer P2 was added, and the tube was inverted 5 times. Within 5 minutes, 350 μL of Buffer N3 was added and the sample was inverted 5 times. This was pelleted for 10 minutes at 13,000 RPM and the supernatant was decanted to a QIAprep spin column. This was centrifuged 60 seconds, and the flow through was discarded. 750 μL Buffer PE was added to the column, and the column was centrifuged for 60 seconds at 13,000 RPM. The flow through was discarded, and the column was centrifuged for an additional 60 seconds. The column was finally transferred to a clean tube, and 50 mL Buffer EB was applied to the center of the column. After waiting 60 seconds, the column was centrifuged for 60 seconds at 13,000 RPM and the flow through was stored at -20°C.

DNA work Protocols

DNA Concentrating – QiaexII: DNA Concentration with QiaexII is accomplished by using combining DNA samples into a single tube, adding 3 volumes of Buffer QX1 and 10 μL of freshly vortexed QIAEXII to the tube, and following the Gel Extraction protocol from immediately after the water bath step.

Gel Electrophoresis: A gel mixture that contained 1x TAE Buffer (4.8% Tris base, 1.1% glacial acetic acid, 0.37% EDTA disodium salt) and 0.7% to 2% agarose was melted in a microwave. This was poured into a gel cast, and a comb was inserted. After the gel solidified and cooled, the comb was removed and the gel was submerged in 1x TAE Buffer. Samples were brought to 1x with loading dye, and added to wells, and the gel was run at 70-120 volts.

Gel Extraction – QiaexII: A band (250 mg or less) is excised from a gel with a razor blade, and transferred to a pre-weighed 1.5 mL tubes. The tube with the gel was re-weighed, the difference being the mass of the gel. 3 volumes of Buffer QX1 and 10 μL of freshly vortexed QIAEXII were added to the tube. The tube was incubated for 10 minutes in a 50^{o}C water bath, vortexing the sample every 2 minutes. The sample was pelleted with a 14,000 RPM spin, and the supernatant aspirated. The pellet was washed with 500 mL of Buffer QX1 and then twice with Buffer PE. The pellet was air dried for 10-15 minutes until the pellet was barely white. 20 μL of TE was added, and the sample was vortexed and incubated for 5 minutes at room temperature. The sample was pelleted at 14,000 RPM, and the supernatant was transferred to a clean tube.

PCR – Standard Taq: A 20 μL PCR reaction is composed of 1 μL 100 pM fw primer, 1 μL 100 pM rv primer, 1 μL template, 2 μL 5x Taq Master Mix (NEB), and 15 μL water. Reactions can have up to 5% DMSO added if necessary. Reactions are carried out in a PCR tube on a thermocycler. Initial denaturation was 95^{o}C for 30 seconds, followed by 35 cycles of 95^{o}C for 20 seconds

denaturing, 45-68°C for 15-60 seconds annealing, and 68°C for ~60 seconds/kb. A final 5 minute extension at 68°C was performed, and the sample was held at 4°C.

PCR – Phusion: A 50 μL PCR reaction is composed of 2 μL 100 pM fw primer, 2 μL 100 pM rv primer, 2 μL template, 25 μL 2x Phusion Master Mix (NEB), and 19 μL water. A 20 μL reaction uses the 1 μL of each primer and template, 10 μL master mix, and 7 μL water. Reactions can have up to 5% DMSO added if necessary. Reactions are carried out in a PCR tube on a thermocycler. Initial denaturation was 98°C for 30 seconds, followed by 35 cycles of 98°C for 10 seconds denaturing, 45-72°C for 10-30 seconds annealing, and 72°C for ~30 seconds/kb. A final 10 minute extension at 72°C was performed, and the sample was held at 4°C.

PCR Purification – Qiagen: 5 volumes of Buffer PB was added to 1 volume of PCR product. The entire mixture was transferred to a QIAquick spin column in a 2 mL collection tube. The sample was centrifuged 30 seconds at 14,000 RPM, and the flow through was discarded. 0.75 mL Buffer PE was added to the column, and it was again centrifuged 30 seconds at 14,000 RPM. The flow through was discarded, and the column was centrifuged for 60 more seconds. The column was then transferred to a clean 1.5 mL tube without a cap, and 50 mL of Buffer EB was applied to the column. The column was incubated 1 minute at room temperature, and then centrifuged for 30 seconds at 14,000 RPM. Finally, the flow through was transferred to a clean tube and stored at -20°C until used.

Sequencing: Sample submitted for sequencing at the UCR Genomics Core facility (Riverside, California) contained a 12 μL total volume with ~500 ng plasmid and 5 pM primer.

Protein work Protocols

Protein Gel: A protein gel was made by mixing 3.06 mL water, 6.25 mL Buffer A (18% Tris base, 0.4% SDS, pH 8.8), 3.12 mL acrylamide, 60 μL 10% APS, and 7 μL TEMED. This was poured into a cast, topped with water and allowed to polymerize for 45 minutes. The water layer was poured off, and the inside of the cast was dried with a piece of filter paper. A stacking gel was made from 2 mL water 2.5 mL Buffer B (6% Tris base, 0.4%SDS, pH 6.8), 500 μL acrylamide, 60 μL 10% APS, and 7 μL TEMED. A comb was added with the appropriate number of lanes, and this was allowed to polymerize for 35 minutes. The comb was removed, the gel was washed and the wells flushed with running buffer (0.3% Tris base, 1.4% glycine, 0.5% SDS). Samples were brought to 1x concentration of Laemmli sample buffer (4x buffer: 13 mL Buffer B, 10 mL glycerol, 2 g SDS, 5 mL β-mercaptoethanol, 50 mg bromophenol blue) and loaded by pipette. The gel was run at 225 volts until the dye front had just run off.

Commassie Staining: After a gel had finished running, it was rinsed gently with distilled water, and placed in a container with enough comomassie stain (0.1% coomassie brilliant blue, 25% methanol, 10% glacial acetic acid, completely dissolved) to completely cover the gel. This was mixed with gentle agitation for 1 hour to overnight, and then destained in destain solution (10% glacial acetic acid, 25% methanol) for 1 hour or until bands retained an intense color but background had become clear. This was then placed between two pieces of cellophane wet with destain solution, bubbles were removed, and the gel was stretched and allowed to dry overnight.

Appendix C: Yeast two hybrid analysis of interactions between RIC8, Gα, and MAPK signaling related proteins.

Introduction:

RIC8 is an essential signaling protein that is involved in Gα regulation and potentially Mitogen Activated Protein Kinase (MAPK) regulation. The link between RIC8 and Gα proteins has been well established in mammals and fungi (Kataria et al., 2013; Siderovski & Willard, 2005; Wright et al., 2011). Given that Gα proteins are involved in MAPK signaling, it has also been theorized that MAPK signaling is controlled by RIC8 (Eaton et al., 2012). What is not known is whether direct physical interaction is involved between any of these signaling proteins.

Materials and Methods:

Yeast haploids were obtained from a variety of previous studies. A yeast two hybrid screen using *N. crassa* GNA-1 as bait revealed a number of novel interactors (Wright et al., 2011). Additionally, a similar screen using RIC8 as bait revealed a group of interactors (Kim and Borkovich, unpublished). Yeast two hybrid strains for a variety of MAPK proteins involved in osmosensing were generated while studying RRG-1 (Jones, 2008). Finally, work has been done to analyze interactions between MAPK components using the yeast two hybrid system (Dettmann et al., 2012). All the haploids used and their sources are listed in table A.C.1.

To obtain diploids, GAD strains were mated with GBK strains (Appendix B). Diploids were grown on SD-Trp-Leu, SD-Trp-Leu-Ade, and SD-Trp-Leu-Ade-His plates. Strains which grew only on SD-Trp-Leu are listed in the Table A.C.2 as DD for Double Dropout, and proteins scored as having no interaction. Strains that grew on SD-Trp-Leu-Ade, but not on SD-Trp-Leu-Ade-His, are

indicated as TD for Triple Dropout, and the two proteins were concluded to have a weak to moderate interaction. Finally, strains which grew on SD-Trp-Leu-Ade-His were listed as QD for quadruple dropout, and were concluded to contain proteins that strongly interact. Data derived from a single experiment that needs to be repeated is indicated with an asterisk (*). Most experiments were performed in duplicate, and when duplicate experiments did not agree the results were indicated by double asterisks (**). Finally, if duplicate experiments did not agree, in most cases a third experiment was performed, and the result which was arrived at twice was reported without any qualifications in the table.

Results:

In total, 281 diploids were generated and tested for this assay. Results for 75% (213) indicated there was no interaction between the two proteins. Only 9% (20 on TD, five on QD) displayed results indicative of a protein-protein interaction based on multiple trials. The remaining 16% are putative interactors that need to be confirmed by retesting. All results are listed in Table A.C.2.

Discussion:

This study produced a small set of interacting proteins, many of which occurred between pathways. Interestingly, the mitogen activated protein kinase kinase MEK-1 interacted with the GNA-1 interactor PDX-1, pyridoxine 1, involved in vitamin B_6 biosynthesis. Also, the MAPK protein STE7 interacted with the unnamed GNA-1 interactor NCU09632, which is predicted to be a phosphodiesterase or alkaline phosphatase. Finally, the RIC8 interactor GEL-1 is a glycolipid-anchored surface protein which interacted with HYM-1, a scaffold for MAPK

components including MAK2, suggesting that while RIC8 may not interact directly with MAPK proteins, it does interact with proteins that themselves interact with MAPK proteins. This data is primarily presented to be a resource for future studies, as much of it needs further validation, but it does point to a number of potentially interesting cross-pathway interactions worth investigating.

Table A.C.1: Yeast haploids used in this study.

NCU#	Gene Symbol	Source	Vector
-	*empty*	Clontech	GAD
-	"	"	GBK
406	*cla-4*	(Dettman et al, 2012)	GAD
"	"	"	GBK
440	*gnb-1*	(Wright et al, 2011)	GAD
"	"	"	GBK
453	-	RIC8 interactor	GAD
455	*ste50*	"	"
636	-	"	"
1162	*gel-1*	"	"
1489	*hpt-1*	(Dettman et al, 2012)	"
"	"	"	GBK
1895	*rrg-1*	(Jones, Dissertation)	GAD
"	"	"	GBK
2234	*mik-11-*^{1007}	(Dettman et al, 2012)	GAD
2393	*mak-2*	"	GBK
2788	*ric8*	(Wright et al, 2011)	GAD
"	"	"	GBK
3071	*os-4*	(Jones, Dissertation)	GAD
"	"	"	GBK
3530	*acw-6*	RIC8 Interactor	GAD
3576	*hym-1*	(Dettman et al, 2012)	GBK
3894	*ste-20*	"	GAD
4612	*ste-7*	"	"
"	"	"	GBK
5206	*gna-3*	(Wright et al, 2011)	GAD
"	"	"	GBK
6182	*nrc-1*	(Dettman et al, 2012)	GAD
"	"	"	GBK
6419	*mek-1*	"	GAD
"	*mek-1*$^{217-518}$	"	"
"	*mek-1*	"	GBK
6493	*gna-1*	(Wright et al, 2011)	GAD
"	"	"	GBK
6550	*pdx-1*	GNA-1 interactor	GAD
6729	*gna-2*	(Wright et al, 2011)	"
"	"	"	GBK
7014	*crp-3*	GNA-1 interactor	GAD
9632	-	RIC8 interactor	"
11324	-	"	"

Table A.C.2: Yeast two hybrid interactions between RIC8, Gα, and MAPK components.

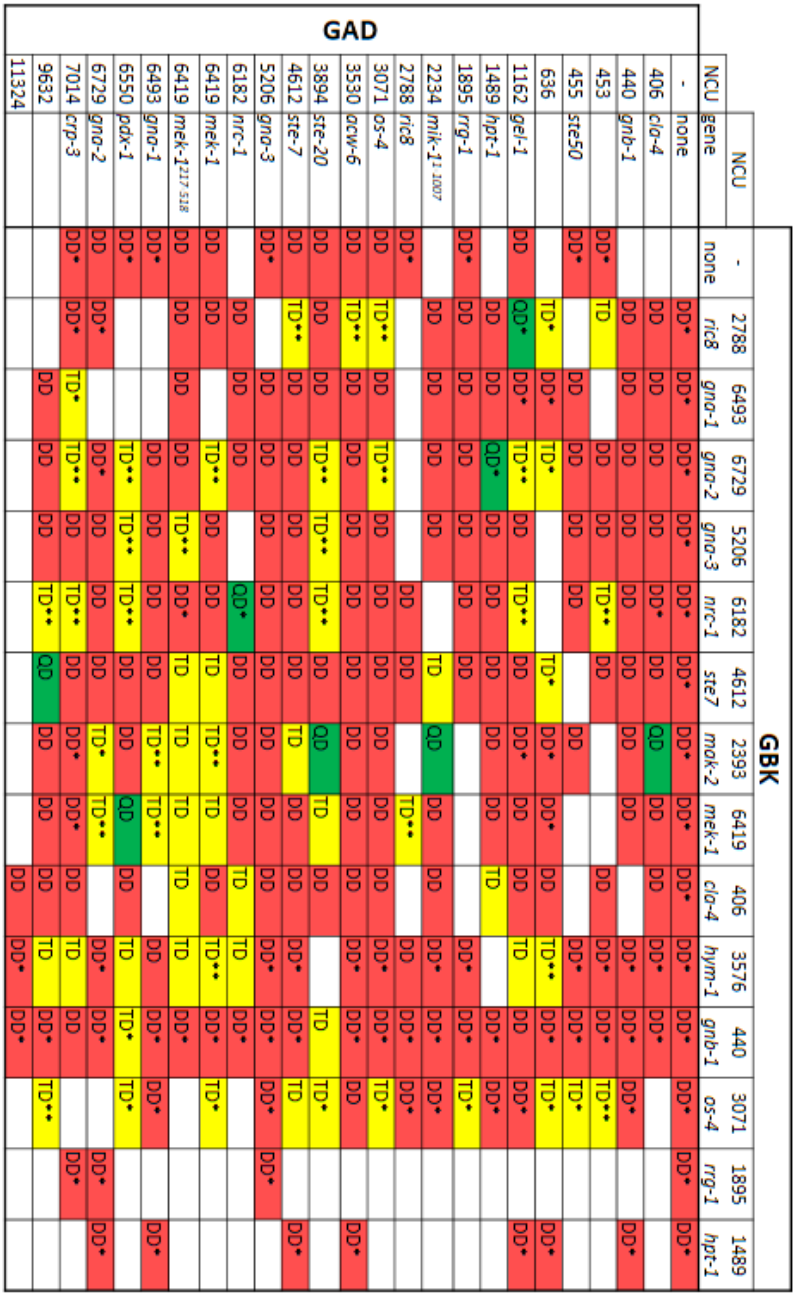

Appendix D: Yeast two hybrid analysis of regions of STE50 essential for interaction with RIC8

Introduction.

Sterile 50 (STE50) is a protein identified by yeast two hybrid screens to interact with RIC8 (Kim, J., unpublished). STE50 in other systems is known to function as a scaffold for MAP kinase (MAPK) signaling (D. Li, Bobrowicz, Wilkinson, & Ebbole, 2005). Studies of STE-50 homologues revealed that it could be subdivided into three domains: RAS, SAM and S/T (Fu et al., 2011). In this chapter, I test truncated forms of STE50 for interaction with RIC8.

Materials and Methods:

Primers described in table A.C.1 were used to make each truncation form for yeast two hybrid analysis. Primer combinations were as follows: SAM_fw and RAS_rv formed STE50_full, SAM_fw and SAM_rv formed SAM_only, S/T_fw and S/T_rv formed S/T only, RAS_fw and RAS_rv formed RAS_only, SAM_fw and S/T_rv formed SAM+S/T, and S/T_fw and RAS_rv formed S/T+RAS. Using 1 μL of a 1:10 dilution of the *ste50* full length vector as template, PCR was performed using the Phusion PCR protocol, with a 1 minute 98^{o}C annealing step and a 3 minute extension step (Appendix B). The fragments were TA cloned into pGEMT vectors, DNA extracted from transformants using Qiagen miniPrep, and then digested with *Eco*RI and *Sal*I in NEB buffer 3 at 37^{o}C for 4 hours (Appendix B). Bands of the expected sizes were gel-extracted: STE50_full (1,450 nt), SAM_only (400 nt), S/T_only (700 nt), RAS_only (350 nt), SAM+S/T (1,100 nt), S/T+RAS (1,050 nt) (Appendix B). GAD and GBK vectors were digested with *Eco*RI and *Sal*I, and similarly gel extracted (Appendix B). Each of the six inserts was ligated into both GAD and GBK

vectors, and transformed into yeast strains AH109 and Y187 respectively. Diploids were formed for each of these with each of the RIC8 truncation by sexual crosses described in appendix B.

Results

The first yeast two hybrid assay performed involved testing full length STE50 with various truncations of RIC8. Here, strains expressing the full length RIC8 with STE50_full grew on SD-Trp-Leu-Ade-His (quadruple dropout; QDO) as expected (Appendix A, Appendix C). The diploids of Δ54C or Δ136C RIC8 with STE50_full also grew on SD-Trp-Leu-Ade-His (QDO), indicating that deletion of the C-terminus of RIC8 does not disrupt interaction with STE50. However, the strain carrying the Δ132N truncation and STE50_full did not grow on SD-Trp-Leu-His or SD-Trp-Leu-Ade (triple dropout, TDO), consistent with no interaction between STE50 and N0termina truncated RIC8. Finally, the strain carrying the double truncations Δ132NΔ54C and Δ132NΔ136C and STE50_full did not grow on TDO or QDO medium, indicating no interaction between the proteins.

The second yeast two hybrid assay performed involved testing various truncations of STE50 with full length RIC8. Here, a strain expressing STE50_full with RIC8 was used as the positive control, where it again grew on QDO medium. The strain carrying the SAM+S/T form of STE50 and RIC8 did not grow on TDO or QDO medium, consistent with a requirement for the RAS domain in STE50 for binding. Yeast expressing the S/T+RAS form of STE50 and RIC8 grew on QDO medium, suggesting that the SAM domain is dispensable for interaction. Individual domains were also tested. Strains expressing the STE50 SAM domain alone with RIC8 did not grown on TDO or QDO medium. However, strains carrying the STE50 S/T domain alone and RIC8 grew on QDO, suggesting that this domain is necessary and sufficient for binding of STE50 to

RIC8. Finally, yeast carrying the STE50 RAS domain grew on TDO, but not QDO, consistent with the RAS domain supporting a weak interaction between STE50 and RIC8.

Discussion

The results of RIC8 truncations with full length STE50 are easily interpreted. The loss of the N-terminus of RIC8 completely eliminates the ability for RIC8 to interact with STE50. This is the same region that was observed to be essential for interaction with GNA-1, suggesting that this region of RIC8 is responsible for binding to multiple partners. In contrast, deletion of the C-terminus did not affect the binding of RIC8 to STE50.

The results for testing RIC8 full length with STE50 truncated forms is less straightforward. A truncation of STE50 removing the SAM domain does not affect the binding to RIC8. Interestingly, the S/T domain alone is able to strongly interact with RIC8, consistent with the observation that the S/T+RAS truncation also interacts with RIC8. Interestingly, the RAS domain alone also interacts, though more weakly, with RIC8, suggesting that the binding domain may be contained partially in the RAS and S/T domains. Further complicating the situation is that the SAM+S/T domains together do not interact, suggesting that the SAM domain may be inhibitory to the interaction. The effect of the SAM domain on interaction presents an interesting question that requires further experimentation, but it is evident that the binding of RIC8 occurs primarily within the S/T and RAS domains of STE50, and somewhat stronger with the S/T than the RAS domain.

Table A.D.1: General primers used for STE50 yeast two hybrid.

Gene	Primer Name	Sequence (5'-3')
ste50	SAM_fw	ACCGGAATTCATGAACTTTGACTCGGGCAC
ste50	SAM_rv	CGTATGTCGACGCCTTCTTTACATCGTAGAC
ste50	S/T_fw	ACCGGAATTCGCTCAAGATGTTCCTATCGAGGAC
ste50	S/T_rv	CGTTATGTCGACTGGCGTCTGTCCTCTGCGGG
ste50	RAS_fw	ACCGGAATTC ACCTGATACCCCTGGTTCC
ste50	RAS_rv	CGGGAGGTATCATATAGGTCGACATAC

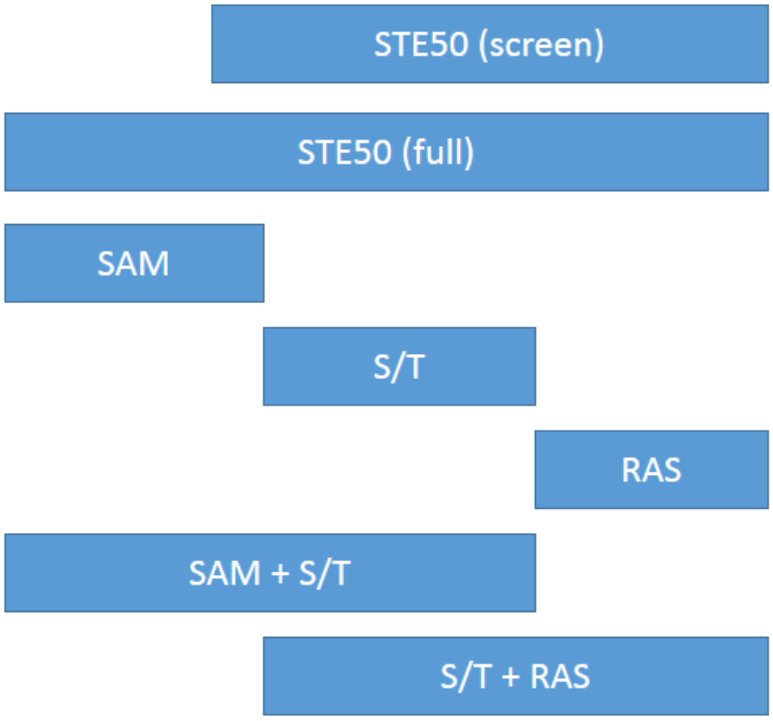

Figure A.D.1 Truncation forms of STE50. The form of STE50 identified in the yeast two hybrid screen contained part of the SAM domain, as well as the entire S/T and RAS domains. To perform further analysis, a full length yeast two hybrid form of STE50 was generated, as well as five distinct truncations. The first three truncations are individual SAM, S/T and RAS domains. The last two contain pairs of adjacent domains, either SAM+S/T or S/T+RAS.

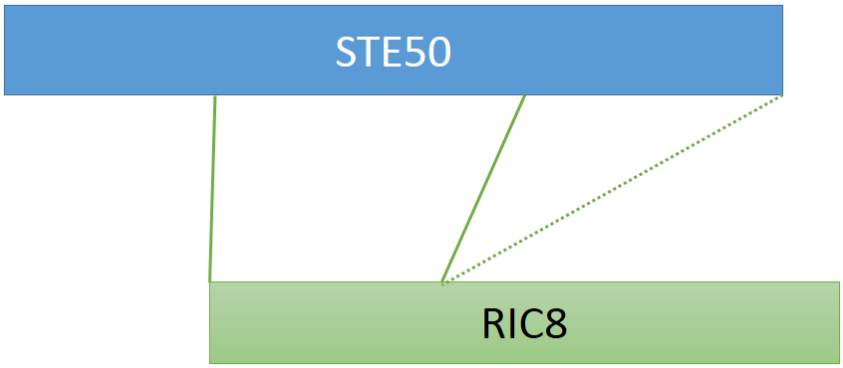

Figure A.D.2: Interaction model of RIC8 with STE50. Data from the truncations of RIC8 revealed that the N-terminus of RIC8 interacts with STE50. Data from the STE50 truncations revealed that the center (S/T domain) is strongly involved in binding RIC8, while the C-terminus (RAS domain) is weakly involved, and the N-terminus (SAM domain) is unnecessary for binding. Thus, the proposed model involves the N-terminus of RIC8 interacting strongly (solid lines) with the central S/T domain of STE50, and weakly (dashed line) with the C-terminal RAS domain.

References:

Afshar, K., Willard, F. S., Colombo, K., Johnston, C. A., McCudden, C. R., Siderovski, D. P., & Gonczy, P. (2004). RIC-8 is required for GPR-1/2-dependent Galpha function during asymmetric division of *C. elegans* embryos. *Cell, 119*(2), 219-230. doi: S0092867404008992 [pii] 10.1016/j.cell.2004.09.026

Aldabbous, M. S., Roca, M. G., Stout, A., Huang, I. C., Read, N. D., & Free, S. J. (2010). The *ham-5*, *rcm-1* and *rco-1* genes regulate hyphal fusion in *Neurospora crassa*. *Microbiology, 156*(Pt 9), 2621-2629. doi: 10.1099/mic.0.040147-0

Alting-Mees, M. A., & Short, J. M. (1989). pBluescript II: gene mapping vectors. *Nucleic Acids Res, 17*(22), 9494.

Backman, T. W., Cao, Y., & Girke, T. (2011). ChemMine tools: an online service for analyzing and clustering small molecules. *Nucleic Acids Res, 39*(Web Server issue), W486-491. doi: 10.1093/nar/gkr320

Bedalov, A., Gatbonton, T., Irvine, W. P., Gottschling, D. E., & Simon, J. A. (2001). Identification of a small molecule inhibitor of Sir2p. *Proc Natl Acad Sci U S A, 98*(26), 15113-15118. doi: 10.1073/pnas.261574398

Bistis, G. N. (1981). Chemotropic interactins between trichogynes and conidia of opposite mating-type in *Neurospora crassa*. *Mycologia, 73*, 959-975.

Bloemendal, S., Bernhards, Y., Bartho, K., Dettmann, A., Voigt, O., Teichert, I., . . . Kuck, U. (2012). A homologue of the human STRIPAK complex controls sexual development in fungi. *Mol Microbiol, 84*(2), 310-323. doi: 10.1111/j.1365-2958.2012.08024.x

Bobrowicz, P., Pawlak, R., Correa, A., Bell-Pedersen, D., & Ebbole, D. J. (2002). The Neurospora crassa pheromone precursor genes are regulated by the mating type locus and the circadian clock. *Mol Microbiol, 45*(3), 795-804.

Borkovich, K. A., Alex, L. A., Yarden, O., Freitag, M., Turner, G. E., Read, N. D., . . . Pratt, R. (2004). Lessons from the genome sequence of *Neurospora crassa*: tracing the path from genomic blueprint to multicellular organism. *Microbiol Mol Biol Rev, 68*(1), 1-108.

Brenk, R., Schipani, A., James, D., Krasowski, A., Gilbert, I. H., Frearson, J., & Wyatt, P. G. (2008). Lessons learnt from assembling screening libraries for drug discovery for neglected diseases. *ChemMedChem, 3*(3), 435-444. doi: 10.1002/cmdc.200700139

Burke, M. D., & Schreiber, S. L. (2004). A planning strategy for diversity-oriented synthesis. *Angew Chem Int Ed Engl, 43*(1), 46-58. doi: 10.1002/anie.200300626

Cases, M., & Mestres, J. (2009). A chemogenomic approach to drug discovery: focus on cardiovascular diseases. *Drug Discov Today, 14*(9-10), 479-485. doi: 10.1016/j.drudis.2009.02.010

Charlie, N. K., Thomure, A. M., Schade, M. A., & Miller, K. G. (2006). The Dunce cAMP phosphodiesterase PDE-4 negatively regulates G alpha(s)-dependent and G

alpha(s)-independent cAMP pools in the Caenorhabditis elegans synaptic signaling network. *Genetics, 173*(1), 111-130. doi: 10.1534/genetics.105.054007

Cock, P. J., Fields, C. J., Goto, N., Heuer, M. L., & Rice, P. M. (2010). The Sanger FASTQ file format for sequences with quality scores, and the Solexa/Illumina FASTQ variants. *Nucleic Acids Res, 38*(6), 1767-1771. doi: 10.1093/nar/gkp1137

Cohen-Fix, O., & Livneh, Z. (1992). Biochemical analysis of UV mutagenesis in Escherichia coli by using a cell-free reaction coupled to a bioassay: identification of a DNA repair-dependent, replication-independent pathway. *Proc Natl Acad Sci U S A, 89*(8), 3300-3304.

Colot, H. V., Park, G., Turner, G. E., Ringelberg, C., Crew, C. M., Litvinkova, L., . . . Dunlap, J. C. (2006). A high-throughput gene knockout procedure for *Neurospora* reveals functions for multiple transcription factors. *Proc Natl Acad Sci U S A, 103*(27), 10352-10357. doi: 0601456103 [pii]10.1073

Davis, R. H. (2000). *Neurospora: Contributions of a Model Organism*. New York: Oxford University Press.

Davis, R. H., & de Serres, F. J. (1970). Genetic and microbiological research techniques for *Neurospora crassa*. *Methods in Enzymology, 17*, 79-143.

Dean, P. M. (2007). Chemical genomics: a challenge for *de novo* drug design. *Mol Biotechnol, 37*(3), 237-245. doi: 10.1007/s12033-007-0037-x

Dettmann, A., Illgen, J., Marz, S., Schurg, T., Fleissner, A., & Seiler, S. (2012). The NDR kinase scaffold HYM1/MO25 is essential for MAK2 map kinase signaling in Neurospora crassa. *PLoS Genet, 8*(9), e1002950. doi: 10.1371/journal.pgen.1002950

Dunlap, J. C., Borkovich, K. A., Henn, M. R., Turner, G. E., Sachs, M. S., Glass, N. L., . . . Xu, J. (2007). Enabling a community to dissect an organism: overview of the *Neurospora* functional genomics project. *Adv Genet, 57*, 49-96. doi: S0065-2660(06)57002-6 [pii]10.1016

Eaton, C. J., Cabrera, I. E., Servin, J. A., Wright, S. J., Cox, M. P., & Borkovich, K. A. (2012). The guanine nucleotide exchange factor RIC8 regulates conidial germination through Galpha proteins in *Neurospora crassa*. *PLoS One, 7*(10), e48026. doi: 10.1371/journal.pone.0048026

Ewing, B., & Green, P. (1998). Base-calling of automated sequencer traces using phred. II. Error probabilities. *Genome Res, 8*(3), 186-194.

Figueroa, M., Hinrichs, M. V., Bunster, M., Babbitt, P., Martinez-Oyanedel, J., & Olate, J. (2009). Biophysical studies support a predicted superhelical structure with armadillo repeats for Ric-8. *Protein Sci, 18*(6), 1139-1145. doi: 10.1002/pro.124

Fitzsimmons, L. F., Flemer, S., Wurthmann, A. S., Deker, P. B., Sarkar, I. N., & Wargo, M. J. (2011). Small-Molecule Inhibition of Choline Catabolism in Pseudomonas aeruginosa and Other Aerobic Choline-Catabolizing Bacteria. *Applied and Environmental Microbiology, 77*(13), 4383-4389. doi: 10.1128/aem.00504-11

Frearson, J. A., & Collie, I. T. (2009). HTS and hit finding in academia--from chemical genomics to drug discovery. *Drug Discov Today, 14*(23-24), 1150-1158. doi: 10.1016/j.drudis.2009.09.004

Fredriksson, R., Lagerstrom, M. C., Lundin, L. G., & Schioth, H. B. (2003). The G-protein-coupled receptors in the human genome form five main families. Phylogenetic analysis, paralogon groups, and fingerprints. *Mol Pharmacol, 63*(6), 1256-1272. doi: 10.1124/mol.63.6.1256

Fu, C., Iyer, P., Herkal, A., Abdullah, J., Stout, A., & Free, S. J. (2011). Identification and characterization of genes required for cell-to-cell fusion in *Neurospora crassa*. *Eukaryot Cell, 10*(8), 1100-1109. doi: 10.1128/EC.05003-11

Galagan, J. E., Calvo, S. E., Borkovich, K. A., Selker, E. U., Read, N. D., Jaffe, D., . . . Birren, B. (2003). The genome sequence of the filamentous fungus *Neurospora crassa*. *Nature, 422*(6934), 859-868. doi: 10.1038/nature01554[pii]

Giles, N. H. (1951). *Studies on the mechanism of reversion in biochemical mutants of Neurospora crassa*. Paper presented at the Cold Spring Harbor Symposium on Quantitative Biology.

Goudreault, M., D'Ambrosio, L. M., Kean, M. J., Mullin, M. J., Larsen, B. G., Sanchez, A., . . . Gingras, A. C. (2009). A PP2A phosphatase high density interaction network identifies a novel striatin-interacting phosphatase and kinase complex linked to the cerebral cavernous malformation 3 (CCM3) protein. *Mol Cell Proteomics, 8*(1), 157-171. doi: 10.1074/mcp.M800266-MCP200

Griffiths, A. J. F. (1982). Null mutants of the A and a mating-type alleles of *Neurospora crassa*. *Can. J. Genet. Cytol., 24:*, 167–176.

Haggarty, S. J., Koeller, K. M., Wong, J. C., Grozinger, C. M., & Schreiber, S. L. (2003). Domain-selective small-molecule inhibitor of histone deacetylase 6 (HDAC6)-mediated tubulin deacetylation. *Proc Natl Acad Sci U S A, 100*(8), 4389-4394. doi: 10.1073/pnas.0430973100

Hampoelz, B., Hoeller, O., Bowman, S. K., Dunican, D., & Knoblich, J. A. (2005). *Drosophila* Ric-8 is essential for plasma-membrane localization of heterotrimeric G proteins. *Nat Cell Biol, 7*(11), 1099-1105. doi: ncb1318 [pii]10.1038

Hollinger, S., & Hepler, J. R. (2002). Cellular regulation of RGS proteins: modulators and integrators of G protein signaling. *Pharmacol Rev, 54*(3), 527-559.

Jamet-Vierny, C., Debuchy, R., Prigent, M., & Silar, P. (2007). IDC1, a pezizomycotina-specific gene that belongs to the PaMpk1 MAP kinase transduction cascade of the filamentous fungus Podospora anserina. *Fungal Genet Biol, 44*(12), 1219-1230. doi: 10.1016/j.fgb.2007.04.005

Jones, C. A. (2008). *Two-Component Signaling Pathways in the Filamentous Fungus, Neurospora crassa.* (Doctor of Philosophy in Biochemistry and Molecular Biology), University of California Riverside, Riverside, CA.

Jones, C. A., Greer-Phillips, S. E., & Borkovich, K. A. (2007). The response regulator RRG-1 functions upstream of a mitogen-activated protein kinase pathway impacting

asexual development, female fertility, osmotic stress, and fungicide resistance in *Neurospora crassa*. *Mol Biol Cell, 18*(6), 2123-2136. doi: E06-03-0226 [pii]10.1091

Kataria, R., Xu, X., Fusetti, F., Keizer-Gunnink, I., Jin, T., van Haastert, P. J., & Kortholt, A. (2013). Dictyostelium Ric8 is a nonreceptor guanine exchange factor for heterotrimeric G proteins and is important for development and chemotaxis. *Proc Natl Acad Sci U S A, 110*(16), 6424-6429. doi: 10.1073/pnas.1301851110

Kays, A. M., & Borkovich, K. A. (2004). Severe impairment of growth and differentiation in a *Neurospora crassa* mutant lacking all heterotrimeric G alpha proteins. *Genetics, 166*(3), 1229-1240. doi: 166/3/1229 [pii]

Kays, A. M., Rowley, P. S., Baasiri, R. A., & Borkovich, K. A. (2000). Regulation of conidiation and adenylyl cyclase levels by the Galpha protein GNA-3 in *Neurospora crassa*. *Mol Cell Biol, 20*(20), 7693-7705.

Kean, M. J., Ceccarelli, D. F., Goudreault, M., Sanches, M., Tate, S., Larsen, B., . . . Gingras, A. C. (2011). Structure-function analysis of core STRIPAK Proteins: a signaling complex implicated in Golgi polarization. *J Biol Chem, 286*(28), 25065-25075. doi: 10.1074/jbc.M110.214486

Kim, H., & Borkovich, K. A. (2004). A pheromone receptor gene, *pre-1*, is essential for mating type-specific directional growth and fusion of trichogynes and female fertility in *Neurospora crassa*. *Mol Microbiol, 52*(6), 1781-1798. doi: 10.1111/j.1365-2958.2004.04096.x MI4096 [pii]

Kim, H., & Borkovich, K. A. (2006). Pheromones are essential for male fertility and sufficient to direct chemotropic polarized growth of trichogynes during mating in *Neurospora crassa*. *Eukaryot Cell, 5*(3), 544-554. doi: 5/3/544 [pii]10.1128

Klattenhoff, C., Montecino, M., Soto, X., Guzman, L., Romo, X., Garcia, M. A., . . . Olate, J. (2003). Human brain synembryn interacts with Gsalpha and Gqalpha and is translocated to the plasma membrane in response to isoproterenol and carbachol. *J Cell Physiol, 195*(2), 151-157. doi: 10.1002/jcp.10300

Kocisko, D. A., Baron, G. S., Rubenstein, R., Chen, J., Kuizon, S., & Caughey, B. (2003). New inhibitors of scrapie-associated prion protein formation in a library of 2000 drugs and natural products. *J Virol, 77*(19), 10288-10294.

Lambreghts, R., Shi, M., Belden, W. J., Decaprio, D., Park, D., Henn, M. R., . . . Loros, J. J. (2009). A high-density single nucleotide polymorphism map for *Neurospora crassa*. *Genetics, 181*(2), 767-781. doi: genetics.108.089292 [pii]10.1534

Li, D., Bobrowicz, P., Wilkinson, H. H., & Ebbole, D. J. (2005). A mitogen-activated protein kinase pathway essential for mating and contributing to vegetative growth in Neurospora crassa. *Genetics, 170*(3), 1091-1104. doi: 10.1534/genetics.104.036772

Li, H., & Durbin, R. (2010). Fast and accurate long-read alignment with Burrows-Wheeler transform. *Bioinformatics, 26*(5), 589-595. doi: 10.1093/bioinformatics/btp698

Li, H., Handsaker, B., Wysoker, A., Fennell, T., Ruan, J., Homer, N., . . . Genome Project Data Processing, S. (2009). The Sequence Alignment/Map format and SAMtools. *Bioinformatics, 25*(16), 2078-2079. doi: 10.1093/bioinformatics/btp352

Li, L., Wright, S. J., Krystofova, S., Park, G., & Borkovich, K. A. (2007). Heterotrimeric G protein signaling in filamentous fungi. *Annu Rev Microbiol, 61*, 423-452. doi: 10.1146/annurev.micro.61.080706.093432

Lipinski, C. A. (2000). Drug-like properties and the causes of poor solubility and poor permeability. *J Pharmacol Toxicol Methods, 44*(1), 235-249.

Lipinski, C. A., Lombardo, F., Dominy, B. W., & Feeney, P. J. (2001). Experimental and computational approaches to estimate solubility and permeability in drug discovery and development settings. *Adv Drug Deliv Rev, 46*(1-3), 3-26.

MacBeath, G. (2001). Chemical genomics: what will it take and who gets to play? *Genome Biol, 2*(6), COMMENT2005.

Maheshwari, R. (1999). Microconidia of *Neurospora crassa*. *Fungal Genet Biol, 26*(1), 1-18. doi: 10.1006/fgbi.1998.1103

Metzenberg, R. L. (1995). The sexual cycle in *Neurospora* from fertilization to ascospore discarge. *Biotechniology of Ectomycorrhizae: Molecular Approaches*, 85-98.

Miller, K. G., Emerson, M. D., McManus, J. R., & Rand, J. B. (2000). RIC-8 (Synembryn): a novel conserved protein that is required for G(q)alpha signaling in the *C. elegans* nervous system. *Neuron, 27*(2), 289-299. doi: S0896-6273(00)00037-4 [pii]

Miller, K. G., Emerson, M. D., & Rand, J. B. (1999). Goalpha and diacylglycerol kinase negatively regulate the Gqalpha pathway in *C. elegans*. *Neuron, 24*(2), 323-333.

Miller, K. G., & Rand, J. B. (2000). A role for RIC-8 (Synembryn) and GOA-1 (G(o)alpha) in regulating a subset of centrosome movements during early embryogenesis in *Caenorhabditis elegans*. *Genetics, 156*(4), 1649-1660.

Neves, S. R., Ram, P. T., & Iyengar, R. (2002). G protein pathways. *Science, 296*(5573), 1636-1639. doi: 10.1126/science.1071550 296/5573/1636 [pii]

Ninomiya, Y., Suzuki, K., Ishii, C., & Inoue, H. (2004). Highly efficient gene replacements in *Neurospora* strains deficient for nonhomologous end-joining. *Proc Natl Acad Sci U S A, 101*(33), 12248-12253. doi: 10.1073/pnas.0402780101 0402780101 [pii]

Oldham, W. M., & Hamm, H. E. (2008). Heterotrimeric G protein activation by G-protein-coupled receptors. *Nat Rev Mol Cell Biol, 9*(1), 60-71. doi: nrm2299 [pii] 10.1038

Pall, M. L. (1993). The use of Ignite (Basta;glufosinate;phosphiothricin) to select transformatns of bar-containing plasmids in *Neurospora crassa. Fungal Genetics Newsletter, 40*, 58.

Pearson, W. R. (2014). BLAST and FASTA Similarity Searching for Multiple Sequence Alignment. *Methods Mol Biol, 1079*, 75-101. doi: 10.1007/978-1-62703-646-7_5

Peterson, R. T., Link, B. A., Dowling, J. E., & Schreiber, S. L. (2000). Small molecule developmental screens reveal the logic and timing of vertebrate development. *Proc Natl Acad Sci U S A, 97*(24), 12965-12969. doi: 10.1073/pnas.97.24.12965

Plamann, M. (2009). Cytoplasmic streaming in neurospora: disperse the plug to increase the flow? *PLoS Genet, 5*(6), e1000526. doi: 10.1371/journal.pgen.1000526

Raju, N. B. (1980). Meiosis and ascospore genesis in Neurospora. *Eur J Cell Biol, 23*(1), 208-223.

Raju, N. B., & Leslie, J. F. (1992). Cytology of recessive sexual-phase mutants from wild strains of *Neurospora crassa*. *Genome, 35*(5), 815-826.

Roca, M. G., Arlt, J., Jeffree, C. E., & Read, N. D. (2005). Cell biology of conidial anastomosis tubes in *Neurospora crassa*. *Eukaryot Cell, 4*(5), 911-919. doi: 10.1128/EC.4.5.911-919.2005

Romo, X., Pasten, P., Martinez, S., Soto, X., Lara, P., de Arellano, A. R., . . . Olate, J. (2007). xRic-8 is a GEF for Gsalpha and participates in maintaining meiotic arrest in *Xenopus laevis* oocytes. *J Cell Physiol, 214*(3), 673-680. doi: 10.1002/jcp.21257

Rossier, C., Ton-That, T. C., & Turian, G. (1977). Microcyclic micronidiation in *Neurospora crassa*. *Exp. Mycol., 1*, 52-62.

Schade, M. A., Reynolds, N. K., Dollins, C. M., & Miller, K. G. (2005). Mutations that rescue the paralysis of *Caenorhabditis elegans ric-8* (synembryn) mutants activate the G alpha(s) pathway and define a third major branch of the synaptic signaling network. *Genetics, 169*(2), 631-649. doi: genetics.104.032334 [pii] 10.1534

Schmid, J., & Harold, F. M. (1988). Dual roles for calcium ions in apical growth of Neurospora crassa. *J Gen Microbiol, 134*(9), 2623-2631.

Siderovski, D. P., & Willard, F. S. (2005). The GAPs, GEFs, and GDIs of heterotrimeric G-protein alpha subunits. *Int J Biol Sci, 1*(2), 51-66.

Simonin, A. R., Rasmussen, C. G., Yang, M., & Glass, N. L. (2010). Genes encoding a striatin-like protein (*ham-3*) and a forkhead associated protein (*ham-4*) are required for hyphal fusion in *Neurospora crassa*. *Fungal Genet Biol, 47*(10), 855-868. doi: 10.1016/j.fgb.2010.06.010

Smith, K. M., Phatale, P. A., Sullivan, C. M., Pomraning, K. R., & Freitag, M. (2011). Heterochromatin is required for normal distribution of Neurospora crassa CenH3. *Mol Cell Biol, 31*(12), 2528-2542. doi: 10.1128/mcb.01285-10

Spring, D. R. (2005). Chemical genetics to chemical genomics: small molecules offer big insights. *Chem Soc Rev, 34*(6), 472-482.

Springer, M. L. (1993). Genetic control of fungal differentiation: the three sporulation pathways of Neurospora crassa. *Bioessays, 15*(6), 365-374. doi: 10.1002/bies.950150602

Springer, M. L., & Yanofsky, C. (1989). A morphological and genetic analysis of conidiophore development in Neurospora crassa. *Genes Dev, 3*(4), 559-571.

Stadler, L. J., & Sprague, G. F. (1936). Genetic Effects of Ultra-Violet Radiation in Maize: I. Unfiltered Radiation. *Proc Natl Acad Sci U S A, 22*(10), 572-578.

Stockwell, B. R. (2004). Exploring biology with small organic molecules. *Nature, 432*(7019), 846-854. doi: 10.1038/nature03196

Tall, G. G., & Gilman, A. G. (2004). Purification and functional analysis of Ric-8A: a guanine nucleotide exchange factor for G-protein alpha subunits. *Methods Enzymol, 390*, 377-388. doi: S0076687904900237 [pii] 10.1016

Tall, G. G., Krumins, A. M., & Gilman, A. G. (2003). Mammalian Ric-8A (synembryn) is a heterotrimeric Galpha protein guanine nucleotide exchange factor. *J Biol Chem, 278*(10), 8356-8362. doi: 10.1074/jbc.M211862200 [pii]

Tonissoo, T., Koks, S., Meier, R., Raud, S., Plaas, M., Vasar, E., & Karis, A. (2006). Heterozygous mice with Ric-8 mutation exhibit impaired spatial memory and decreased anxiety. *Behav Brain Res, 167*(1), 42-48. doi: S0166-4328(05)00368-2 [pii] 10.1016/j.bbr.2005.08.025

Turner, G. E., & Borkovich, K. A. (1993). Identification of a G protein alpha subunit from *Neurospora crassa* that is a member of the Gi family. *J Biol Chem, 268*(20), 14805-14811.

Vignal, A., Milan, D., SanCristobal, M., & Eggen, A. (2002). A review on SNP and other types of molecular markers and their use in animal genetics. *Genet Sel Evol, 34*(3), 275-305. doi: 10.1051/gse:2002009

Wang, H., Ng, K. H., Qian, H., Siderovski, D. P., Chia, W., & Yu, F. (2005). Ric-8 controls *Drosophila* neural progenitor asymmetric division by regulating heterotrimeric G proteins. *Nat Cell Biol, 7*(11), 1091-1098. doi: ncb1317 [pii] 10.1038

Weber, L. (2000). High-diversity combinatorial libraries. *Curr Opin Chem Biol, 4*(3), 295-302.

Wells, J. A., & McClendon, C. L. (2007). Reaching for high-hanging fruit in drug discovery at protein-protein interfaces. *Nature, 450*(7172), 1001-1009. doi: 10.1038/nature06526

Westergaard, M., & Mitchell, H. K. (1947). *Neurospora*. V. A syntehtic medium favoring sexual reproduction. *Am J Bot., 34*(573-577).

Wilkie, T. M., & Kinch, L. (2005). New roles for Galpha and RGS proteins: communication continues despite pulling sisters apart. *Curr Biol, 15*(20), R843-854. doi: S0960-9822(05)01150-4 [pii] 10.1016/j.cub.2005.10.008

Wright, S. J., Inchausti, R., Eaton, C. J., Krystofova, S., & Borkovich, K. A. (2011). RIC8 is a guanine-nucleotide exchange factor for Galpha subunits that regulates growth and development in *Neurospora crassa*. *Genetics, 189*(1), 165-176. doi: 10.1534/genetics.111.129270

Xiang, Q., Rasmussen, C., & Glass, N. L. (2002). The *ham-2* locus, encoding a putative transmembrane protein, is required for hyphal fusion in *Neurospora crassa*. *Genetics, 160*(1), 169-180.

Yu, J. H. (2006). Heterotrimeric G protein signaling and RGSs in *Aspergillus nidulans*. *J Microbiol, 44*(2), 145-154. doi: 2371 [pii]